POLITECNICO
MILANO 1863

SCUOLA DI INGEGNERIA INDUSTRIALE
E DELL'INFORMAZIONE

Preliminary Sizing of Hydrogen-Burning Jetliner for Direct Operating Cost Optimization

TESI DI LAUREA MAGISTRALE IN
AERONAUTICAL ENGINEERING
INGEGNERIA AERONAUTICA

Author: **Hamid Mohammadi**

Student ID: 926787
Advisor: Prof. Lorenzo Trainelli
Co-advisor: Prof. Carlo E.D. Riboldi
Academic Year: 2022-23

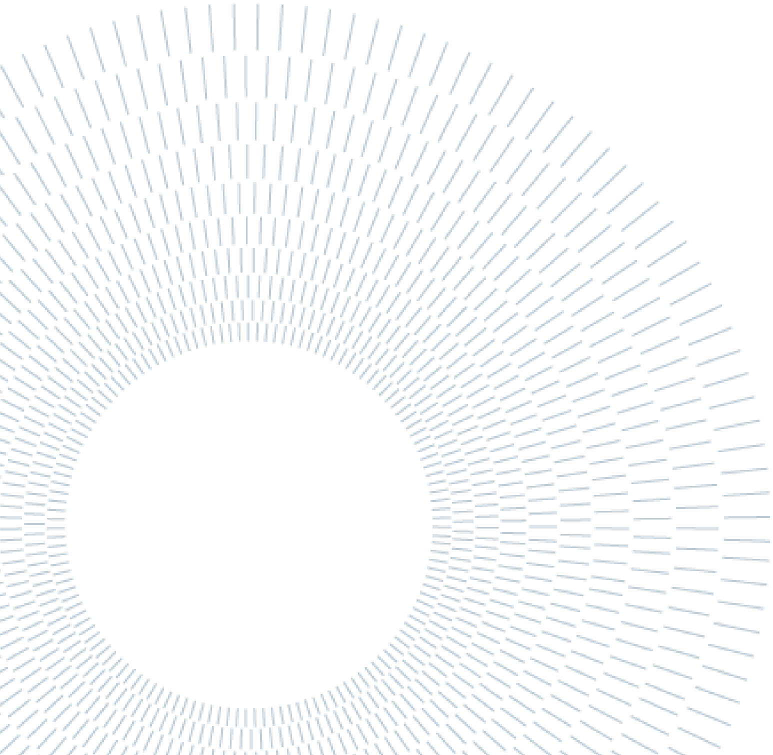

Abstract

The research objectives of this thesis are to conduct a comprehensive design study on the use of LH2 (liquid hydrogen) as a direct burning aviation fuel in passenger aircraft and to minimize direct operating costs associated with LH2 fuel usage. The main focus is on adapting the current tube and wing jetliner configuration to accommodate LH2 as a fuel source. The ultimate goal is to find optimal solutions for narrowbody and widebody aircraft that not only meet market demands but also significantly reduce their environmental impact.

To achieve this, a design tool called HYPERION was used to analyze the sizing of LH2 burning passenger aircraft and model the associated costs. The goal was to find optimal solutions for narrowbody (NB) and widebody (WB) aircraft, while maintaining the conventional tube and wing configuration to avoid radical changes and new technology investments. The analysis involved varying the number of seats, design range, and wing parameters. Eventually according to the figure of merit parameters, the best solution were selected.

Based on market studies and average aircraft utilization, a range of scenarios were examined for NB aircraft, including 180 number of passengers (PAX) to 220 PAX with a design range of 2,000 km to 6,000 km. For WB aircraft, scenarios ranged from 250 PAX to 400 PAX with a design range of 6,000 km to 15,000 km. In a systematic assessment, at the both classes, technology level, number of abreast, wing aspect ratio, wing sweep angle, wing relative thickness and cruise speed were optimized. To obtain the best solution, the analysis considered parameters such as maximum takeoff mass, fuel mass, and direct operating cost (DOC), which represents the cost per available seat per km and DOC per hour.

The main message of the project is, through family planning, it is possible to meet market demands competitively with the kerosene-burning version of the aircraft. However, there are limitations in terms of range and passenger capacity. The LH2 mid-range narrowbody class (in the class of A321neo) and large widebody (in the class of A350-1000) LH2 burning passenger aircraft have constraints in terms of range and passenger capacity. Additionally, while fuel prices do affect operational assumptions, they have a negligible effect on the optimal solution.

The best solutions found in this study are the basic variant of NB with a design range of 4,000 km and 200 passengers, and the basic variant of WB with a design range of 12,000 km and 350 passengers. These solutions not only cover the maximum market demand but also provide the possibility of family planning for shorter and longer derivatives. Additionally, these combinations are economically feasible for airliners to operate.

Key-words: Aircraft Design, Hydrogen Burning Aircraft, Preliminary Sizing, Direct Operating Cost, HYPERION, Narrowbody, Widebody.

Abstract in Italiano

Gli obiettivi di ricerca di questa tesi sono analizzare l'impatto dell'utilizzo di LH2 come carburante di velivoli commerciali, minimizzandone i costi operativi diretti. L'idrogeno è introdotto a bordo di velivoli a corto e lungo raggio in configurazione tubo-ala, opportunamente modificata. L'obiettivo è trovare soluzioni ottimali per gli aeromobili narrowbody e widebody che soddisfino le esigenze del mercato riducendo al contempo l'impatto ambientale.

Per raggiungere questo obiettivo, è stato utilizzato HYPERION, una metodologia di progetto preliminare di velivoli, che permette di dimensionare aerei che bruciano idrogeno per poi modellarne i costi associati. L'obiettivo era trovare soluzioni ottime in termini di costi operativi per gli aeromobili narrowbody (NB) e widebody (WB), mantenendo la configurazione tradizionale tubo e ala, per evitare cambiamenti radicali anche nella configurazione del velivolo. L'analisi è basata sulla variazione del numero di posti, il raggio d'azione e i parametri dell'ala. Alla fine, è stata selezionata la combinazione migliore in base alle cifre di merito introdotte.

Sulla base degli studi di mercato e dell'utilizzo medio degli aeromobili, sono stati esaminati una serie di scenari per gli aeromobili NB, che portano da 180 PAX a 220 PAX con il raggio d'azione da 2,000 km a 6,000 km. Per gli aeromobili WB, i velivoli considerati portano da 250 PAX a 400 PAX, con un raggio d'azione tra 6,000 km e 15,000 km. In una valutazione sistematica, in entrambe le categorie, sono stati ottimizzati il livello tecnologico, il numero di posti a sedere, il rapporto di allungamento dell'ala, l'angolo di freccia dell'ala, lo spessore relativo dell'ala e la velocità di crociera. Per ottenere la soluzione migliore, l'analisi ha considerato parametri come la massa massima al decollo, la massa del carburante e il costo operativo diretto (DOC), che rappresenta il costo per posto disponibile per chilometro, e il DOC per ogni ora di volo.

Il messaggio principale della tesi è che, attraverso un'analisi dei requisiti della missione di riferimento, è possibile soddisfare le richieste del mercato con velivoli alimentati ad idrogeno, in modo che siano compatitivi con i rispettivi velivoli a cherosene. Tuttavia, gli aeromobili passeggeri a idrogeno di classe narrowbody (simili all'A321neo) e widebody (nella classe dell'A350-1000) hanno vincoli in termini di raggio e capacità passeggeri. Inoltre, sebbene i prezzi del carburante influenzino le ipotesi operative, hanno un effetto trascurabile sulla soluzione ottimale.

Le migliori soluzioni trovate in questo studio sono la variante di base di NB con una raggio di 4,000 km e 200 passeggeri, e la variante di base di WB con un raggiogu di 12,000 km e 350 passeggeri. Queste soluzioni non solo coprono la massima domanda di mercato, ma offrono anche la possibilità di sviluppare de lle famiglie di velivoli, garantendo agli operatori una certa versatilità. Inoltre, queste combinazioni sono economicamente sostenibili per le compagnie aeree.

Parole chiave: Progettazione di velivoli, Aeromobili a brucia di idrogeno, Dimensionamento preliminare, Costo operativo diretto, HYPERION, Narrowbody, Widebody.

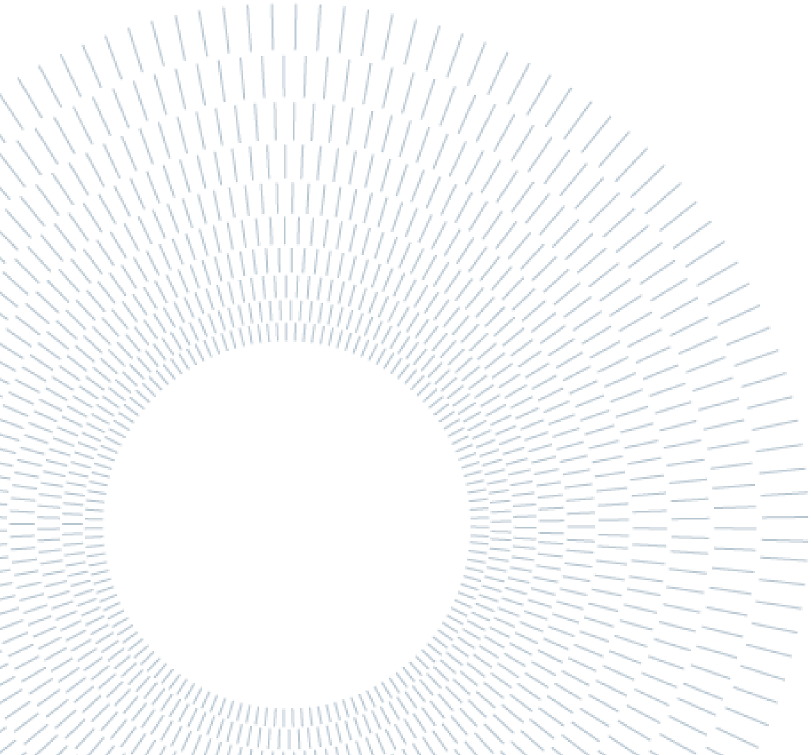

Contents

Abstract .... **iii**

Abstract in Italiano .... **v**

Contents .... **ix**

Introduction **13**

- Motivation 13
- Research Objective 16
- Methodology and Terminology 19
- Background of LH2 Burn Aircraft 23
- Chapters Overview 27

1 Market Study and Performance Requirements **29**

- 1.1. Traffic Demand 29
- 1.2. Current Fleet 31
- 1.3. Market Outlook 32
- 1.4. Average Utilization 34
  - 1.4.1. NB Utilization 36
  - 1.4.2. WB Utilization 36
- 1.5. Performance Requirements 37
  - 1.5.1. NB Performance Requirements 37
  - 1.5.2. WB Performance Requirements 37

2 Cost Model **41**

- 2.1. DOC 42
  - 2.1.1. Fuel Cost 43
  - 2.1.2. Crew Wage 44
  - 2.1.3. Maintenance Cost 45
  - 2.1.4. Ownership Cost 47
  - 2.1.5. Insurance Cost 47
  - 2.1.6. Navigation Fee 47
  - 2.1.7. Airport Fees 48
- 2.2. RDTE & ACQ 48
- 2.3. Purchasing Price 51

2.4. A321 Case Study 52

3 Framework of Design Trade off 55

3.1. Advancement of Engine 55

3.2. Advancement of Wing 56

3.2.1. Pitch-up Tendency 57

3.2.2. Drag Divergence Mach number 58

3.3. Fuselage Arrangement and Size 59

3.4. Aerodynamic Coefficients 61

3.4.1. Max Lift Coefficient 61

3.4.2. Drag Coefficient Increment 62

3.5. Oswald Efficiency 62

3.6. Economical Cruise Mach Number 64

3.7. Method Sensitivity Analysis 65

4 Narrowbody Design Study 67

4.1. Baseline NB Aircraft 67

4.2. Engine and Material Technologies Trade off 68

4.3. Range and PAX Trade off 69

4.4. Wing Parameters Trade Off 71

4.5. Cruise Speed Trade Off 74

4.6. NB Design Solution 75

5 Widebody Design Study 79

5.1. Baseline WB Aircraft 79

5.2. Number of Abreast Trade Off 79

5.3. Range and PAX Trade off 80

5.4. Wing Parameters Trade Off 82

5.5. Cruise Speed Trade Off 85

5.6. WB Design Solution 85

6 Summary and Conclusion 89

Bibliography 93

A Appendix A 99

A.1. NB trade off trend 99

A.2. WB Trade off trend 100

B Appendix B 103

B.1. NB HYPERION Output of Final Solution 103

B.2. WB HYPERION Output of Final Solution 105

List of Figures 107
List if Tables 111
List of abbreviations 113
List of symbols 115
Acknowledgments 119

Introduction

This chapter provides an overview of the motivation behind working on LH2 aircraft and the background of research activities in this area. It also outlines the research objectives and methodology used in this thesis.

Motivation

The aviation industry is one of the fastest-growing sources of greenhouse gas emissions, with carbon dioxide (CO2) emissions projected to double by 2050 compared to current levels (Figure 0.1). Currently, the aviation industry accounts for about 2.5% of global carbon emissions annually, and 4% in Europe [1].

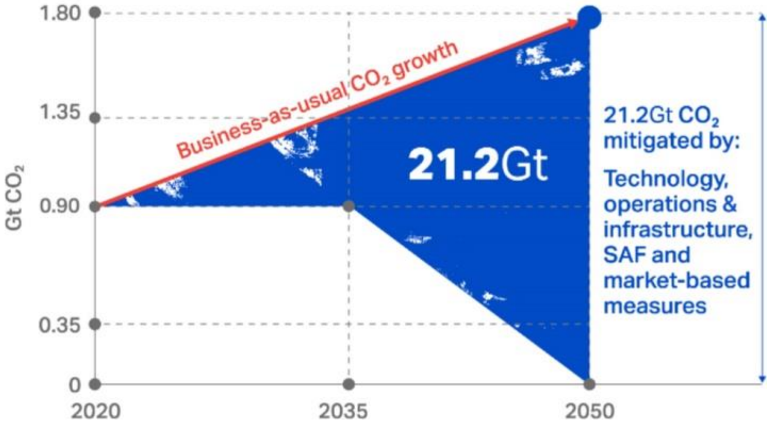

Figure 0.1: Aviation carbon emissions to be subsided by 2050 [2].

Emissions are directly related to fuel burn and flight range. Figure 0.2 illustrates the cumulative number of flights and CO2 emissions based on flying distance. It is evident from the figure that while only 10% of flights occur on routes longer than 3,000 km, these flights contribute to over 50% of fuel consumption and CO2 emissions. Similarly, 5% of flights longer than 7,000 km consume 20% of the total fuel. This indicates that a significant portion of CO2 emissions is generated by intercontinental flights [73]. Long-haul flights consume more fuel, and emissions are directly proportional to flight distance.

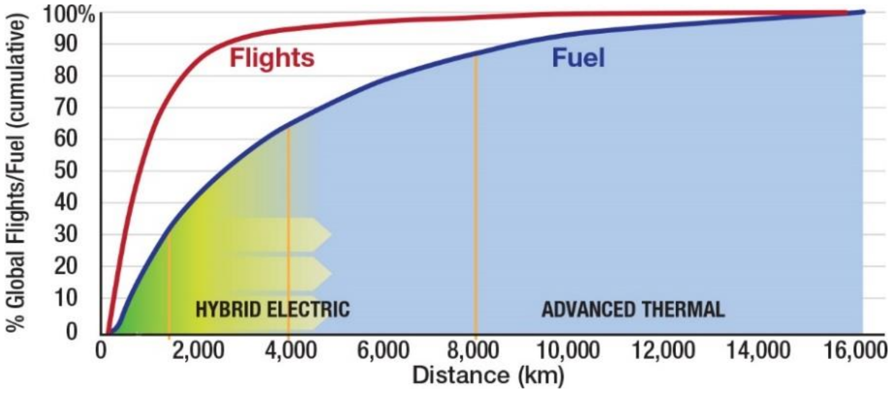

Figure 0.2: Share of global flights and CO2 emissions vs flight distance [3].

Figure 0.3 also demonstrates the distribution of CO2 emissions among different aircraft categories. Narrowbody aircraft, which are the most common type of aircraft in service and form the backbone of aviation transport, contribute the most to CO2 emissions.

Typically, narrowbody and regional aircraft operate short-range flights, but the carbon intensity of these flights, measured in grams of CO2 per revenue passenger kilometer, is nearly twice that of long-haul flights [4].

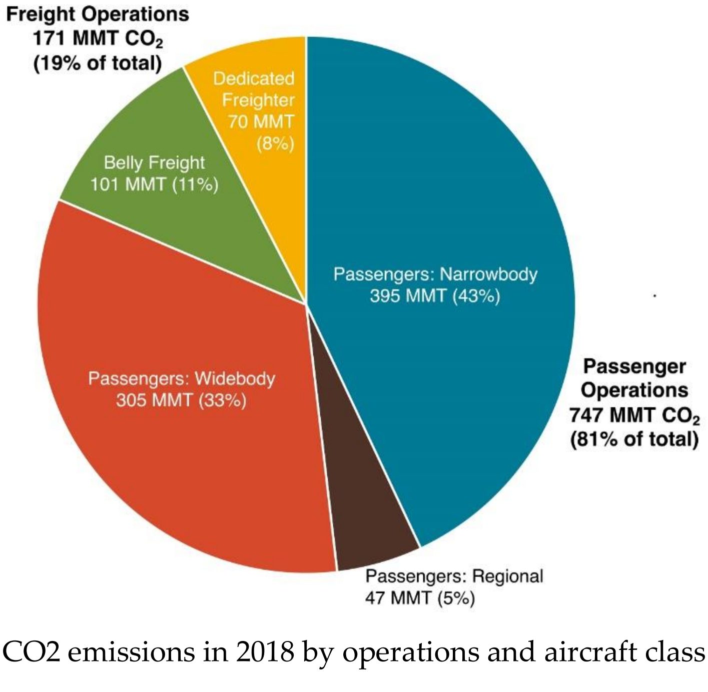

Figure 0.3: CO2 emissions in 2018 by operations and aircraft class [5].

Several governments are implementing decarbonization policies, particularly in the field of air transport operations and fuel types. Limitations on short-haul European flights are increasing, with Norway setting an ambitious goal to electrify all domestic flights by 2040. In France, domestic flights that compete with high-speed rail are prohibited. Consequently, the number of European flights covering distances less than 400 km is expected to decrease in the future. Another form of restriction is airport capacity limits, as seen with the Dutch government's recent decision to limit annual movements at Amsterdam Schiphol airport to 440,000, down from 500,000 in 2018 and 2019 [6].

Europe has also implemented measures to promote the use of Sustainable Aviation Fuel (SAF). Starting in 2025, operators will be required to use 2% SAF, with the percentage increasing to 5% by 2030, 32% by 2040, and 63% by 2050. That is convenient to know that currently, the cost of SAF is at least three times higher than kerosene [6].

In October 2021, the International Air Transport Association (IATA) released a roadmap to achieve net-zero carbon emissions by 2050 (Figure 0.4). Following this roadmap aligns air transport with the goals of the Paris Agreement to limit global warming to 1.5°C. The use of SAF plays a major role in reducing emissions. Additionally, the design and development of aircraft that utilize alternative fuels instead of kerosene is a revolutionary technology being researched by aircraft manufacturers.

Improving and developing new technologies is another solution for carbon reduction. Fuel efficiency in aircraft operations has improved by an average of over 2% per year between 2009 and 2019 [1], but further actions are necessary. Improving aerodynamic efficiency, implementing drag reduction techniques, and developing new and sometimes radical configurations are ongoing research endeavors in the aviation sector.

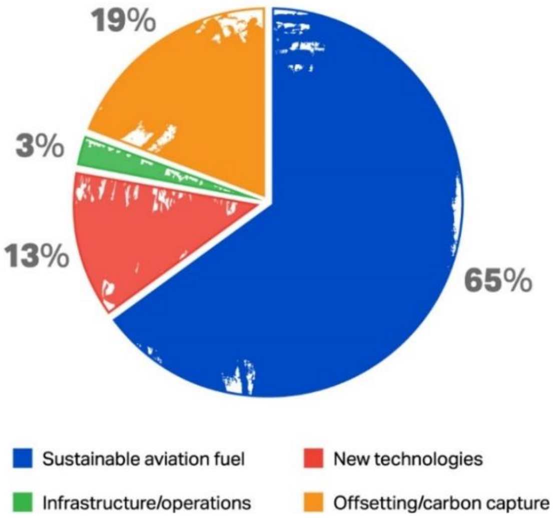

Figure 0.4: Contribution to achieving Net Zero Carbon in 2050 [2].

LH2 is a net-zero carbon fuel that is currently being strongly considered as a promising technology. Extensive government funding for hydrogen research as an alternative fuel for transportation is underway. Hydrogen combustion produces water vapor as its primary byproduct, but water emitted at high altitudes due to low temperatures can form Cirrus clouds. The impact of these clouds on global warming requires extensive research to fully understand their effects.

Even though hydrogen has a lot of potential, the new fuel contains numerous challenges in production, transport, distribution, and fueling in operational aspects. Additionally, there are challenges in adapting it to propulsion systems and finding solutions for onboard carrying. LH2 has ten times lower density compared to kerosene and a boiling temperature of -253 °C, which are major obstacles in its development as an aviation fuel.

Furthermore, like other green energy sources, hydrogen is not able to compete with kerosene fuel in terms of energy efficiency. Figure 0.5 shows the level of efficiency of energy delivery, illustrating that kerosene fuel delivers twice the amount of energy to aircraft propulsion compared to the energy required to extract, refine, and transport the fuel.

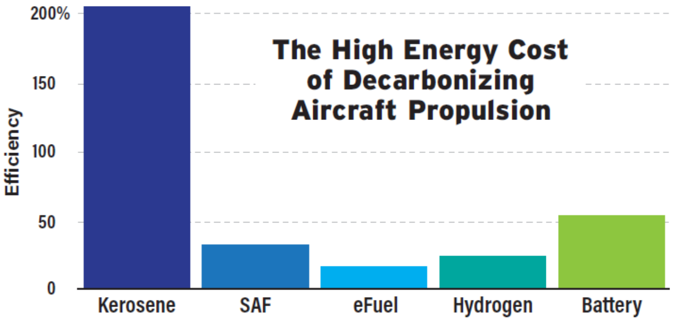

Figure 0.5: Efficiency of energy delivery to the aircraft propulsion [7].

Overall, technology challenges increase operational costs. Introducing any new technology to the market needs to be economically compatible with existing products. That is why economic analysis and design for a profitable LH2 burning aircraft are vital. This has been the main driver behind the thesis.

Research Objective

The use of hydrogen as a fuel source for aircraft has been divided into two categories: fuel cell powertrain aircraft and direct burning hydrogen aircraft. Fuel cell powertrain aircraft are more suitable for shorter distances, such as commuter and regional flights. These aircraft use a fuel cell system to convert hydrogen into electricity, which then powers the aircraft's electric motors. This type of aircraft is considered to be the most energy-efficient, environmentally friendly, and cost-effective option for fast and affordable travel.

The UNIFIER19 project [15], conducted by the Aerospace Department of Politecnico di Milano and funded by the European Commission, focused on the design study of fuel cell powertrain aircraft. This research aimed to develop an aircraft that could compete with highways and high-speed rail in terms of efficiency and cost-effectiveness.

The second category of hydrogen-powered aircraft considered in this thesis is the potential replacement for kerosene-burning aircraft. These aircraft directly burn hydrogen fuel in a turbine engine, similar to traditional jet engines. They are capable of long range transport and superiorly meeting the restrictions of fuel cell powertrain aircraft in terms of range and speed requirements and can also economically compete with current jet liners. For more details on Hydrogen aircraft and its effect of aviation transport, readers are referred to [73].

The objective of this investigation is to set a group of cases in the NB and WB class to cover market requirements and carry out preliminary sizing by HYPERION (HYbrid PERformance SimulatION) for a clean sheet design. By using a cost model, the cases were assessed to find the optimum solution in terms of DOC.

Figure 0.6 illustrates the fundamental objective of this work, which is the combination of PAX and design range. In the NB class, the number of seats ranges from 180 to 220, with a design range of 2000 km to 60000 km. For WB cases, the number of seats ranges from 250 to 400, with a design range of 6000 km to 15000 km.

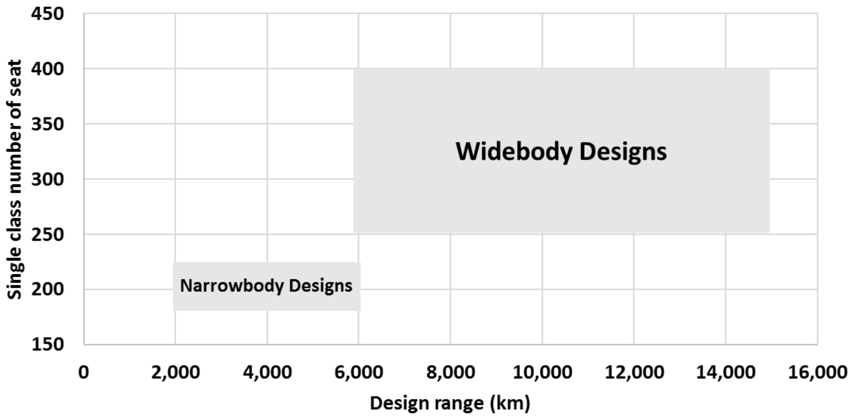

Figure 0.6: The range of cases in terms of PAX and design range evaluated for NB and WB.

Another aim is to identify the effect of fuel price on optimum solutions. Reasonable LH2 price and moderate incremental were assumed, and their influence on DOC was evaluated.

Obtaining the best combination of wing parameters to comply with mission requirements is another aim of these assessments. Wing parameters and operational speed are coupled variables. In this study, wing parameters are taken as the primary variable and optimum cruise speed as the secondary variable.

The real-life flight range of airliners is different from the design range. The ability to serve longer-range flights is a valuable option in terms of operational flexibility for airline operators, but daily flight utilization range is usually a couple of times less than the design range. Hence, DOC is a function of the average stage length. Based on available data, stage length is determined for each class and cost analysis is performed.

Even though LH2 has a higher energy density (MJ/kg) compared to kerosene, its gravity density (kg/m^3) is lower by several times. Nevertheless, LH2 stored at one bar requires four times the volume of kerosene fuel for the same energy amount. Therefore, it leads to a demand for a higher fuel tank volume for LH2. Figure 0.7 shows the relative tank size of LH2 and kerosene for a typical aircraft in the A320 class.

On the other hand, the boiling temperature of -253 °C requires a cryogenic intensive isolated wall tank, and by heat transfer, we have gaseous hydrogen. The fuselage accommodates the tank and gets elongated compared to the kerosene version. This extra part of the fuselage causes an increment in drag and structural weight.

In this level of conceptual design, for simplicity, a one-piece cylindrical tank is assumed to be a suitable solution for carrying the fuel and gases. This concept of tank location is also followed by Airbus in the ZEROe project. However, the FAA requires at least two tanks for redundancy in case one starts to leak, and for other safety reasons [74].

During a flight, as the LH2 is consumed, the center of gravity (c.g.) shifts aft. This may potentially cause c.g. range problems. However, based on the analysis presented in [75], it is determined that in the case of the A320, the c.g. travel remains well within the c.g. envelope. Therefore, the assessment of c.g. travel analysis is skipped.

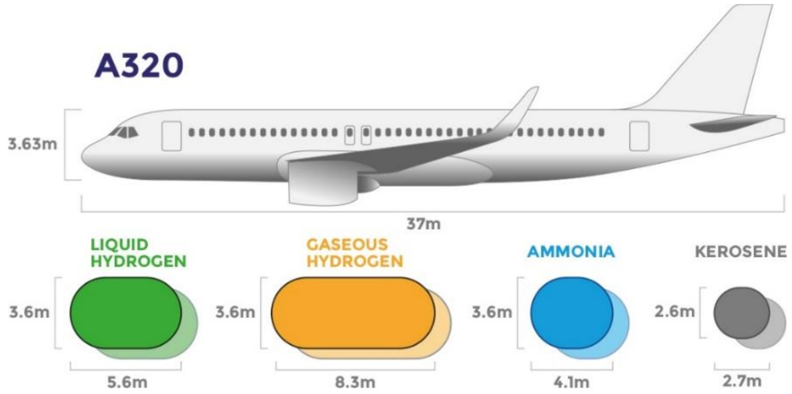

Figure 0.7: Relative tank size for different zero-carbon emission fuels, with kerosene provided for comparison [8].

Furthermore, due to the low weight of fuel, the LH2 design has a much lighter takeoff weight than the kerosene design and requires less wing area to be able to operate from a runway of a given length. The combination of a large fuselage and small wing naturally leads to a lower L/D, which represents aerodynamic efficiency [9].

Regarding to the longer fuselage, the slenderness ratio (fuselage length / fuselage diameter) is higher than that of kerosene aircraft. A higher slenderness ratio creates more flexibility of the fuselage and higher friction drag. This issue is one of the important restriction parameters of LH2 aircraft.

Although the main aim of the project is to find the level of economic compatibility between LH2 and kerosene jetliners, we need enough data about the aircraft, which preliminary sizing provides us in just a few minutes thanks to HYPERION.

Methodology and Terminology

The methodology used in this study follows the classical aircraft design process. Based on a set of performance and mission requirements, an aircraft is preliminarily sized, and a cost model is used with realistic assumptions to obtain DOC parameters.

Figure 0.8 simplifies the classical steps of the design and development process of a jetliner. The complete process is divided into design, manufacturing of a prototype, and testing phases.

Aircraft design encompasses activities that lead to the creation of a new flight vehicle. It starts as a vision and finishes with the bending of metal or cutting of Prepreg cloth for composites according to detailed design drawings. This phase is crucial as all features in the life cycle of an aircraft, both positive and negative, are determined at this point [10].

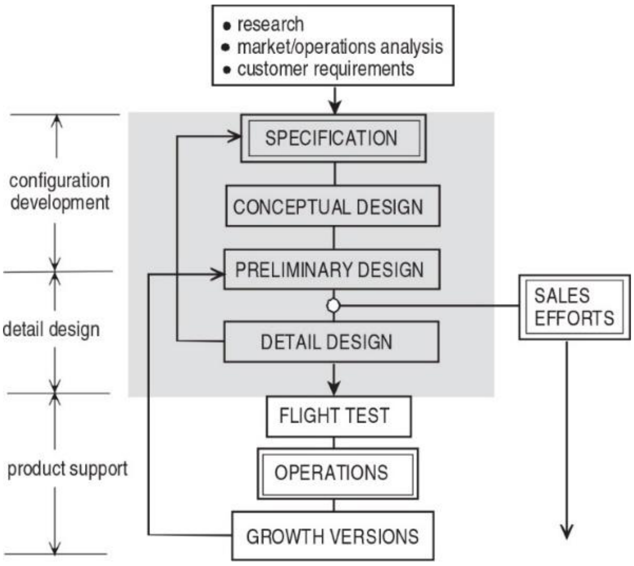
• research
• market/operations analysis
• customer requirements
configuration development
detail design
product support
SPECIFICATION
CONCEPTUAL DESIGN
PRELIMINARY DESIGN
DETAIL DESIGN
FLIGHT TEST
OPERATIONS
GROWTH VERSIONS
SALES EFFORTS

Figure 0.8: Schedule of the civil airplane development process [11].

The aircraft design process is divided into conceptual design, preliminary design, and detail design. These phases are typically organized as depicted in Figure 0.9.

The conceptual design phase, which is most important, determines the feasibility of meeting the requirements, and the design decisions made during this phase drive over 70% of the life cycle cost of the aircraft [10].

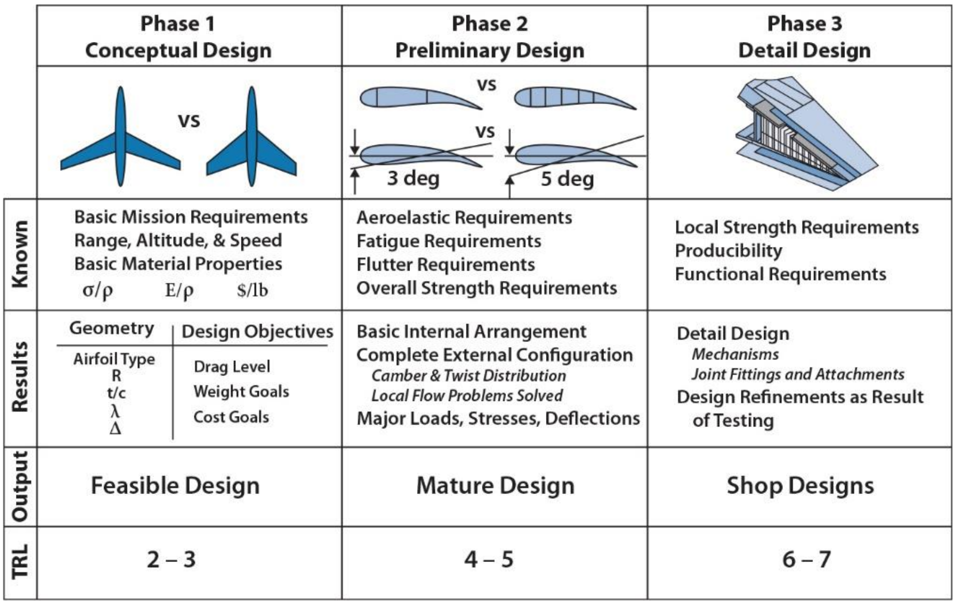

	Phase 1 Conceptual Design	Phase 2 Preliminary Design	Phase 3 Detail Design
	vs	vs vs 3 deg 5 deg	
Known	Basic Mission Requirements Range, Altitude, & Speed Basic Material Properties σ/ρ E/ρ $/lb	Aeroelastic Requirements Fatigue Requirements Flutter Requirements Overall Strength Requirements	Local Strength Requirements Producibility Functional Requirements
Results	Geometry: Airfoil Type R t/c λ Δ Design Objectives: Drag Level Weight Goals Cost Goals	Basic Internal Arrangement Complete External Configuration *Camber & Twist Distribution* *Local Flow Problems Solved* Major Loads, Stresses, Deflections	Detail Design *Mechanisms* *Joint Fittings and Attachments* Design Refinements as Result of Testing
Output	Feasible Design	Mature Design	Shop Designs
TRL	2 – 3	4 – 5	6 – 7

Figure 0.9: The three phases of aircraft design [10].

The conceptual design phase begins with preliminary sizing analysis. Preliminary sizing is the process of numerically determining basic aircraft parameters, such as take-off mass, empty mass, fuel mass, take-off thrust, wing area, wing aspect ratio, maximum required lift coefficient in cruise, takeoff and landing. It has been shown in Figure 0.10 the input for this stage is the mission specification obtained from customer requirements and market demands.

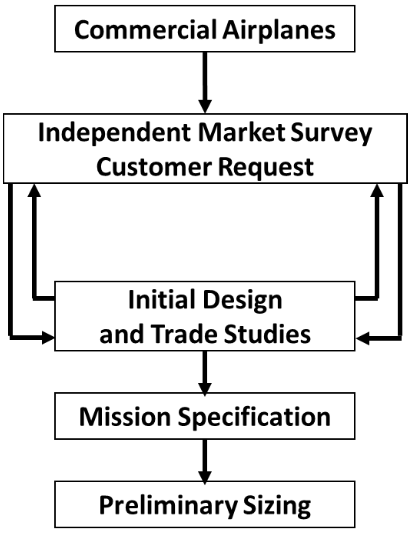

Figure 0.10: Evolution of mission specification and its relation to preliminary sizing [12].

Market survey in terms of demands for the number of PAX and flight range are professional activities that are outside the scope of this project. Therefore, this project is limited to reflecting the results of market analysis from consulting groups specializing in aviation market studies and data released by major passenger aircraft manufacturers. These data have been used to establish cases that will be analyzed in the preliminary sizing.

To extract performance requirements, assumptions were made based on existing aircraft products. The Airbus A320 was used as a reference for NB aircraft, and the B787-8 was used for WB aircraft to determine performance requirements such as takeoff and landing run, cruise and maximum Mach number, rate of climb, etc.

According to the classification presented by [11], NB and WB aircraft are categorized as follows:

- Narrow body jet aircraft seating between 110 and 220 passengers on a single-aisle single deck. This class is mostly used for short and medium distances.
- Wide body jet aircraft seating at least 220 passengers on one or two twin-aisle passenger decks. WB aircraft serve long-haul flights.

Preliminary sizing was conducted using HYPERION design tools which developed by the Department of Aerospace Science and Technology of Politecnico di Milano. Inputs include range, payload mass, engine parameters, lift coefficients, increment drag coefficient due to landing gear and flap, Oswald efficiency, wing parameters, mission parameters, and certification standards. The computation tools provide thrust loading, wing loading, sizing matrix, takeoff mass, fuel mass, operating empty mass, and other constituent mass items of operating empty mass. It also simulates flight missions and provides time history of flight parameters. For more details on HYPERION, readers are referred to [13] and [14].

The findings of preliminary sizing are highly dependent on the assumptions regarding aerodynamic coefficients. The dominant assumption is that Oswald factor, lift and drag coefficients are in line with those of current aircraft in production.

Hydrogen aircraft will require significant research and development, investments, and accompanying regulation to ensure safety. Several technological advancements need to occur in the fields of aircraft production, maintenance, and operational infrastructure. Compared to kerosene aircraft, LH2 aircraft have different costs for fuel and related infrastructure, aircraft ownership, operations, and maintenance.

Regarding the aircraft platform, the increased cost is mainly due to the expenses associated with the LH2 tank structure integrated into the fuselage, the heightened complexity of fuel distribution, increased propulsion costs, and larger aircraft size.

Total maintenance costs for LH2 aircraft might rise due to the larger airframe and hydrogen tanks, which may require checks that are more frequent. Maintenance costs for the propulsion system could also increase due to higher combustion temperatures.

Fuel costs encompass all expenses related to fuel production and the necessary infrastructure for distribution, storage, and refueling of airplanes. However, by 2050, LH2 fuel prices are expected to approach those of kerosene due to higher demand for LH2 and improvements in production costs [73].

Handling and safety regulations would need to be re-evaluated for LH2 use in aviation, given its radically different properties compared to conventional jet fuel. Fuel companies, airports, airplane manufacturers, and airlines would also need to collaborate to ensure infrastructure development and safe and economically affordable passenger transfer.

Establishing parallel refueling infrastructures at airports and modifying parking stands to accommodate larger aircraft lead to increased operational costs. Although these changes are cause of increase airport fees, but the exact effects on costs are uncertain and difficult to estimate at present.

Additionally, LH2 refueling considerations and procedures would result in longer turnaround times and consequently fewer flight cycles. This would particularly affect crew costs, potentially increasing DOC and reducing productivity.

All of the aforementioned issues necessitate radical changes in current cost models. A reliable cost method specifically designed for hydrogen aviation transport is currently unavailable, to the best knowledge of the author. However, the aim of the project is cost optimization by trading off various variable parameters. It is reasonable to solve the problem without disrupting the overall parameters by relying on existing cost models, as the optimum point is not dependent on the exact value of FoM.

Outputs of the sizing are inputs of cost assessment. The cost assessment is performed with an accepted method in DOC estimation. It is based on modified DAPCA IV model [15]. The model has been discussed in chapter two. In addition to the sizing output, assumptions on operational cost have remarkable influence of cost output which are closely connected to how airline business model is. In addition, DOC is close couple to block hour. Block hour is the time between closing aircraft doors at origin airport to opening at destination airport.

Finally, selection of the best case upon the best values of Figures of Merit (FoM). Relay on definition by [Nicolai], “The FoM is similar to a requirement except that it is initially known only to the customer and is not overtly specified. The FoM is important to the customer and will be used as a “tie breaker” in selecting the winning design. It is often said that meeting the requirements gets you invited to the dance, but meeting the FoM gets you out on the dance floor”. FoMs in this study are CASK, DOC/BH, block fuel and MTOM.

Background of LH2 Burn Aircraft

The meaning of LH2 burn aircraft is to use LH2 as fuel in a jet engine. The history of LH2 burning aircraft dates back to the 1950s when a modified Martin B-57B (Figure 0.11) successfully made the first flight of a hydrogen-fueled jet aircraft in 1957. This aircraft was powered by a specially adapted Wright J65 engine and was developed by NASA for the U.S. Air Force to research the potential benefits of hydrogen fuel for high-altitude aircraft [16].

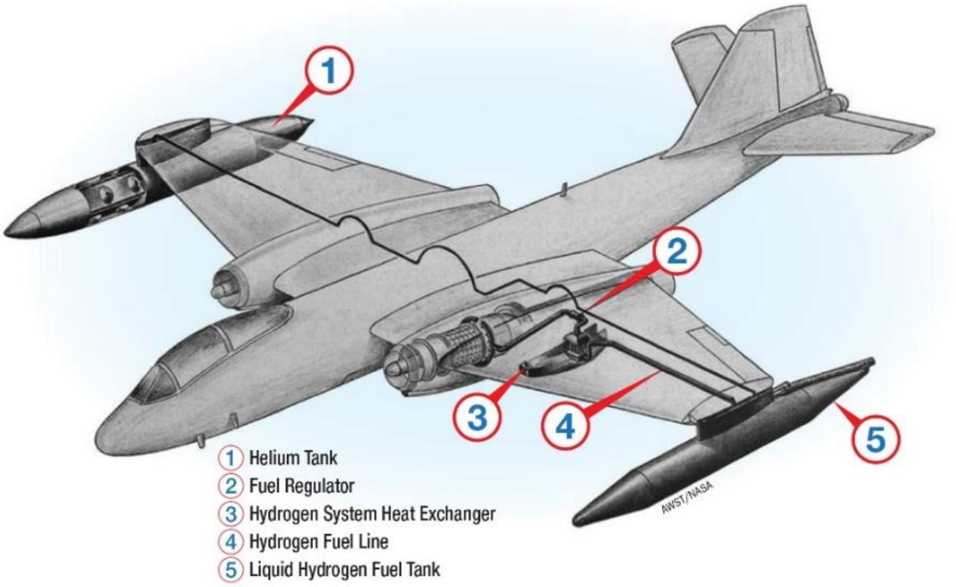
1
2
3
4
5
1 Helium Tank
2 Fuel Regulator
3 Hydrogen System Heat Exchanger
4 Hydrogen Fuel Line
5 Liquid Hydrogen Fuel Tank
AWST/NASA

Figure 0.11: Project Bee, Hydrogen powered B-57B [16].

In 1973, NASA sponsored a series of studies conducted by Lockheed to further explore the potential of hydrogen in aircraft. These studies aimed to assess the feasibility of using hydrogen fuel in commercial transport aircraft and determine its advantages and disadvantages compared to conventional Jet A1 fuel. The studies also aimed to identify any problems and technological requirements associated with the use of LH2 and outline a roadmap for the development of the necessary technology. Two classes of transport aircraft, supersonic (Figure 0.12) and subsonic (Figure 0.13), were studied during this time [9].

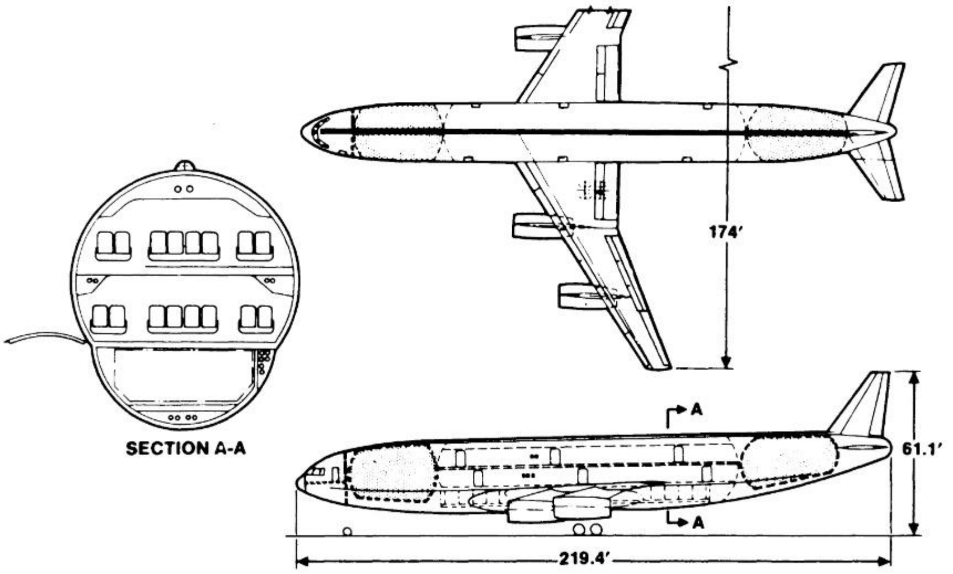
174′
SECTION A-A
A
A
61.1′
219.4′

Figure 0.12: General arrangement LH2-fueled subsonic passenger, 400 PAX, 5500 nm, M 0.85. [9].

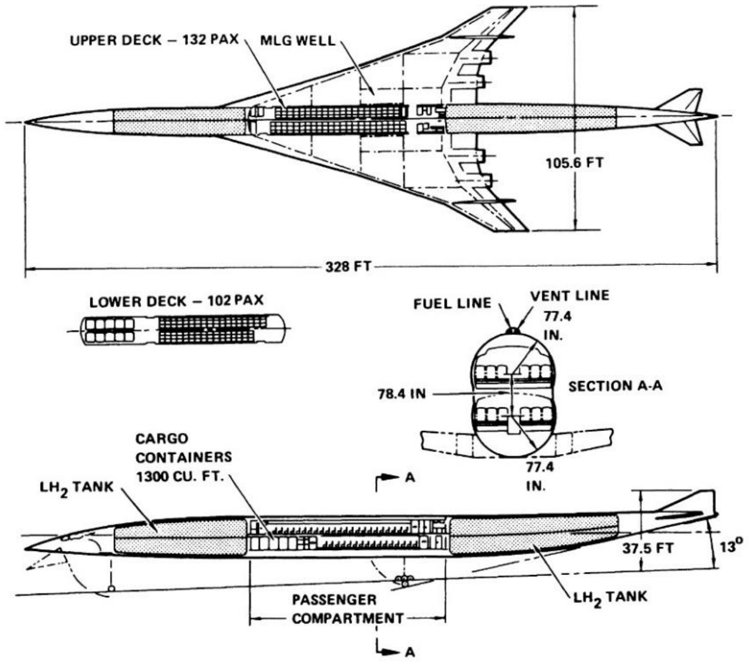
UPPER DECK – 132 PAX
MLG WELL
105.6 FT
328 FT
LOWER DECK – 102 PAX
FUEL LINE
VENT LINE
77.4 IN.
78.4 IN
SECTION A-A
77.4 IN.
CARGO CONTAINERS 1300 CU. FT.
LH2 TANK
A
37.5 FT
13°
PASSENGER COMPARTMENT
LH2 TANK
A

Figure 0.13: General arrangement LH2-fueled supersonic passenger, 234 PAX, 4200 nm, M 2.7 [9].

In 1988, Tupolev design bureau flew a modified Tu-154 aircraft with one engine burning hydrogen. This aircraft, known as the Tu-155 (Figure 0.14), was equipped with a cryogenic fuselage tank and served as an alternative fuel testbed. The project also studied the feasibility of using liquid hydrogen and liquid natural gas as fuels. The Tu-155 recorded approximately 100 flight hours, but only a few hours were tested using LH2 fuel, with methane fuel being used for the rest. The Tu-155 demonstrated that it is feasible to use liquefied gas as a fuel, but its fuel system was deemed too heavy to be practical [17].

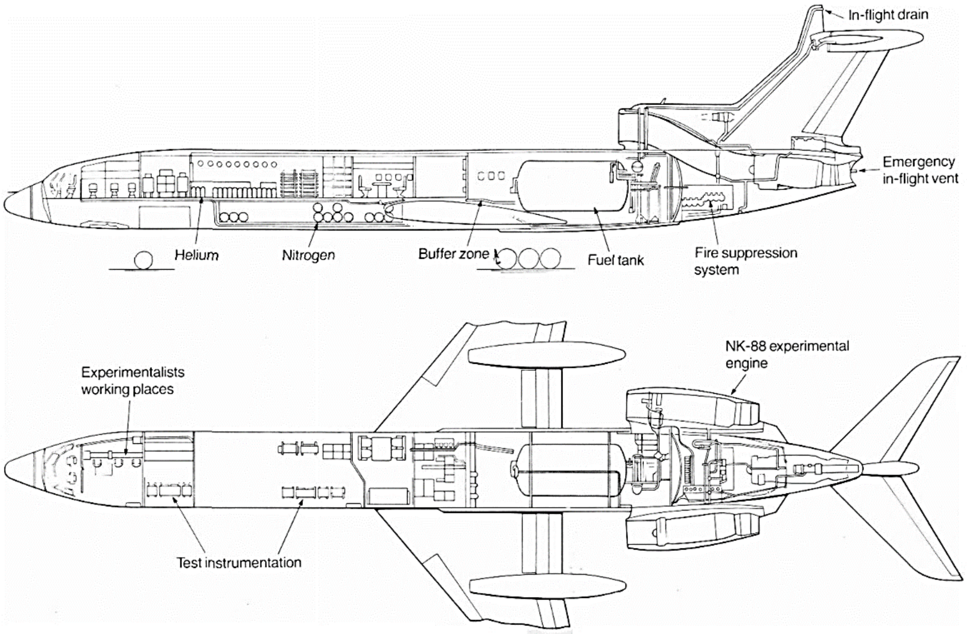
In-flight drain
Emergency in-flight vent
Helium
Nitrogen
Buffer zone
Fuel tank
Fire suppression system
NK-88 experimental engine
Experimentalists working places
Test instrumentation

Figure 0.14: Tu-155 inboard profile [18].

Between 1990 and 1993, Deutsche Airbus and Tupolev design bureau collaborated on a study to investigate the feasibility of converting airliners to operate on liquid methane and hydrogen. This work contributed to the development of a derivative gas-fueled Airbus A300 demonstrator (Figure 0.15).

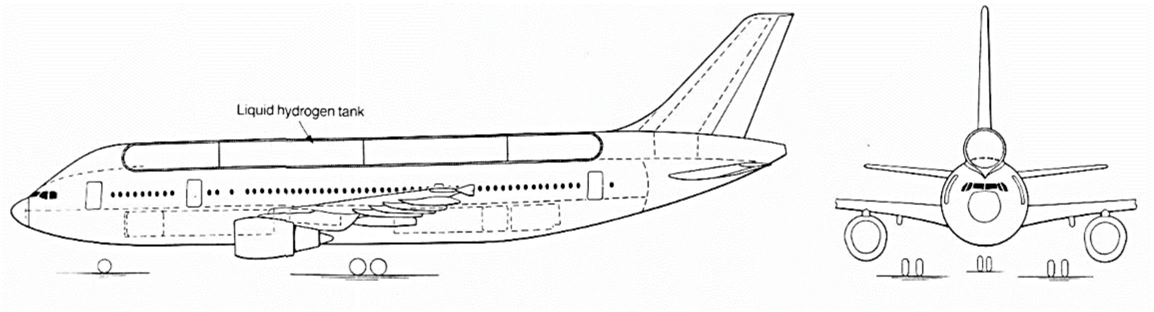
Liquid hydrogen tank

Figure 0.15: Hydrogen fueled Airbus A300 [19].

In 2000, the European Commission established the CRYOPLANE program under the leadership of Airbus. The aim of this program was to conduct a comprehensive system analysis to provide a decision basis for future technology development. The study covered all relevant technical, environmental, and strategic aspects related to the development and introduction of liquid hydrogen as an aviation fuel. Various aircraft types, ranging from regional turboprops to very large long-range jet aircraft with different tank locations, were studied during the project. Figure 0.16 shown its concept for short and medium range aircraft [20].

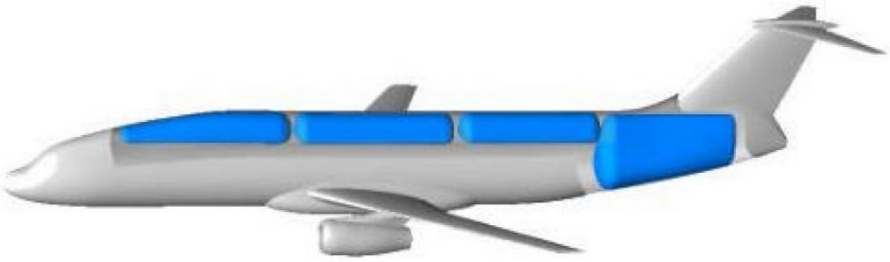

Figure 0.16: CRYOPLANE concept for short and medium range aircraft [20].

In 2018, the European Commission launched the EnableH2 project under the Horizon 2020 program, which was coordinated by Cranfield University. This project included experimental and analytical work on combustor design, fuel and heat management systems. The project also implemented technology studies for wing and tube configurations, as well as blended wing body configurations [21].

The UK government-funded the FlyZero project in 2018 to accelerate the introduction of zero-emission commercial aircraft. This project was led by the Aerospace Technology Institute (ATI).

After developing three aircraft concepts (Figure 0.17), including a regional airliner (75 PAX, 800 nm), a narrowbody (180 PAX, 2,400 nm), and a midsize widebody (280 PAX, 5,250 nm), the study concluded that focusing on the development of a Boeing 767-class aircraft would make the most significant contribution to achieving net-zero carbon emissions in aviation by 2050.

The final FlyZero concept report stated that hydrogen-powered aircraft could be competitive with SAF powered aircraft using technology available by 2030. The study also showed that hydrogen-powered aircraft have the potential to address 100% of short-haul flights and 93% of long-haul flights [22].

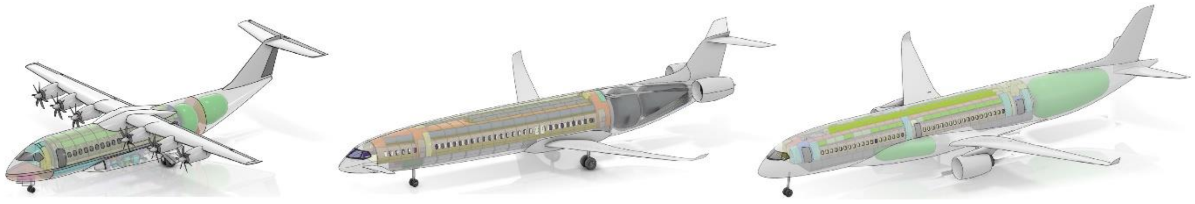

Figure 0.17: ATI concepts for FlyZero[1] [23].

In September 2020, Airbus presented three concept (Figure 0.18) studies for liquid hydrogen-powered aircraft. These concepts included a regional turboprop, a narrowbody in the class of A320, and a blended wing body (BWB) design. The regional turboprop would accommodate 100 passengers and have a range of 1,000 nm, while the narrowbody would accommodate 120-200 passengers and have a range of 2,000 nm with a cruise speed of Mach 0.78. The conventional tube and wing layout with a large portion of the aft fuselage dedicated to hydrogen storage were targeted for the first two concepts.

---

[1] In the figure, the aircraft are not the same scale.

In those preliminary studies, Airbus has concluded that of the various options, liquid hydrogen combustion is the most realistic technology for producing a carbon-neutral aircraft. Although SAF is a low-risk and affordable solution for long-haul flying [24].

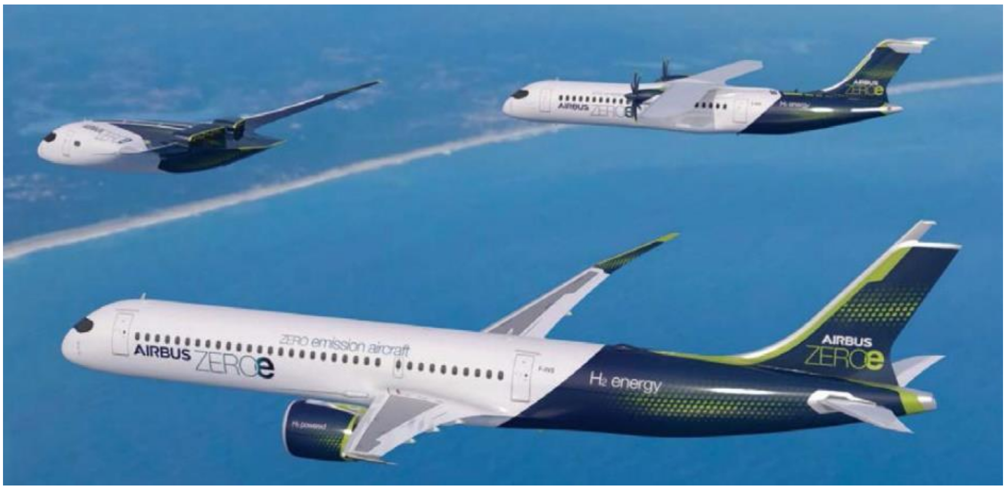

Figure 0.18: Airbus concepts for low carbo aviation [24].

Chapters Overview

Following this introduction to the motivation, objectives, methodology, and a brief review of the history of LH2 burning aircraft projects, the following sections are part of the work:

Chapter one provides a summary of traffic demand vision, current and future market trends in the NB and WB aircraft classes. It discusses average utilization in terms of passenger and range, as well as performance requirements for each aircraft class.

Chapter two presents the cost model used in this study. It includes a set of assumptions, methodology, and validation study on the A321 aircraft.

Chapter three introduces the framework of the design study and trade-off structure. It provides formulation, assumptions, and a short description of the technical background of the methods considered for preliminary sizing. In addition, to verification of the method a case study based on A320 is presented.

Chapter four and five explain analysis and trade off results for NB and WB cases consequently. Both chapters close with the optimum solution for each class.

Chapter six provides a summary and offers possible future developments of the thesis.

The Appendix A and B contain some trends and the output of HYPERION for NB and WB optimum solutions.

1 Market Study and Performance Requirements

Market research and analysis, including determining passenger demand and flight range, are essential components of any development project. These activities help identifying the specific requirements and specifications for a new product. The primary goal of a commercial aircraft program is to generate sufficient profit for both the manufacturing company and the operator.

Reliable forecasts about the demand and requirements for new aircraft are obtained from continuous market monitoring and close negotiations with major airline operators. Through a conceptual design activity based on market requirements, the management board of the company is able to make decisions about kicking off a new project.

In this case, environmental issues have led to increasing pressure from governments and communities, forcing aircraft manufacturer to develop net zero carbon aircraft. Hence, profitable products guarantee the sustainability of the business.

In this chapter, in addition to reviewing the current fleet in service and its activity, market forecasts and average utilization of passenger aircraft are reported.

1.1. Traffic Demand

Presently, the demand for passenger traffic is approximately 10 trillion RPK. Over the next twenty years, it is projected to increase to 20 trillion RPK (Figure 1.1). The growth in demand is closely tied to Gross Domestic Product (GDP), with air travel typically expanding at twice the rate of GDP in emerging economies and aligning more closely with GDP growth in advanced countries (Figure 1.2) [6].

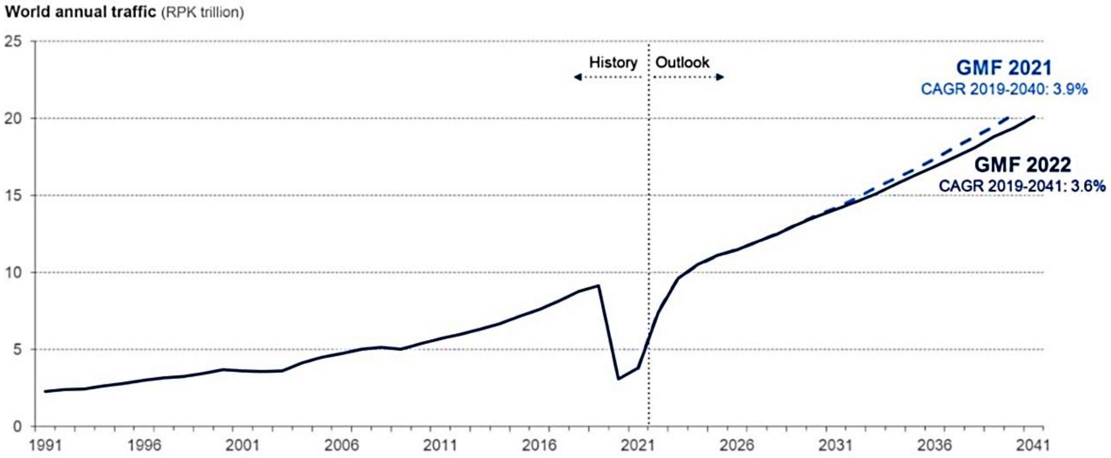

Figure 1.1: World annual air traffic [25][2].

GDP growth is determined by two main factors: population growth and productivity growth. It is anticipated that the GDP will be lower compared to the previous decade due to the decrease in China's GDP and its population reduction.

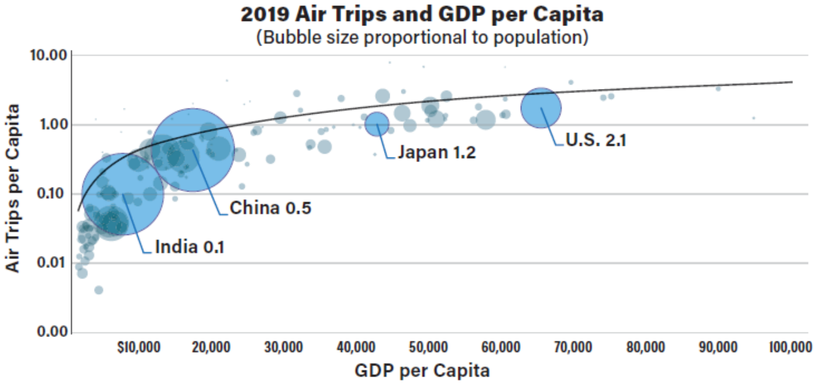

Figure 1.2: Trend of GDP vs air trip [26].

The days of consistent and easy 5% air travel growth are no longer feasible. Two significant factors influencing traffic growth are the lower global GDP and decarbonization policies [6]. The twenty-year forecast indicates that the world GDP will remain at a long-term average of 2.6% [27].

Looking ahead, the vision for the next twenty years suggests that the demand for passenger traffic will grow annually by 3.6% [25] to 3.8%. Cargo traffic is expected to grow at a rate of 4.1% due to a 2.9% increase in international trade, while the jet fleet is projected to expand by 2.8% [27]. In summary, airline fleets are expected to nearly double in size over the next 20 years to accommodate the doubling of air passenger demand.

---

[2] The break in the chart is due to pandemic.

1.2. Current Fleet

In 2019 (before the pandemic), the number of airplanes in service for airlines was 25,900, with NB aircraft making up 64% of the total and WB aircraft making up 18% (Figure 1.3). The major players in the NB class are the B737 and A320 families, while in the WB class, the major aircraft are the A330, B777, and B787 (Figure 1.4).

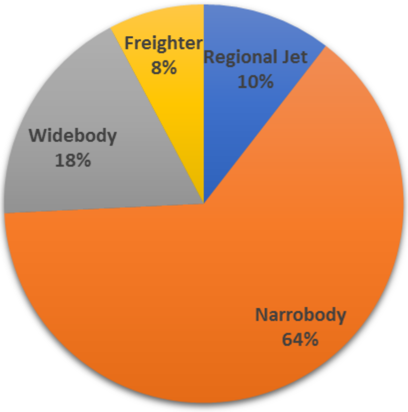

Figure 1.3: World 2019 fleet share [27].

However, by the beginning of 2020, the fleet had dropped to 22,880 aircraft in-service, a decrease of 12% compared to 2019 [25]. This decline was due to the COVID-19 pandemic, which caused a severe crisis in the aviation industry ever faced. Aircraft deliveries fell by 35% in 2020, and air travel demand dropped by 66%.

During the period of 2020 to 2022, there was a significant reduction in WB aircraft due to grounded fleets, which need to additional cost to running service and a lack of sufficient market demand [27] [28].

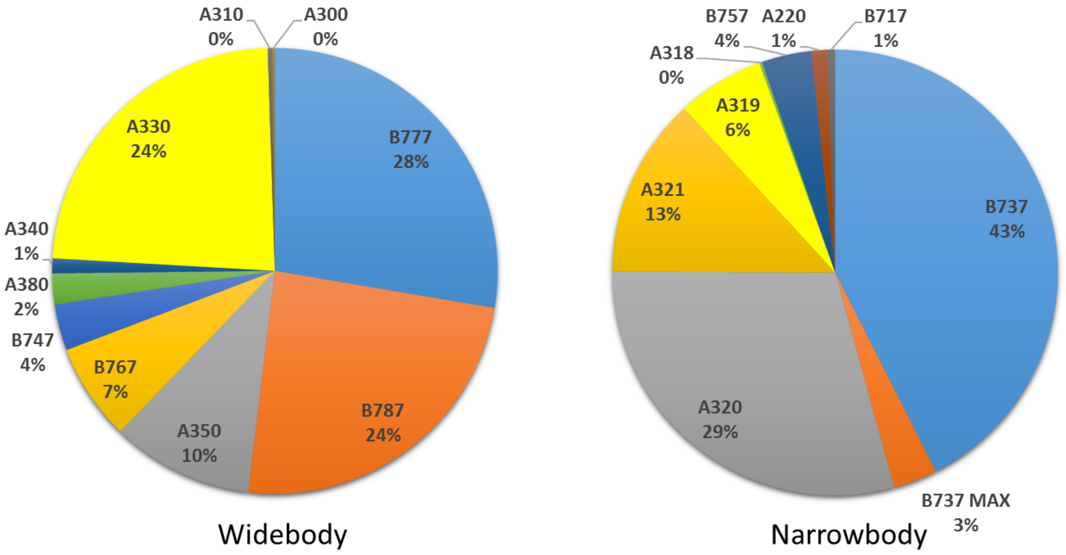

Figure 1.4: Current fleet share by type [28].

1.3. Market Outlook

Looking ahead to the next twenty years, it is forecasted that the fleet will reach 47,000 aircraft by 2041 [25] [27]. During this period, approximately 40,000 aircraft will be delivered. Airbus and Boeing are expected to deliver 80% of these aircraft [28]. New NB deliveries will account for 75% of total deliveries, while WB deliveries will make up 20% of the total.

The fleet will growth 50%. The 80% of current fleet will retired and only 20% enough as advance as to stay in service. In Figure 1.5 the share of demands by 2041 are plotted [6].

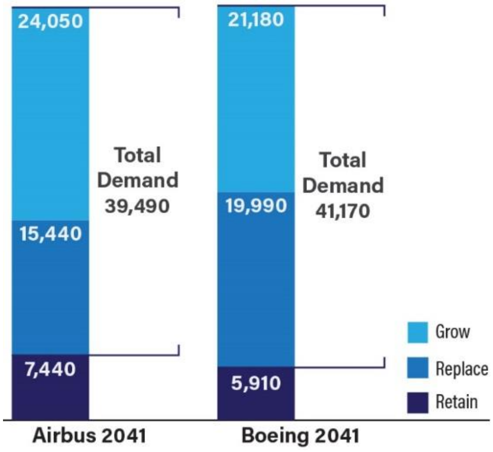

Figure 1.5: Demand for new aircraft by 2041 [6].

The backlog list of major manufacturers shows that orders are primarily focused on new generation NB with capacities ranging from 150 to 200+ seats. These aircraft offer improved passenger number, range and fuel efficiency. As of the beginning of 2023, the class accounted for 91% of Airbus orders [29] and 79% of Boeing orders [30]. Flexible point-to-point routes, made possible by the growing range capabilities of new NB, are favored by the market.

However, some airline operators believe that future growth prospects depend on New Midsize Airplanes (NMA). The NMA would fill the gap between NB and WB aircraft and would be used for up gauging from NB routes to use a new 225 to 265 seat aircraft with 4,000 to 5,000 nm range to create new city-pair opportunities beyond their current route networks and as replacements for current aircraft in the class. Airbus A321neo orders strongly dominate the backlog picture (Figure 1.6) for all jets in the 180 to 250 seat [31].

However, WB aircraft have faced multiple crises in the past. The demand for hub-and-spoke networks by this class is declining, and WB was already experiencing overcapacity with larger jetliners before the pandemic. Furthermore, the demand for

WB jets heavily relies on international air traffic, which was severely impacted by the pandemic and is taking longer to recover. The pandemic has also accelerated the preference for NB aircraft, particularly the A321neo, for international routes. In summary, the market trend for most of this decade indicates that the market share value for NB to WB aircraft will be 70 - 30 [32].

The increasing role of third-party finance has exacerbated the problem for WB aircraft. This is because lessors and other financiers prefer to finance NB aircraft due to their much larger client base [32].

The crisis faced by the WB class is not applicable to the entire category. Smaller WB with increased range and improved economics have enabled airlines to operate profitably on long-haul city pairs that were previously not feasible for nonstop flights. In this class, small WB aircraft make up two-thirds of the market share, while medium-sized of WB account for one-third [27].

The Boeing 787 and Airbus A350 will continue to play a central role in the $1.1 trillion the WB market, with the mid-sized 250-300 seaters accounting for almost 70% of the delivery value in the sector. The remaining 30% will be competed for by the A350-1000 and B777-9 in the highest capacity markets (Figure 1.7) [28].

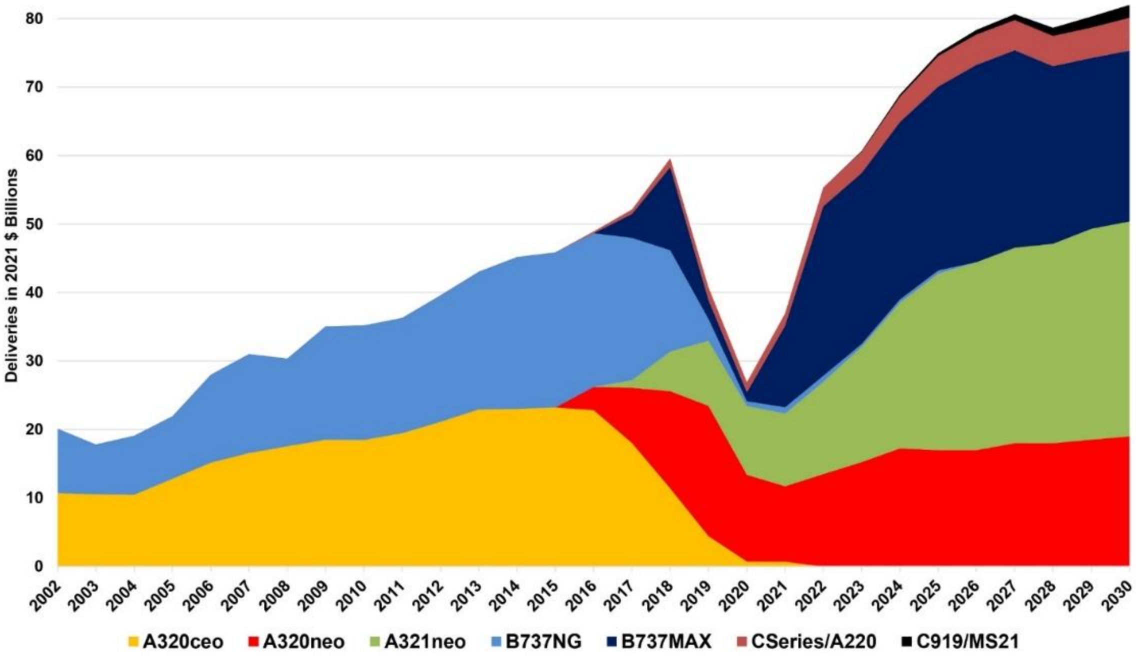

Figure 1.6: Forecast of NB aircraft Orders [33].

In conclusion, the most favorable airliners with respect to orders in 2040 will be the A321neo in the NB class and small WB aircraft with 300 passengers. These choices are driven by the market demand for these types of aircraft.

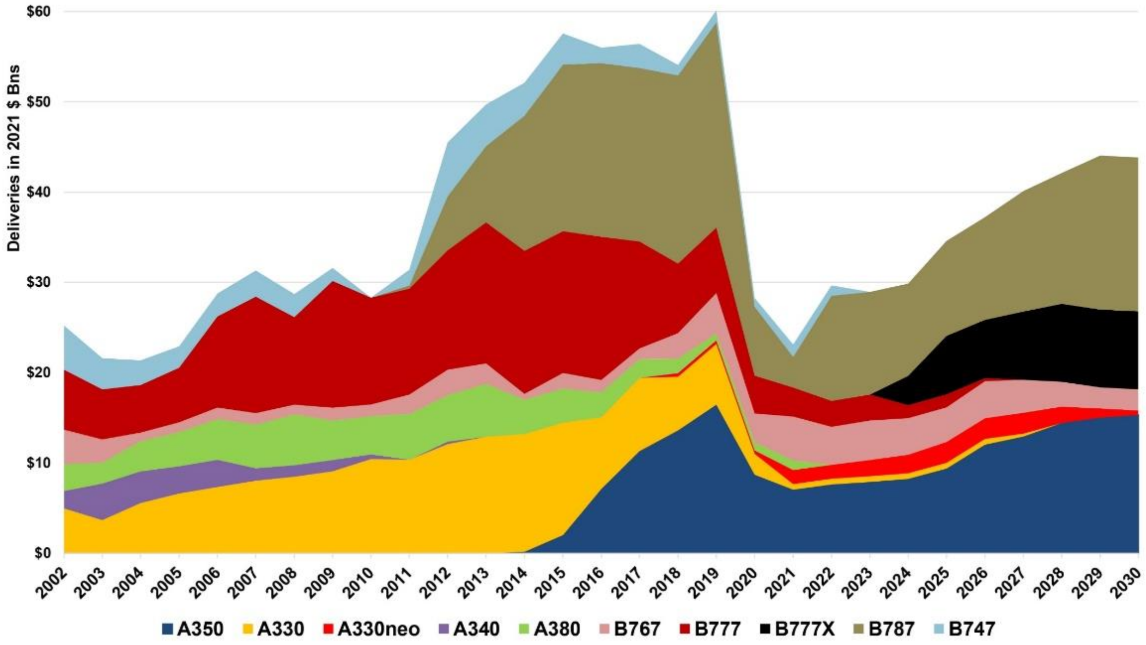

Figure 1.7: Forecast of WB aircraft Orders [33].

1.4. Average Utilization

The aim of this part of work is to gain insight into how NB and WB aircraft are used in passenger transport. It is important to consider the average utilization and reasonable range when selecting optimum parameters for aircraft. Assuming the maximum range for finding optimum cost parameters is not a sensible idea.

The average route length based on the top 50 busiest global air routes (domestic and international) is 1,123 km [34]. Airliners use different classes of aircraft for different average stage lengths. Figure 1.8 extracted based on 30 busiest rout, divided to short haul, medium haul and long haul with respect of world's parts [35]. Short-haul flights are typically less than 1,500 km with average 742 km, medium-haul flights are between 1,500 km and 4,000 km with average 2,128 km, and long-haul flights are over 4,000 km with average 5,171 km [3]. NB aircraft are commonly used for short and medium-haul flights, while WB aircraft are used for long-haul flights.

---

[3] This definition used in this work is matched by Eurocontrol definition of flight range.

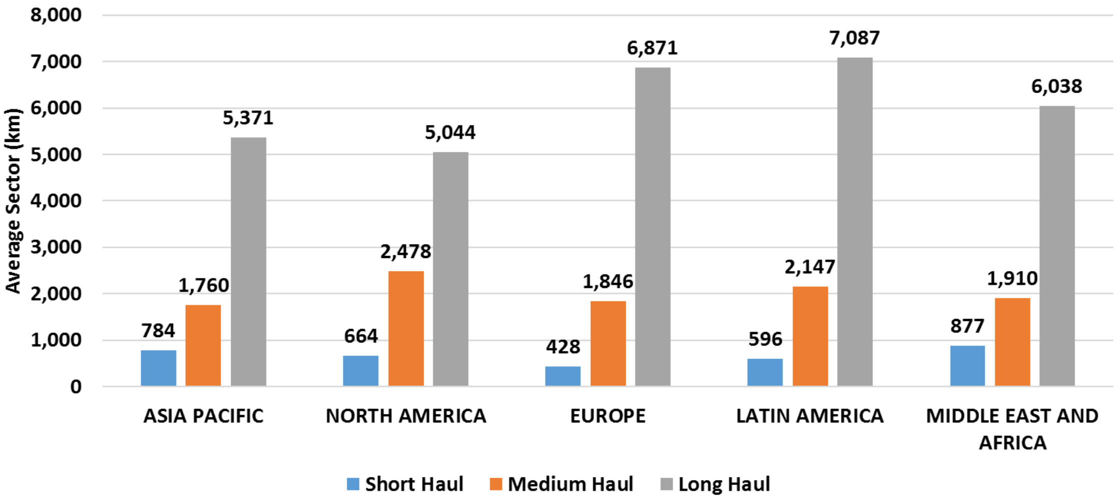

Figure 1.8: Average flight stage divided in short, medium and long haul.

In all continents, short-haul sectors are less than 1,000 km, medium-haul sectors are less than 2,500 km, and the average length of long-haul flights is not greater than 7,100 km.

Furthermore, the stage length is proportional to the flight cycle. Decreasing the range and increasing cruise speed can result in higher flight cycles. It shown by Figure 1.9. Which means more passengers transported by the airline and potentially higher profits.

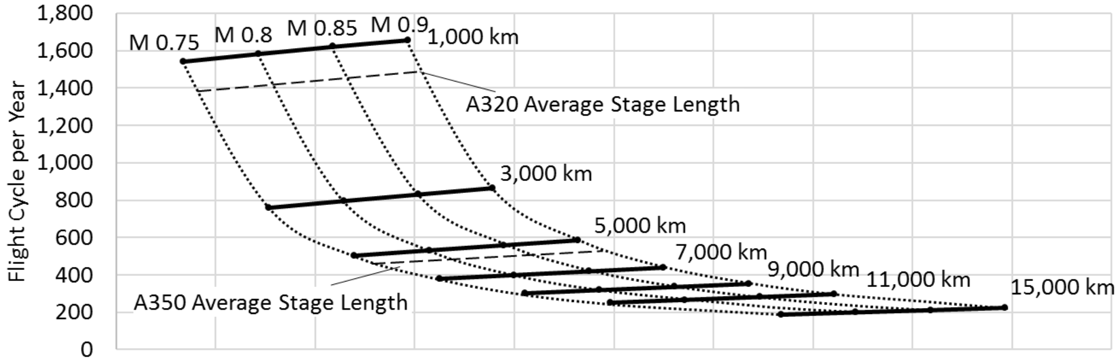

Figure 1.9: Relation between stage length and cruise speed with flight cycle.

It would be advantageous to have a best estimate of real-life aircraft in terms of stage length or flight duration and number of passengers for preliminary sizing. This would provide a more efficient concept in terms of profitability. For example, Airbus planned the A320 for a 25-year design service life with 48,000 cycles or 60,000 hours. However, based on airline experience, the actual average flight duration was 1.82 hours. Airbus adjusted the trade cycles to 37,500 cycles or 80,000 hours based on usage [36].

In the reference [37], the results of an extended study on seat-range density are highlighted. In the thesis, the statistical data were used to find a realistic vision for the utilization of NB and WB aircraft.

1.4.1. NB Utilization

The utilization of NB aircraft is typically up to 4,000 km, depending on the type of aircraft. The major sector utilization of the B737 and A320 are 1,100 km and 1,480 km respectively, with an average of 1,300 km (Figure 1.10) [38]. Therefore, a cost study based on the average utilization of NB aircraft with a 1,300 km stage length is reasonable.

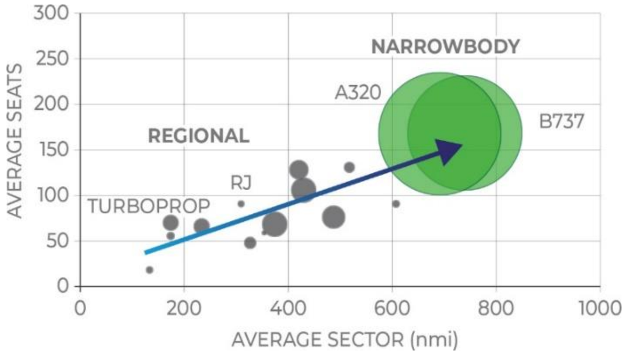

Figure 1.10: Relationship between aircraft size and sector distance in NB [38].

1.4.2. WB Utilization

For WB aircraft, the longest sectors are between 13,500 km and 15,350 km based on the top 10 longest air routes. However, these routes contribute to a tiny portion of WB flight services. WB aircraft mostly cover sectors up to 12,000 km.

The average sectors of the B787 and A350 are 5,230 km and 5,550 km, respectively (Figure 1.11). Approximately 85% of A350-900 flights are up to 9,300 km [39]. Therefore, a logical reference for cost study of WB aircraft would be a 5,550 km stage length.

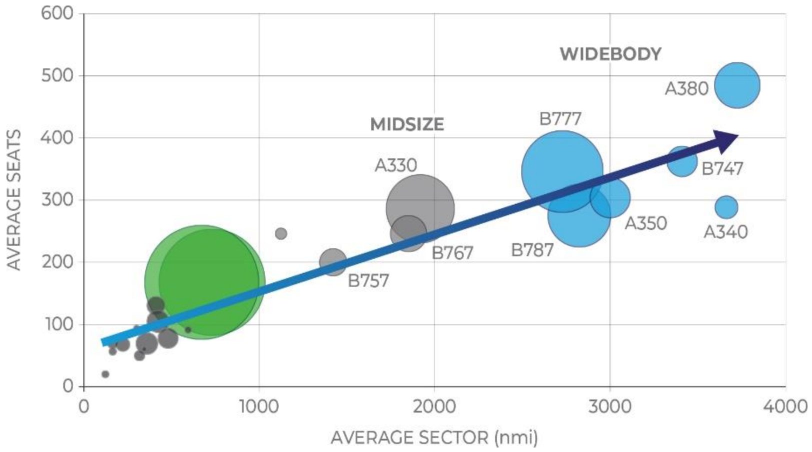

Figure 1.11: Relationship between aircraft size and sector distance in WB [38].

1.5. Performance Requirements

The design of an aircraft is a delicate balance between various competing requirements, so the best answer is the right answer and it is crucial to find the optimal solution. Performance requirements play a significant role in the design process, and they serve as the primary input. In this step of work based on performance characteristics of major aircraft in service a set of performance parameters have been set.

To ensure the success of next-generation LH2 airliners, it is essential to surpass the current market leaders such as the B787 and A320neo families while also bridging the gap between NB and WB aircraft. Without competitive performance characteristics, these new aircraft will not attract market attention. Therefore, it is logical to define the parameters as closely as possible to those of the existing top players.

1.5.1. NB Performance Requirements

Table 1.1 presents some important performance parameters of major airliners in the NB class. A range of requirements has been set in Table 1.3 that align with the values of other NB aircraft. In Chapter 4, these parameters are further discussed and traded off against values for the number of passengers and range proportion.

1.5.2. WB Performance Requirements

Similarly, Table 1.2 provides the parameters for the most favorable WB aircraft currently in service. As with the NB class, a set of performance parameters has been defined in Table 1.3. For certain parameters mentioned as To Be Determined (TBD), their values will be determined through design trade-offs discussed in Chapter 5.

Table 1.1: Selected performance parameters of NB aircraft [40].

Parameters	A320-200	A320neo	A321-100	A321neo	B737-700	B737 MAX8
Approach Speed (km/hr) *	252	252	268	271	241	264
Cruise Mach Number	0.78	0.78	0.78	0.78	0.785	N/A
Max Cruise Mach Number	0.82	0.82	0.82	0.82	0.82	N/A
ROC Max (ft/min)	2,500	2,500	2,500	N/A	N/A	N/A
Takeoff Distance (ft)	5,730	5,600	7,350	6,310	5,580	7,000
Landing Distance (ft)	4,890	4,890	5,500	5,130	4,950	5,000
Range (km)	3,610	3,650	2,355	4,460	5,110	6,130
Max PAX Number	186	186	230	239	149	189
Number of Abreast	6	6	6	6	6	6
*** Estimated**						
Approach Speed @ MLM						
Stall Speed @ Landing configuration, MLM						
ROC Max @ S/L						
Takeoff distance @ MTOM, S/L, ISA+15 °C						
Landing Distance @ MLM, S/L, ISA						
Range @ Max PAX number						
Max PAX number @ single class or Max certified						

Table 1.2: Selected performance parameters of WB aircraft [40].

Parameters	A330-200	A350-900	B787-8	B777-200
Approach Speed (km/hr) *	250	259	N/A	248
Cruise Mach Number	0.82	0.85	0.85	0.84
Max Cruise Mach Number	0.86	0.89	0.9	N/A
ROC Max (ft/min) @ S/L	N/A	N/A	N/A	N/A
Takeoff Distance (ft)	8,300	9,070	8,950	8,430
Landing Distance (ft)	5,750	6,500	5,360	5,100
Range (km)	10,370	15,030	12,020	12,730
Max PAX Number	406	343	359	440
Number of Abreast	8	9	9	10
*** Estimated**				
Approach Speed @ MLM				
Stall Speed @ Landing configuration, MLM				
Takeoff distance @ MTOM, S/L, ISA+15 °C				
Landing Distance @ MLM, S/L, ISA				
Range @ Max PAX number				
Max PAX number @ single class or Max certified				

Table 1.3: Performance parameters aimed for LH2 NB and LH2 WB aircraft.

Parameters	NB LH2	WB LH2
Approach Speed (km/hr) *	250	277
Cruise Mach Number	TBD	TBD
Max Cruise Mach Number	TBD	TBD
ROC Max (ft/min) @ S/L	2,500	2,500
Takeoff Distance (ft)	7,000	8,500
Landing Distance (ft)	5,000	6,500
Range (km)	TBD	TBD
Max PAX Number	TBD	TBD
Number of Abreast	6	TBD
*** Estimated**		
Approach Speed @ MLM		
Stall Speed @ Landing configuration, MLM		
Takeoff distance @ MTOM, S/L, ISA+15 °C		
Landing Distance @ MLM, S/L, ISA		
Range @ Max PAX number		
Max PAX number @ single class or Max certified		

2 Cost Model

This section provides a summary of the methodology used to assess aircraft costs at the conceptual design level. This method is recommended by [41] and [10] and has been calibrated using current aircraft operation data.

Cost estimation during conceptual design is largely based on statistics, but many assumptions have a significant influence on the results. For a detailed description of the methodology and assumptions, please refer to [41] and [15].

One crucial aspect of any cost analysis is determining the fiscal base year. Due to inflation, the value of actual dollars spent in each year of the program, past, present, and future, differs. That is why constant-year dollars are used as a reference in cost estimation and project planning. In this study, 2020 has been selected as the basic fiscal year.

The life cycle cost of a commercial aircraft, from concept to disposal, includes Research Development, Test, and Evaluation (RDT&E) costs, Acquisition (ACQ) costs, and operations costs.

RDT&E costs cover the entire cost of basic research to advanced development efforts required to mature technologies and engineering, as well as the development and fabrication activities that lead to prototype samples and flight tests for performance improvement and certification by a type certification of new aircraft.

The ACQ cost includes the cumulative cost of Q samples of aircraft, which consists of engineering, tooling, quality control, labor and material costs, as well as expenses for installed items such as engines, APU, avionics, etc.

The cost of one flight is divided into direct operating costs (DOC) and Indirect Operating Costs (IOC). DOC includes all expenses that must be paid for the flight, including fuel, ownership, maintenance, insurance, airport fees, navigation costs, and crew wages. IOC includes airline running costs such as general administration costs, facility expenses, ticketing and promotion expenses, and taxes. The cost of airline operations strongly depends on the business model. Roughly, the IOC to DOC proportion is 30 - 70. In the design for cost, we only consider DOC.

Aircraft companies recover RDT&E and ACQ costs through a fair profit when selling the aircraft. Therefore, RDT&E and ACQ costs are included in the ownership cost, which is a share of DOC.

2.1. DOC

In this section, we will discuss the different cost components of DOC that, when aggregated, compute the cost of one flight. In [15], some of the DOC methods were reviewed, and one adopted method was presented and used for the research objective. Figure 2.1 summarizes the major components of DOC.

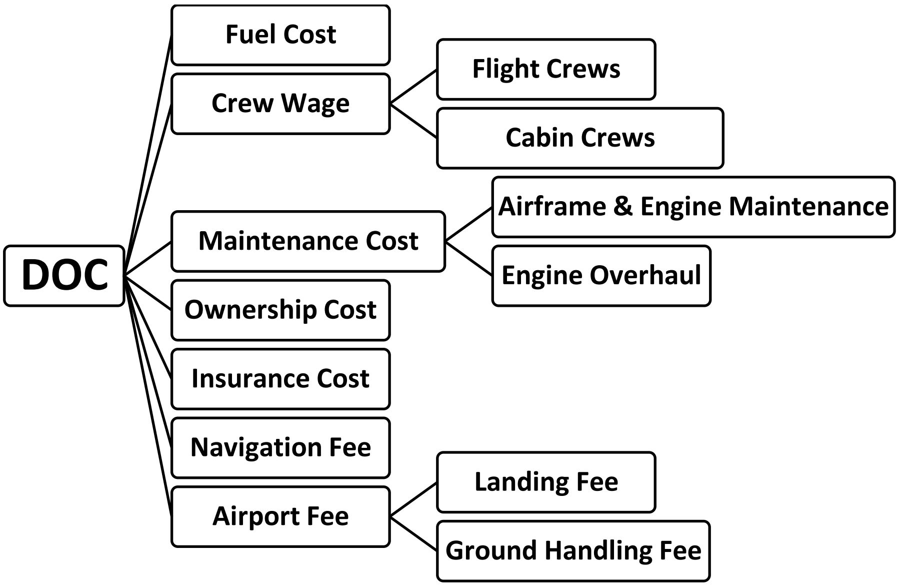
DOC
Fuel Cost
Crew Wage
Flight Crews
Cabin Crews
Maintenance Cost
Airframe & Engine Maintenance
Engine Overhaul
Ownership Cost
Insurance Cost
Navigation Fee
Airport Fee
Landing Fee
Ground Handling Fee

Figure 2.1: DOC items.

The major part of DOC is proportional to the Block Hour (BH), which is computed by Flight Hours (FH) that are linear in distance. The remaining part of DOC is a function of Flight Cycle (FC). The flight profile between the departure and arrival points determines the flight time. In Figure 2.2, a typical operational flight profile for NB cases cost analysis is depicted[4]. BH and FC are computed by Equations (2.1) and (2.2).

$$\boldsymbol{BH = FH + 0.33} \tag{2.1}$$

$$\boldsymbol{FC = \frac{3750}{(BH+0.5)}} \tag{2.2}$$

---

[4] It is necessary to avoid misunderstanding that the typical operational profile is different from the design profile, which must satisfy the design regulations set by EASA CS-25. The airworthiness regulations regarding the passenger aircraft mission profile have been taken into account in HYPERION during the preliminary sizing.

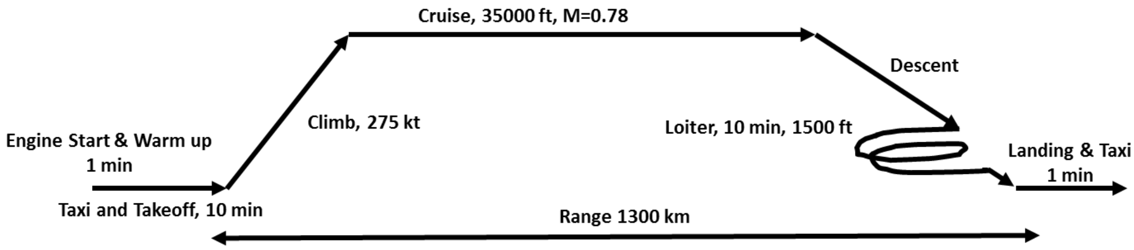
Cruise, 35000 ft, M=0.78
Descent
Climb, 275 kt
Loiter, 10 min, 1500 ft
Engine Start & Warm up
1 min
Landing & Taxi
1 min
Taxi and Takeoff, 10 min
Range 1300 km

Figure 2.2: Flight profile for NB cases analysis.

However, it is important to note that the real cost parameters are strongly dependent on the business model followed and how airlines operate. Based on statistical data, Figure 2.3 provides a realistic description of this point. In the same flight sector, every airline reports different values of CASK. Additionally, the figure presents an order of DOC vs flight distance.

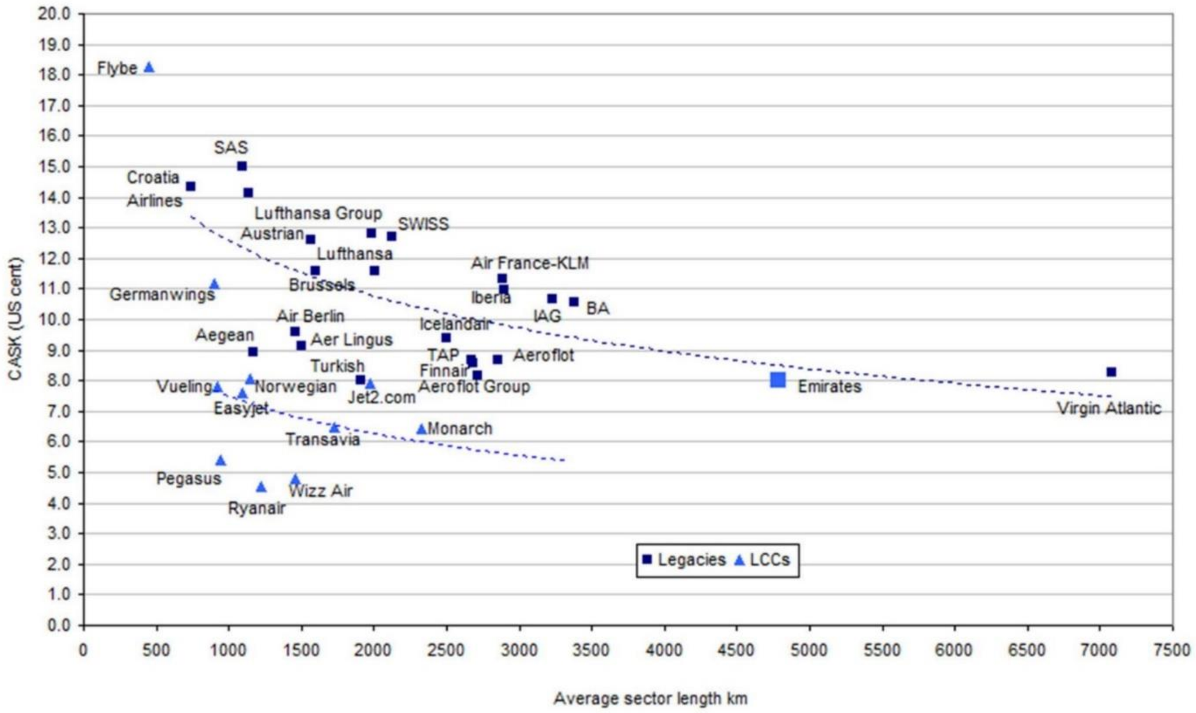

Figure 2.3: CASK vs flight distance based on airlines data in 2012 [72].

2.1.1. Fuel Cost

The cost of fuel is one of major components of the DOC. The significance of the cost is not only to compute the DOC. After airline traffic demand, the ratio of fuel cost to ownership cost is an important factor in the market health of jetliners [42].

Fuel burn for an aircraft is proportional to the distance flown and almost linearly proportional to the weight of the aircraft. The block fuel (BF) per hour, which is the average fuel burned divided by the BH, multiplied by the BH and fuel price, provides the fuel cost through Equation (2.3). In this study, the BF per hour is based on mission design fuel consumption per hour. Figure 2.4 shows the fuel burn per kilometer for an A321-200 aircraft in different sectors as a sample of the parameter order.

$$DOC_{fuel} = BF/hr.BH.P_{fuel} \tag{2.3}$$

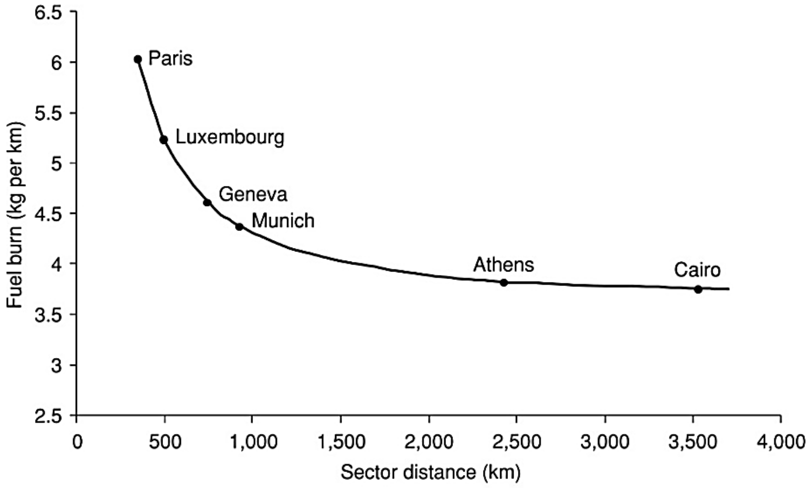

Figure 2.4: The impact of sector distance on fuel burn of A321-200 on routes from London [43].

For LH2 burning aircraft, the fuel price is assumed to be 2 $/kg for an optimistic scenario and 3 $/kg for a moderate increment scenario based on a 2035 forecast (Figure 2.5), converted to 2020 as the reference year [44].

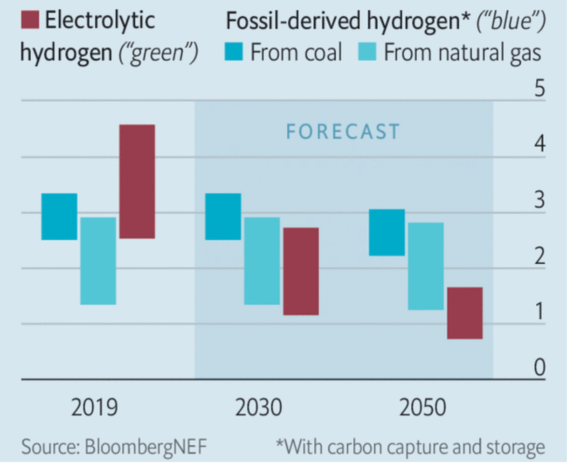

Figure 2.5: Cost of LH2 per kg, fiscal base year 2019 [44].

2.1.2. Crew Wage

The crew wage includes both flight crew and cabin crew. The number of pilots required depends on the flight duration, with two pilots typically sufficient for flights shorter than 6,000 km. Trips longer than 8 hours require a third pilot, and beyond 12 hours, a fourth pilot is mandatory [45].

The number of cabin crew is determined by the number of seats, with a typical ratio of one crew member per 40 seats. Lower ratios are employed to increase onboard service level in full-service flights. Reference [46] suggests a ratio of one crew member per 35 seats for NB aircraft and one per 30 seats for WB aircraft, but safety requirements limit this to one per 50 seats [45].

Pilot wages are typically higher than co-pilot wages, and pilots flying larger airplanes are usually paid more than those flying smaller ones. The wage of cabin crew members is usually half that of pilots. Table 2.1 reports the hourly wages considered in this study, and the share of crew wage in DOC can be calculated using Equations (2.4).

$$\boldsymbol{DOC_{crw} = N_P \times S_{p/h} + N_{CP} \times S_{cp/h} + N_{FA} \times S_{fa/h}} \tag{2.4}$$

Table 2.1: Crew wage.

Parameters	$/hr
Pilot for NB	70
Co-Pilot for NB	60
Pilot for WB	90
Co- Pilot for WB	75
Cabin Crew	40

2.1.3. Maintenance Cost

Maintenance costs for airframes and engines are computed separately in this method. The airframe maintenance cost is determined based on maintenance man-hours per flight hour (MMH/FH) and labor cost. The engine maintenance cost consists of the sum of overhaul cost and expenses for Life-Limited Parts (LLP) replacement. Table 2.2 provides MMH/FH for some passenger aircraft, and in Table 2.4 overhaul and LLP costs of selected engines by publicly available data are presented.

The cost is not a fixed value for a type of aircraft. It is dependent on the age of the aircraft, the average flight hours per flight cycle, how many aircraft of that type are utilized by the airline, the skillfulness of the airline to keep the aircraft operational, etc.. Table 2.3 shows the maintenance cost per flight hour for selected aircraft, which presents a good vision to check the cost estimation result with real costs.

Table 2.2: MMH/FH for selected aircraft [10].

Aircraft	MMH/FH
L1011	14.1
DC-10-10	11
B757	9.1
B767	11.4
B777	10.2
A320-200 [AO&OG 5.1999]	3.7

Table 2.3: Maintenance cost for selected aircraft, based on 2013 [47].

Aircraft	Fleet size	Daily utilization (hr/day)	FH/FC	Average age (year)	Maintenance cost ($/FH)
B757	180	9	2.7	19	850
B767	220	9.5	3.5	18	900
B777	450	11.7	5.1	8	1,800
B737	75	6.3	1.3	20.5	850
B737 NG	650	9	1.9	7.3	700
B747-400	150	10.2	5.1	16.5	1,700
A320	890	8.4	1.8	8.2	900
A330	300	10.8	4.1	8.6	1,400
A340	125	11.5	7.3	14.2	1,500
E-190/195	155	6.7	1.5	4.8	700

Additionally, modern engines typically require visits to the shop for overhaul and LLP replacements every 15,000 FC for NB aircraft and every 5,000 FC for WB aircraft. Airframes typically require structural inspections every 6 years during the overhaul procedure.

Table 2.4: Overhaul cost of selected engine [48].

Engine	Thrust (lb)	FC	Overhaul and LLP Cost (M$)
CFM56-5B6/3	23,500	16,500 - 17,500	3.3 - 3.5
V2524-A5 S1	24,000	15,000 - 16,000	3.2 - 3.4
LEAP-1A24	24,400	16,500 - 17,500	3.3 – 3.6
PW1124G	24,490	16,500 - 17,500	3.2 – 3.5
CF6-80E1A4	70,000	4,600 – 5,000	6.2 – 6.6
PW4168	68,000	4,700 – 5,100	6.2 – 6.6
Trent 772	71,200	5,000 – 5,400	6.6 – 7
GE90-110B	110,000	3,200 – 3,600	9.5 – 10.5
Trent XWB-84	84,000	3,300 – 3,700	6.4 – 6.8

Due to the significant use of composite materials in recent and future aircraft, a linear reduction in MMH/FH is assumed based on the share of composite material [49]. Older version aircraft have 20% composite material, while newer versions have more than 50%, resulting in a 30% decrease in MMH/FH.

For engine maintenance cost estimation, half of the engine price for NB aircraft and one-third for WB aircraft are considered based on survey data.

2.1.4. Ownership Cost

There are various methods to calculate ownership costs for a flight, and these can lead to large differences when comparing airliners' DOC. Ownership costs are determined by factors such as interest rate, depreciation period, and residual value. A fair interest rate of 5% is typically used for business purposes, and at the end of the service life, the value of the aircraft is assumed to be 10% of its price.

Commercial aircraft are usually depreciated over 12-15 years and in some case 20 years, but in this study, a 15-year depreciation period is used as the reference for computation. The Equations (2.5) is used to calculate the share of ownership cost in the DOC of a flight.

$$\boldsymbol{DOC_{own}} = \frac{\boldsymbol{P_{ac}}}{\boldsymbol{FC}}\left[\boldsymbol{IR}\frac{(\boldsymbol{1}+\boldsymbol{IR})^{\boldsymbol{DP}}-\boldsymbol{f_{RV}}}{(\boldsymbol{1}+\boldsymbol{IR})^{\boldsymbol{DP}}-\boldsymbol{1}}\right] \tag{2.5}$$

2.1.5. Insurance Cost

The cost of insurance for a passenger aircraft is typically 0.5% of its value per year. The share of this cost in a flight can be calculated using the Equation (2.6) provided.

$$\boldsymbol{DOC_{ins}} = \boldsymbol{P_{ac}}\,\boldsymbol{f_{ins}}/\boldsymbol{FC} \tag{2.6}$$

2.1.6. Navigation Fee

Navigation fees are charges imposed by countries' Civil Aviation Organizations (CAO) for aircraft flying through their airspace to cover the cost of Air Traffic Control (ATC) and navigational services provided.

The cost is usually based on the weight of the aircraft, the region's charge rate, and the distance of the flight. However, in some countries, it is solely dependent on the distance, and in a few countries, it is a fixed charge.

Table 2.5 provides the cost for en-route charges for an A321 flight in selected countries [43]. Additionally, en-route ATC fees may increase due to implemented carbon tax policies by countries.

The reference rate for Western Europe is $65 per 100 km, and the cost can be calculated using the Equation (2.7) provided [15].

$$\boldsymbol{DOC_{Nav} = 65\left(\frac{D_f}{100}\right)\left(\frac{MTOM}{50}\right)^{0.5}} \tag{2.7}$$

Table 2.5: En-route charges for Airbus A321, 2001 (per 700 km overflight) [43].

Country	En-route fee ($)	Distance-related
Japan	717	No
Germany	560	
Italy	465	
France	431	
Spain	405	
India	362	No
Argentina	330	
Australia	167	
Indonesia	142	
USA	141	
Egypt	125	No
South Africa	125	
Korea	92	No
Brazil	28	

2.1.7. Airport Fees

Airport fees are paid to the airport and include landing and ground handling fees. The landing fee is dependent on the MTOM of the aircraft, while the ground handling fee is proportional to the number of PAX. The rates for these fees vary at different airports. As a rough estimate, the landing fee can be assumed 11.5 $/ton [50], and the ground handling fee can be assumed to be $18 per passenger. It can obtain by Equation (2.8).

$$\boldsymbol{DOC_{arp} = 11.5 \times MTOM + 18 \times PAX} \tag{2.8}$$

2.2. RDTE & ACQ

RDT&E and ACQ assessment involve various cost items, as shown in Figure 2.6 and have been discuss in this section. The overall cost can be calculated using Equation (2.9).

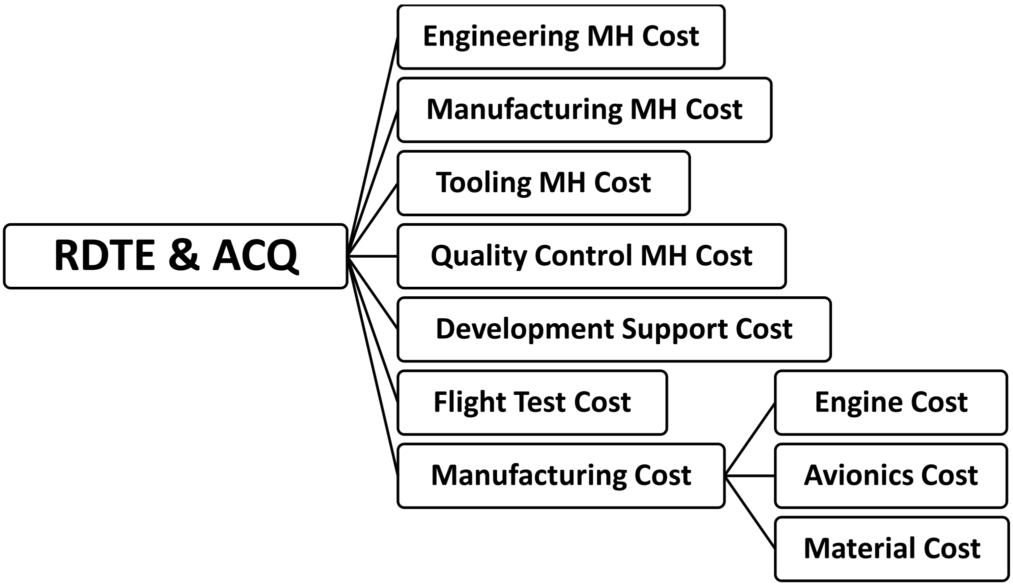
RDTE & ACQ
Engineering MH Cost
Manufacturing MH Cost
Tooling MH Cost
Quality Control MH Cost
Development Support Cost
Flight Test Cost
Manufacturing Cost
Engine Cost
Avionics Cost
Material Cost

Figure 2.6: Items of RDT&E and ACQ cost.

$$\boldsymbol{C_{RDTE\,\&\,ACQ} = \left(H_{eng}R_e + H_{tool}R_t + H_{mfg}R_m + H_{qc}R_q\right)f_{mat} + C_{dev} + C_{FT} + C_{mat} + \left(C_{eng}N_{eng} + C_{avio}\right)Q} \tag{2.9}$$

The method utilizes regression formulas for many cost items, including engineering, manufacturing, tooling, quality control, development support, and manufacturing material costs. The cost of avionics and engines is treated as purchased equipment. The regressions are based on factors such as empty mass, maximum velocity, and production quantity.

The costs of engineering, tooling, manufacturing, and quality control are determined by multiplying the respective man-hours by the appropriate hourly rates provided in Table 2.6. Development support, flight test, and manufacturing material costs are estimated using relevant regression formulas. Equation (2.10) to (2.16) formulated above-mentioned items.

Engineering Hours:

$$\boldsymbol{H_{eng} = 5.18M_e^{0.777}V^{0.894}Q^{0.163}} \tag{2.10}$$

Manufacturing Hours:

$$\boldsymbol{H_{mfg} = 10.5M_e^{0.82}V^{0.484}Q^{0.641}} \tag{2.11}$$

Tooling Hours:

$$\boldsymbol{H_T = 7.22M_e^{0.777}V^{0.696}Q^{0.263}} \tag{2.12}$$

Quality Control Hours:

$$\boldsymbol{H_{QC} = 0.133 H_{mfg}} \tag{2.13}$$

Development Support Cost:

$$\boldsymbol{C_{dev} = 67.4 M_e^{0.63} V^{1.3}} \tag{2.14}$$

Flight Test Cost:

$$\boldsymbol{C_{FT} = 1947 M_e^{0.325} V^{0.822} FTA^{1.21}} \tag{2.15}$$

Manufacturing Material Cost:

$$\boldsymbol{C_{mat} = 31.2 M_e^{0.921} V^{0.621} Q^{0.799}} \tag{2.16}$$

Table 2.6: Labor rate at 2020 [15].

Sector	Rate ($)
Engineering, Re	129
Tooling, Rt	132
Quality Control, Rq	121
Manufacturing, Rm	110

Composite materials for aircraft structures are lighter but cost more than conventional aluminum. The increasing complexity of design and developments implemented by composite materials has been measured by the material factor, which is applied to engineering, manufacturing, tooling, and quality control costs.

The material factor can be determined using Equation (2.17) and Table 2.7. It is calculated as the sum of the corresponding percentage of each material in the empty mass multiplied by the partial cost factors. In the case of recent new aircraft like the B787, the material factor is 1.38.

$$\boldsymbol{f_{mat}} = \sum (\%_{\boldsymbol{mat\,i}} \times \boldsymbol{f_{mat\,i}}) \tag{2.17}$$

The value of Q, representing the production quantity to be produced in five years [41], is typically determined based on economic considerations. For passenger aircraft projects, a reasonable value for Q is in the order of 200 samples.

Table 2.7: Material factor [15].

Material	Factor
Aluminum	1.0
Carbon-Epoxy	1.45
Fiberglass	1.15
Steel	1.75
Titanium	1.45

Engine prices are determined based on publicity data surveys of purchasing orders over the last 30 years. The price of the engine is generally proportional to its thrust. In the case of NB engines, the thrust does not change significantly, so a constant value can be used. However, for WB engines, the thrust varies significantly, and a trend of engine thrust vs. price is used as a reference. Lead to availability of Trent family purchasing data [51], the trend price of the family provided and shown in Figure 2.7.

The price data for avionics is difficult to find, but a suggested value of $5,000 per pound [41] is applied for commercial aircraft avionics in both NB and WB cases.

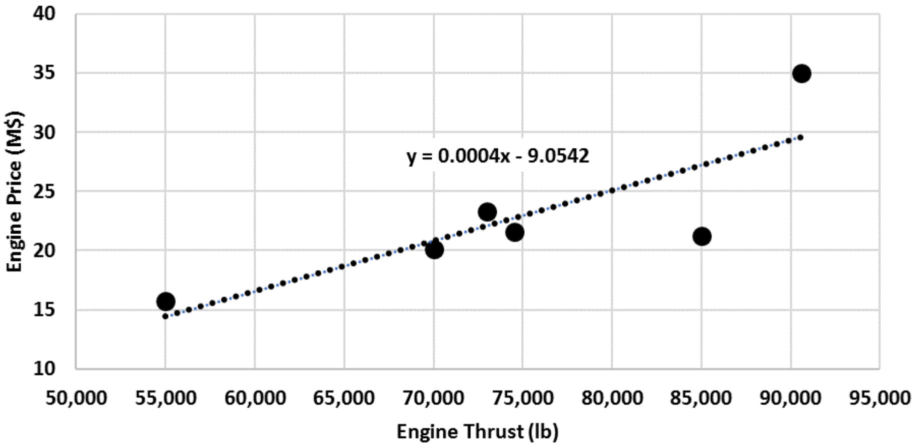

Figure 2.7: Rolls-Royce Trent family thrust vs price (based on 2020) [51].

2.3. Purchasing Price

RDT&E and ACQ costs are recurring based on the number of aircraft produced. The flyaway (production) cost of the aircraft includes the per capita cost of each Q number of manufactured aircraft, as well as the interior cost. The flyaway cost is determined by Equation (2.18).

$$C_{aircraft} = \frac{C_{RDTE\,\&\,ACQ}}{Q} + C_{interior} \tag{2.18}$$

The interior cost is influenced by the class of aircraft and the business model of the airline operator. In the case of WB aircraft, passengers on long-haul flights prioritize comfort over short-haul flights. However, if the airline follows a low-cost carrier (LCC) business model, their orders are typically for high-density seating arrangements with minimal galleys and lavatories. The reference [52] provides the reported order of interior cost for both classes of aircraft. In this project, the price of $25,000 per PAX is used for WB aircraft and $9,250 per PAX for narrow-body (NB) aircraft.

The purchasing price of a civil aircraft is determined by factors such as the flyaway cost, profit margin, spare parts, and other services. The prediction of these factors is difficult and depends on marketing strategy and the details of the purchasing contract. Aircraft manufacturers typically use market-based pricing strategies. It is not reasonable to expect the purchase price to be equal to what is found in the market.

In this study, a profit margin of 35% and a spares factor of 1.1 are included in the aircraft unit price. The purchasing price is calculated using Equation (2.19).

$$\boldsymbol{P_{ac} = C_{aircraft} f_{invest} f_{spares}} \tag{2.19}$$

2.4. A321 Case Study

The cost model was applied to the A321, and its CASK and purchasing data are reported in [43] and [40].

The purchasing price of the aircraft is dependent on the engine type and customization of the interior. Based on fiscal year 2020, the price list of the A321 is $133.4 M. However, the estimated price using the method is $135.2 M. The deviation is approximately 1%, indicating that the method accurately estimates RDTE, ACQ, and purchasing prices.

To assess the method in terms of DOC, the aircraft was evaluated across a range of sectors (Figure 2.8). As shown in the figures, the method correctly estimates the trend of cost, but the numerical results for sectors less than 1,000 km are offset. It should be noted that the reported data for the A321 in [43] does not mention the business model, assumptions, and depreciation strategy of ownership costs, which significantly influence the results.

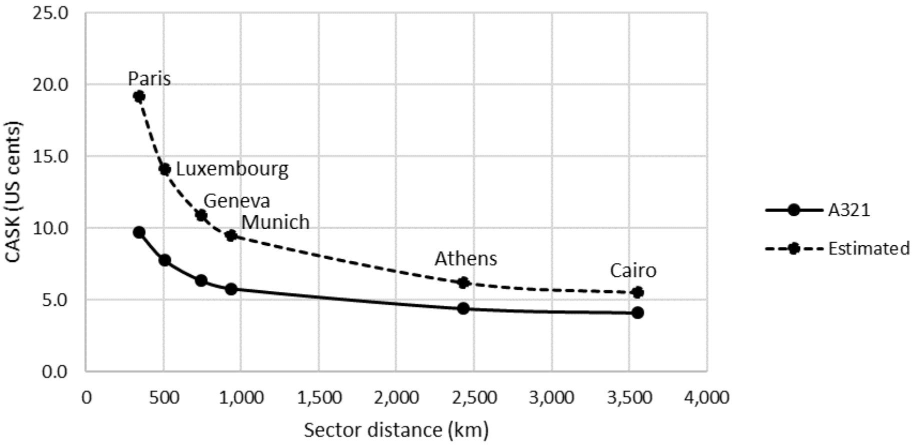

Figure 2.8: CASK vs sector distance for Airbus A321 on routes from London (2020) [43].

In the case of average utilization of a NB aircraft like the A321, the method was used to analyse different components of DOC (Figure 2.9). The major parts of DOC are airport fees, fuel costs, and ownership costs.

Fuel costs, which represent the cruise efficiency of the aircraft, account for 18% of DOC. The largest element is the ownership cost, accounting for 43% of DOC. This indicates that DOC is strongly influenced by production costs. To lower DOC, technological improvements that reduce production cost of the aircraft are more essential than technological advancements that improve cruise efficiency.

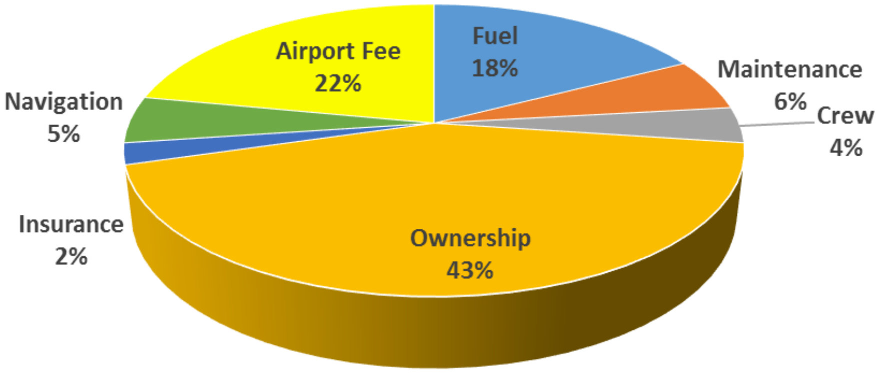

Figure 2.9: A321 DOC at stage length 1,300 km.

3 Framework of Design Trade off

To determine the trade-off matrix, certain key parameters need to be specified. Some of these parameters include the engine bypass ratio (BPR) and Mach drag divergence of the wing, which are assumed to be at a certain technology level by the entry into service (EIS) in 2035. Other parameters are input into HYPERION to size each case. This chapter provides a brief summary of the theoretical background and logical assumptions of the progressive design trade-off.

3.1. Advancement of Engine

Advances in turbofan technology have been delivering efficiency improvements averaging 1.5% per year [53]. The majority of these improvements come from increasing the BPR and, therefore, the fan diameter. However, the larger dimensions of the engine require changes in design to fit under the wings for common tube and wing configurations. Figure 3.1 shows the application of different engines during the aircraft upgrading process, with the latest higher BPR engines being used in the B737, with modifications such as tilting the inboard wing up, increasing wing dihedral, and modifying the upper surface of the wing to accommodate the engine installation.

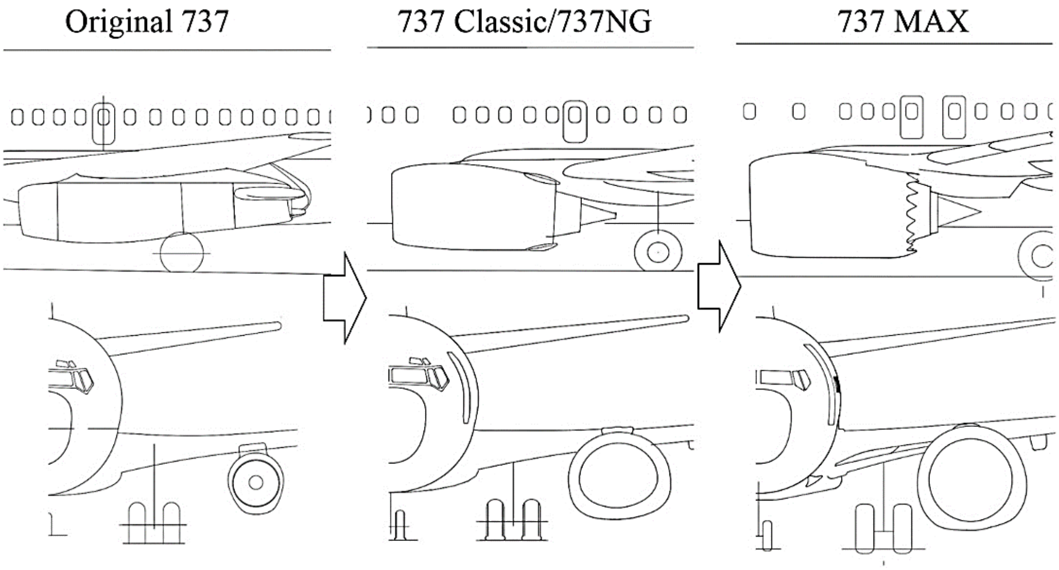

Figure 3.1: Boeing 737 nacelle evolution [54].

Increasing the BPR can reduce the thrust-specific fuel consumption (TSFC). Figure 3.2 shows the effects of BPR on TSFC for a family of engines with a constant core overall pressure ratio (OPR) and turbine entry temperature (TET). However, component losses, power offtake, inlet loss, higher nacelle drag, and weight can lead to lower efficiency of the installed engine. To achieve a further BPR of 10, which is crucial to achieving higher efficiency, other technologies such as geared turbofan (GTF) and composite fan blades are key elements.

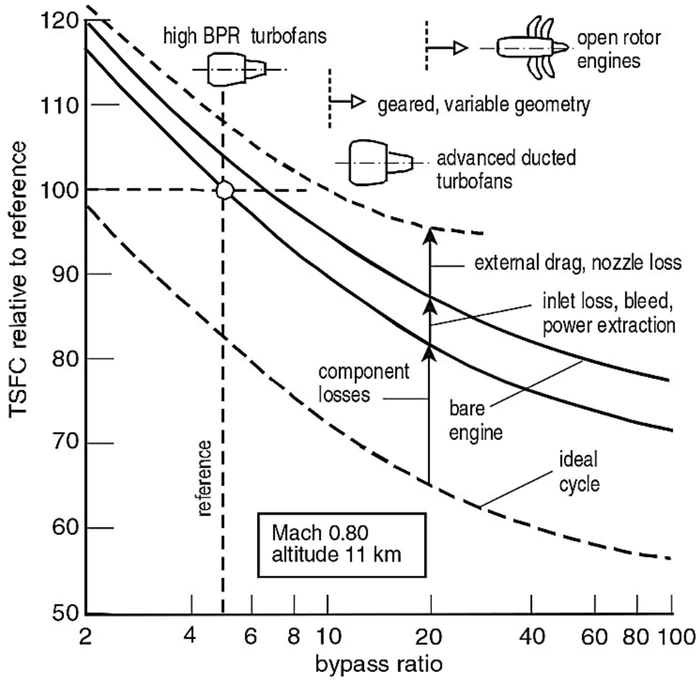

Figure 3.2: Effects of turbofan BPR on TSFC in cruise conditions [11].

However, conventional tube-and-wing aircraft configurations restrict the maximum BPR to around 12, which leaves limited room for improvement in engine efficiency. By the way, LH2 burning in engine provides higher TET, which allows to smaller engine core. Therefore, BPR=12 is conservatively considered the highest potential value of BPR in this study.

3.2. Advancement of Wing

Wing advancements are expressed in terms of an increase in the drag rise Mach number for a given wing sweep, thickness-to-chord ratio (t/c), and cruise lift coefficient, as well as improvements in flow control over the wing. The trade-off of wing parameters needs to define a logical set of wing sweep, AR and t/c. These parameters are interconnected to avoid achieving a patch-up tendency and drag divergence.

It is useful to explain that the reason for considering these factors is to reduce the number of cases that need to be studied during the systematic process. In other words, by focusing on studying pitch up boundary and implementing drag divergence, we can have a smaller matrix of wing parameter variables.

3.2.1. Pitch-up Tendency

Wings with sweep back suffer from a significant pitch-up moment near and at stall. Increasing the sweep angle increases the loading on the outer wing, leading to flow separation. The loss of lift in that region shifts the aerodynamic center forward in close or exceed the center of gravity, potentially causing pitch-up.

The effect of pitch-up tendency depends on the sweep angle at 25% of chord (c/4) and the AR. Passenger aircraft typically require high AR for better cruise efficiency and a high sweep angle to favor a higher cruise Mach number. However, the phenomenon of pitch-up tendency restricts having both parameters at higher values due to a pitch-up boundary. Advancements in the leading edge (LE) of the wing and LE high lift devices allow this nominal boundary to be exceeded [55].

An empirical trend (Figure 3.3) and equation presented by [56] suggests that for a given AR, the highest value for sweep should be less than the result of Equation (3.1). In the trade-off study, this boundary has been respected. It is worth mentioning that the wing taper ratios (λ) of passenger aircraft vary from 0.2 to 0.3, but the effect of λ on sweep limitation is negligible within this range.

$$\boldsymbol{\Lambda_{c/4limit} \leq 23.436\left[\ln\left(17.714(2-\lambda)\right) - \ln AR\right]} \tag{3.1}$$

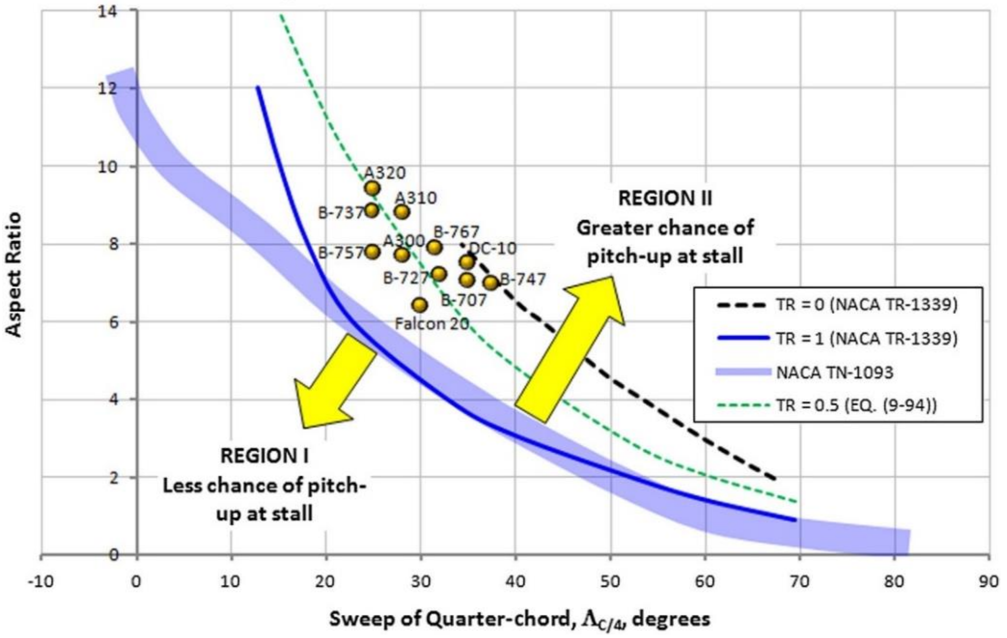

Figure 3.3: Empirical pitch-up boundary for sweep back wing [56].

3.2.2. Drag Divergence Mach number

The selection of the sweep angle and t/c ratio of a wing must ensure that the drag increase of the aircraft is not too high at the required cruise Mach number. The drag divergence Mach number (MDD) is defined as the Mach number where the wave drag amounts to 0.0020 (Figure 3.4). The relation between MDD and the design cruise Mach number (MCR) is determined by the selected wing parameters.

According to Airbus and Boeing, MDD is taken equal to MCR [57]. Based on experience at Fokker [58], the following Equation (3.2), is recommended to set MDD in relation to the required MCR. Through the formula, it's possible to determine Mach number proportion to the upper possible value of average wing t/c.

$$\mathbf{M}_{\boldsymbol{DD}} = \boldsymbol{M_{CR}} + \mathbf{0.02} \tag{3.2}$$

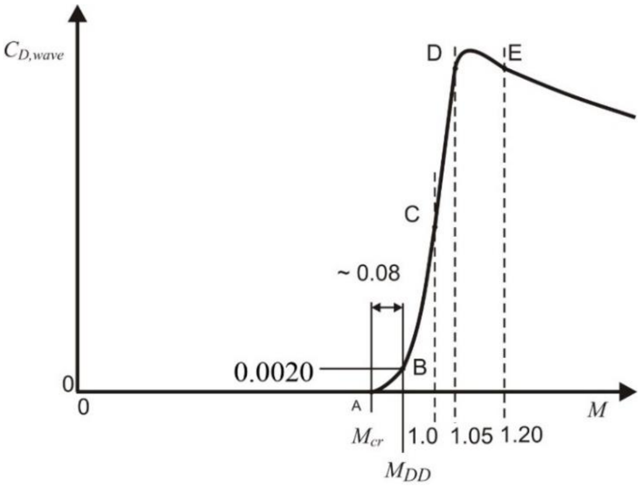

Figure 3.4: MDD definition[5].

The upper limit of the average wing t/c ratio has been determined to achieve a limited amount of compressibility drag at the design Mach number[6]. The aerodynamic wing design technology has a large effect on this limit. The upper limit is related to the drag divergence Mach number by Equation (3.3) [11].

The M* parameter depends to the technology level and it rise by improvement of transonic aerodynamic design of wing. Figure 3.5 shown the improvement of drag rise characteristic based on L1011 wing due to improvement of wing transonic aerodynamic [59].

---

[5] Please pay attention to avoid mixing up Mcr as a symbol for critical Mach number and MCR as a symbol for cruise Mach number.

[6] it's taken equal to cruise Mach number in this study.

$$\mathbf{M}_{DD}\cos\Lambda_{c/4}+\frac{\overline{t/c}}{\cos\Lambda_{c/4}}+0.1\left[\frac{1.1C_L}{\left(\cos\Lambda_{c/4}\right)^2}\right]^{1.5}=M^*\quad,M^*=0.95 \tag{3.3}$$

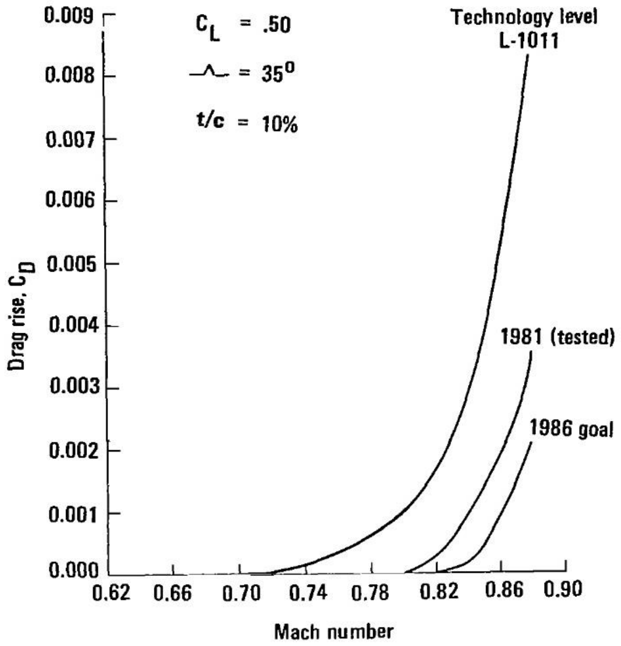

Figure 3.5: Improvement of drag rise Mach number by advancement of aerodynamic at constant wing seep, t/c and lift coefficient [59].

3.3. Fuselage Arrangement and Size

The HYPERION design tool requires the definition of fuselage length and diameter based on the kerosene burning version. The internal layout of seats, including the number of abreast and number of PAX, defines the internal cabin length and width.

The selection of the right fuselage cross-section not only affects the basic economic characteristics of the aircraft but also has a major influence on adaptability to ever-changing market conditions [60]. Therefore, the internal width of the fuselage is one of the most important design decisions.

To determine the fuselage cross-section and length, the method presented in [46] and [61] has been applied. The width of the cabin is determined by the width of seat, armrest, and aisle using Equation (3.4) and (3.5) for NB and WB aircraft respectively (Figure 3.6). To find the fuselage diameter, Equation (3.6) has been applied.

$$\mathbf{W}_{Cabin}=n_{Abreast}(\mathbf{W}_{Seat}+\mathbf{W}_{Armrest})+2\mathbf{W}_{Armrest}+2\mathbf{W}_{Clearance}+\mathbf{W}_{Aisle} \tag{3.4}$$

$$\mathbf{W}_{Cabin}=n_{Abreast}(\mathbf{W}_{Seat}+\mathbf{W}_{Armrest})+3\mathbf{W}_{Armrest}+2\mathbf{W}_{Clearance}+2\mathbf{W}_{Aisle} \tag{3.5}$$

$$\mathbf{D}_{\boldsymbol{Fus}} = \mathbf{1.045W}_{\boldsymbol{Cabin}} + \mathbf{0.084} \tag{3.6}$$

The theoretical cabin length can be estimated using Equation (3.7) based on the number of seats. Additional space for seat arrangement, the service facilities must be provided. Therefore, the actual cabin length is determined by the sum of about 35% of the theoretical length and the flight deck length using Equation (3.8). The fuselage length is defined by the cabin length and fuselage diameter through Equation (3.9). Typical values of the above-mentioned parameters are reported in

Table 3.1 for estimation of length and diameter.

$$\mathbf{L}_{\boldsymbol{Cabin\ theo}} = \frac{\boldsymbol{n_{PAX}}}{\boldsymbol{n_{Abreast}}} \boldsymbol{L_{seat\ pitch}} \tag{3.7}$$

$$\mathbf{L}_{\boldsymbol{Cabin\ actu}} = \mathbf{1.35\ L}_{\boldsymbol{Cabin\ theo}} + \boldsymbol{L_{Flight\ deck}} \tag{3.8}$$

$$\mathbf{L}_{\boldsymbol{Fus}} = \mathbf{L}_{\boldsymbol{Cabin\ actu}} + \mathbf{1.6}\ \boldsymbol{D_{Fus}} \tag{3.9}$$

Table 3.1: Typical cabin parameters dimension.

Parameter	Dimension (m)
Width of seat	0.46 – 0.51
Width of armrest	0.025 – 0.04
Width of clearance	0.025 – 0.05
Width of Aisle	0.48 – 0.51
Seat pitch for NB (single class)	0.71 (28-inch)
Seat pitch for WB (single class)	0.81 (32-inch)
Flight deck length	2.28 – 2.67

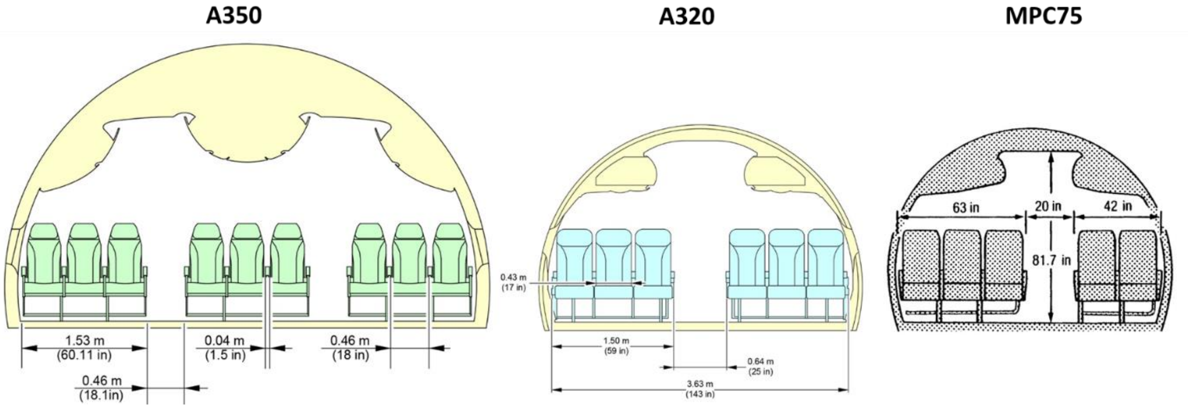

Figure 3.6: Fuselage cross section in NB and WB.

3.4. Aerodynamic Coefficients

To run HYPERION, it is necessary to define the maximum lift coefficient and the increment in drag coefficient in different configurations. These parameters are typically based on previous experiences and refined in the design cycle.

The purpose of this section is to find as realistic as possible values for C_{Lmax} in takeoff, landing, and ΔC_D due to flap deflection in those phases, as well as landing gear (LDG) extension.

3.4.1. Max Lift Coefficient

The maximum lift coefficient is determined based on aerodynamic characteristics provided in [58] and [62]. The values reported in Table 3.2 are based on stall speed tests and represent $C_{L\,max\,1g}$. This maximum lift coefficient varies slightly over the center of gravity range and determines the minimum steady flight speed at a given aircraft weight.

Table 3.2: C_{Lmax} at landing and takeoff configuration of selected aircraft [58].

Parameters	**MPC75[7]** [62]	**A320-200**	**A330-200**	**B737-800**	**B757-200**	**B767-200**	**B777-200**
C_{Lmax} landing	2.9	2.6	2.5	2.5	2.6	2.2	2.4
C_{Lmax} takeoff	2.6	2.4	2.3	2.2	2.4	2	2.3

LH2 airliners will have a dry wing instead of current wet wing passenger aircraft. The empty space in wing box may allow allocating some onboard systems, which it provide partially root bending relief during a gust or pull-up maneuver, especially at near MTOM [74]. In addition, in the case of using the space to accommodate flap and wing control surfaces mechanisms, allows for the smaller of external fairing of high lift devices and control surfaces and less disturbance. This provides the potential for a higher lift coefficient due to flap deflection. Therefore, slightly higher values for lift coefficients of NB and WB aircraft have been taken into account, as presented in Table 3.3.

Table 3.3: C_{Lmax} at landing and takeoff configuration for NB and WB.

Parameters	**NB**	**WB**
C_{Lmax} landing	3.0	3.0
C_{Lmax} takeoff	2.5	2.5

---

[7] MPC75 was a project to design and development of an aircraft in the class of A319 which carried out by Deutsche Airbus in early 90s.

3.4.2. Drag Coefficient Increment

HYPERION calculates the zero-lift drag coefficient of the aircraft using equivalent skin-friction method. This method uses the aircraft geometry to determine the wetted area, and trend data of the equivalent skin-friction coefficient provides a good estimation of the friction parameter. The coefficient is then multiplied by the dynamic pressure and wetted area to obtain the zero-lift drag. However, to account for the landing gear (LDG) and flap in the drag estimation, the design tool needs to determine the impact of these elements on the C_{D0}.

The same approach used for determining the C_{Lmax} is applied to the drag coefficient. Table 3.4, based on publicity data, presents the ΔC_D values for LDG[8] and flap. The size of the aircraft strongly affects the amount of C_D for these components, which is why the coefficients are different for NB and WB aircraft based on their sizes. Relaying to the data in Table 3.5, the drag increment for NB and WB aircraft is determined.

Table 3.4: $\Delta C_{D\ LDG}$ and $\Delta C_{D\ Flap}$ for selected aircraft.

Parameters	MPC75 [Aero Data]	B777-200 [Obert]
C_{D0}	0.0186	0.014
$\Delta C_{D\ LDG}$	0.0285	0.012
$\Delta C_{D\ Flap\ LN}$	0.051	0.077
$\Delta C_{D\ Flap\ TO}$	0.019	0.029

Table 3.5: $\Delta C_{D\ LDG}$ and $\Delta C_{D\ Flap}$ for NB and WB.

Parameters	NB	WB
$\Delta C_{D\ LDG}$	0.025	0.015
$\Delta C_{D\ Flap\ LN}$	0.05	0.075
$\Delta C_{D\ Flap\ TO}$	0.015	0.03

3.5. Oswald Efficiency

The Oswald efficiency (e) factor is another parameter that varies based on design parameters and must be computed and fed into HYPERION for each case. The Oswald factor reflects the deterioration of aircraft lifting properties due to deviation from an elliptical lift distribution.

---

[8] In hydrogen aircraft, the elongation of the fuselage results in the need for longer and heavier landing gear, which also increases drag [74]. However, the specific elongation of the fuselage determines the increase in landing gear length. To simplify the analysis and avoid complicating the optimization of overall parameters, a constant value for the drag increment of the landing gear has been assumed.

As shown in Equation (3.10), a lower e value results in higher induced drag. For a typical passenger aircraft, induced drag accounts for 70% to 80% of total drag in the second segment climb and 40% during the cruise phase [63]. Therefore, it is important to accurately estimate this parameter during preliminary sizing.

$$\mathbf{C}_{D} = \mathbf{C}_{D0} + \mathbf{C}_{Di} = \mathbf{C}_{D0} + \frac{C_L^2}{\pi . AR . e} \tag{3.10}$$

The Oswald factor is influenced by several factors, including the wing planform, presence of a fuselage, nacelles, and other components, Mach number, and zero-lift drag coefficient.

To find an appropriate method for trade-off design studies, a literature survey was conducted using main design references, and the A320 aircraft was evaluated for its Oswald factor value (Table 3.6). Due to its ease of use and accuracy, the Shevell method [64] was selected, and its method formulations are presented in Equations (3.11) to (3.13).

Table 3.6: Real and estimated Oswald factor of A320 in cruise condition.

	A320 experimental [65]	**Shevell**	**Torenbeek**	**Raymer**	**Schaufele** [66]	**Obert**
Oswald factor	0.78	0.8	0.78	0.49	0.8	0.79

$$e = \frac{1}{(\pi . AR . k) + {}^{1}\!/_{0.99s}} \tag{3.11}$$

$$k = \left(0.38 + 57 \times 10^{-6} \Lambda_{c/4}^2\right) C_{D0} \tag{3.12}$$

$$s = 1 - 1.556 \left(\frac{D_{Fus}}{b}\right)^2 \tag{3.13}$$

In the above equation, by increasing the AR at a constant sweep angle, wing span and C_{D0}, the Oswald factor decreases. It may seem paradoxical that a higher AR leads to higher induced drag, but this can be explained by the fact that the fuselage causes a loss in lift, resulting in an irregular spanwise lift distribution. Therefore, in addition to considering a higher AR, the width of the fuselage relative to the wing span is essential, and the fuselage size must be taken into account at the early stage of design [67].

3.6. Economical Cruise Mach Number

The range R is the distance that an airplane can travel with a given amount of fuel. The range is calculated by integrating the specific air range (SAR). In the optimization of cruise performance for jet aircraft, it is typically assumed that the TSFC is independent of flight speed, which is generally accurate. According to Equation (3.14), to achieve maximum range, the $(M.L/D)_{max}$ must be selected by choosing an appropriate M_{CR} [11].

$$\boldsymbol{SAR = \frac{dR}{dW_f} = \frac{a.M.L/D}{W.TSFC}} \tag{3.14}$$

Typically, a plot of ML/D as a function of C_L for different Mach numbers is developed to find the maximum value of ML/D [66]. This procedure was carried out at McDonnell Douglas and Lockheed, and it is expected that a similar procedure would be followed at Boeing [74].

In Figure 3.9, the plot for the DC-10 is shown. These curves demonstrate the significant impact of compressibility drag rise on the $(L/D)_{max}$ in cruise as the M_{CR} increases. These curves illustrate that while the $(L/D)_{max}$ decreases significantly at Mach numbers beyond M=0.75, the maximum value of ML/D continues to increase up to at least M=0.825. This indicates that $(ML/D)_{max}$ occurs at a Mach number where some level of compressibility is present.

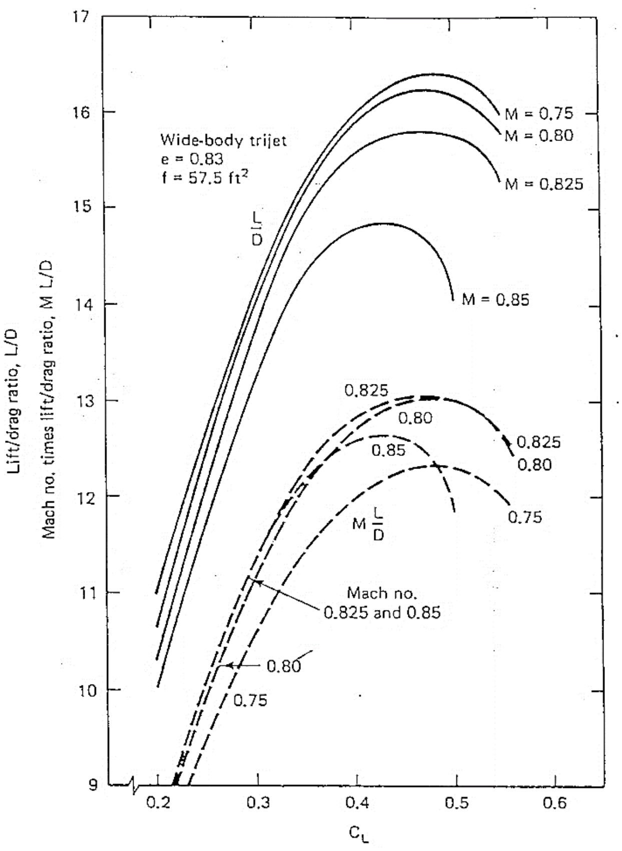

Figure 3.7: Mach number time aerodynamic efficiency of DC-10 [64] [76].

The aforementioned method ultimately determines the optimal cruise Mach number, which minimizes fuel consumption or maximizes flight range. While fuel efficiency is crucial in commercial transport design, the primary objective is to generate profit and return on investment for the airline operator.

Therefore, the DOC for commercial transport emphasize the need for higher cruise speeds due to increased utilization of the aircraft by the airline. Higher utilization leads to reduced insurance costs and depreciation contributions to the DOC. Additionally, crew costs and maintenance expenses (both airframe and engine) decrease as flight time is reduced.

As a result, the DOC typically decreases with increasing Mach number (increased productivity) until the additional costs associated with increased airframe weight and cost due to wing sweep or thickness reduction, along with the increased fuel consumption at higher Mach numbers, outweigh the time-related cost reductions (refer to Figure 3.8) [76].

In conclusion, this thesis has chosen a method and procedure that directly assesses the DOC in relation to cruise Mach number rather than the method provides the cruise Mach number with respect to minimum fuel weight.

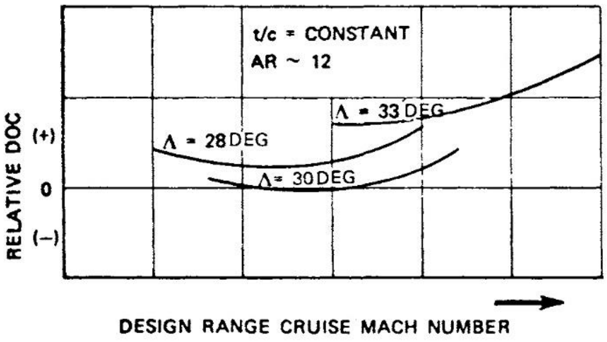

Figure 3.8: Typical trade off cruise Mach number optimization for DOC [76].

3.7. Method Sensitivity Analysis

To demonstrate the sensitivity of the design tool, assumptions and methodology to trade-off studies, a kerosene burning NB case with 198 passengers was sized based on the requirements mentioned in Table 1.3.

The A320 aircraft was selected for comparison and justification of the results. The engine technology was kept the same as the A320. A sensitivity analysis of major operational and geometry parameters was conducted, providing insight into the effectiveness of varying these parameters on sizing. The findings indicate that the model and method are sensitive to:

1. Design range (Figure 3.9 a)
2. Cruise Mach number (Figure 3.9 b)

3. Wing parameters, specifically AR (Figure 3.9 d)

There is insensitivity to cruise altitude. Additionally, the cost of DOC decreases with increasing Mach number up to a point where the increment of fuel burned cost outweighs the reduction in block time. Optimum values for aspect ratio and cruise speed are found near the values of the A320. In summary, the method has enough potential to be applied to design studies.

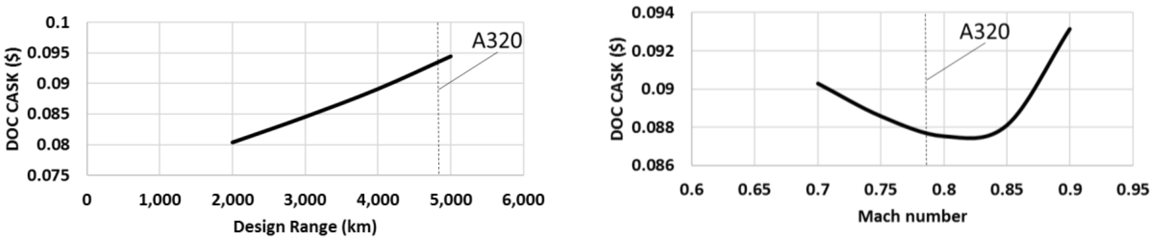

(a) Design range sensitivity.

(b) Cruise Mach number sensitivity.

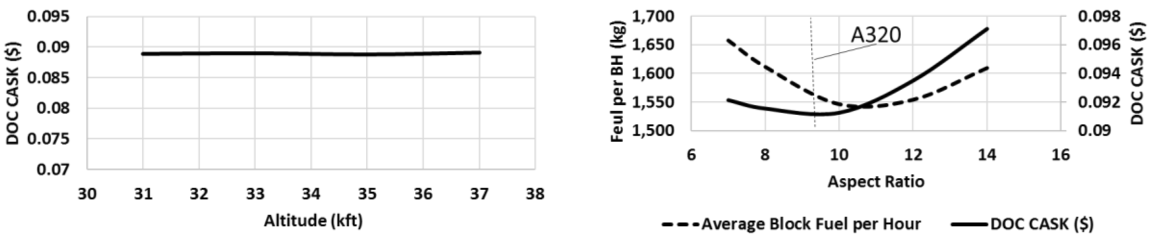

(c) Cruise altitude sensitivity.

(d) Aspect ratio sensitivity.

Figure 3.9: Method trade off sensitivity study for a kerosene burning aircraft in class of A320.

4 Narrowbody Design Study

This chapter presents a trade-off design study for NB aircraft and provides analysis results for all cases. The effects of technology, variations in design range and passenger capacity, wing parameters, and cruise Mach number on the cost of DOC are examined.

In order to conduct a trade-off analysis, a reference is needed to systematically recognize the variation of FoM due to variable parameters. Parametric design studies were conducted to determine the optimum aircraft, and interesting results were observed.

The chapter aims to answer two questions:

1. What are the best parameters in terms of minimizing DOC?

2. Does a change in fuel price have an effect on the optimum solution? Therefore, two fuel prices were considered in the economic analysis for each combination of variables.

4.1. Baseline NB Aircraft

The baseline for the NB aircraft trade study (A-1) is an aircraft with a capacity of 198 passengers, a seat pitch of 28 inches, and a design range of 3,700 km. It meets the performance requirements outlined in Table 1.3. The characteristics and results of the A-1 design case are listed in Table 4.1.

Table 4.1: NB baseline case design parameters.

Parameter	**A-1**
Max Take off Mass (kg)	71,218
Operating Empty Mass (kg)	47,257
Empty Mass (kg)	43,658
Payload Weight (kg)	18,414
Fuel (kg)	5,344
Engine Mass (kg)	5,017
Average Block Fuel per Hour (kg)	1,002
Wing Area (m^2)	112.5
Each Engine Thrust	126.3 kN (28,390 lb)
DOC CASK (\$) @ 1,300 km stage, LH2 2 \$/kg	0.081
DOC / BH (\$/hr) @ 1,300 km stage, LH2 2 \$/kg	9,229

4.2. Engine and Material Technologies Trade off

The trade-off between engine and material technologies is examined to understand how the application of high BPR engines and advanced composite materials affect DOC. New advanced technologies typically increase the manufacturing cost of an aircraft, but they also have the potential to reduce DOC.

The old engine has a BPR of 6, while the newer one has a BPR of 12, resulting in reduced fuel burn. Additionally, based on publicity data (Figure 4.1), the early advanced aircraft has at least a composite share of 50% of the total structure weight, compared to 15% for the old aircraft. This increase in composite share leads to weight and MMH reduction, which favors DOC reduction.

Table 4.2 shows the results of substituting new technology instead of the old technology. The version with the old technology (A-0) has roughly 15% higher MTOM and 14% for DOC, and there is a significant reduction in mission fuel, with the new technologies decreasing fuel consumption by 36%.

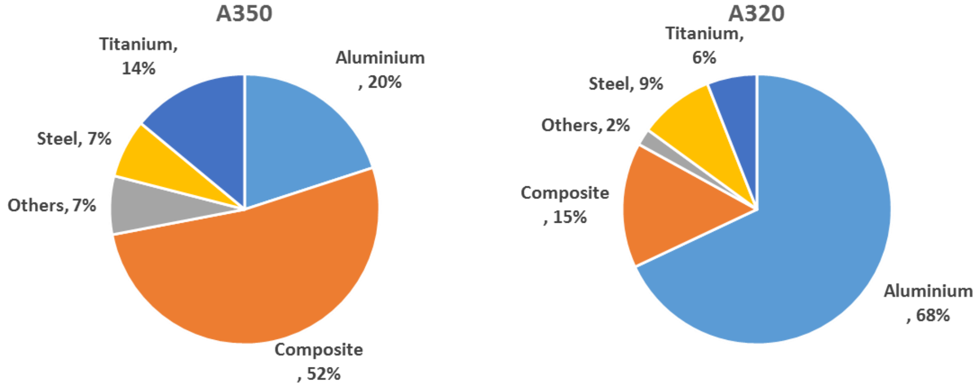

Figure 4.1: Share of materials in new and old passenger aircraft, A350 and A320 [68] [69].

Table 4.2: The Effect of implement higher technology in NB cost and design parameters.

Parameters	A-1	A-0	Δ
Max Take off Mass (kg)	71,218	81,736	-12.9%
Operating Empty Mass (kg)	47,257	54,945	-14.0%
Empty Mass (kg)	43,658	51,346	-15.0%
Payload Weight (kg)	18,414	18,414	0.0%
Fuel (kg)	5,344	8,180	-34.7%
Engine Mass (kg)	5,017	5,738	-12.6%
Average Block Fuel per Hour (kg)	1,002	1,534	-34.7%
Wing Area (m^2)	112.5	129.1	-12.9%
Each Engine Thrust	126.3 kN (28,390 lb)	143 kN (32,140 lb)	-11.7%
DOC CASK ($) @ 1,300 km stage, LH2 2 $/kg	0.081	0.093	-12.9%
DOC / BH ($) @ 1,300 km stage, LH2 2 $/kg	9,229	10,569	-12.7%
Purchasing Price (M$)	119.8	125.9	-4.8%

4.3. Range and PAX Trade off

The trade-off between range and passenger capacity is also studied to understand their effects on DOC. A set of range-PAX combinations is defined, and as expected, the gain is greater at lower ranges and higher passenger capacities.

The interaction between PAX and design range is shown in Figure 4.2, which demonstrates a linear increase in DOC with both PAX and range. The sensitivity of DOC to variations in PAX is greater than to variations in range, with a PAX step of 20 having a larger impact than a range step of 1,000 km. In the Figure 4.3 changing OEM with respect to design range and PAX are presented. The mass increase linearly by increasing the two parameters.

Fuselage length is related to PAX and design range, and it directly contributes to the wetted area and mass of the fuselage structure. Increasing PAX and range leads to an increase in slenderness. The elongation of the fuselage in terms of slenderness is worth studying, as it provides an opportunity to evaluate it based on previous experiences in passenger aircraft design.

The optimum zone for this parameter is between 10 and 11, according to data survey results [61] [70]. From Figure 4.4, it can be observed that all cases except for a range of 2,000 km and less than 180 PAX are outside the optimum value range. Additionally, in order to avoid breaking historical height records[9], a range of 6,000 km with 200 PAX should be maintained.

In conclusion, when selecting the best combination of range and passenger capacity, it is important to consider that a NB LH2 aircraft must be capable of covering current NB routes while also meeting the increasing demand for using this class of aircraft on current small WB routes (as mentioned in Section 1.3).

In addition, to cover domestic and intracontinental flights, the aircraft range must be at least 2,500 km, which is the most concentrated request by the market (Figure 4.5). Although for the possibility of carrying trans-Atlantic, flights typically need at least 5,500 km. Those demands should be satisfied through family planning. In other words, it’s necessary to have a basic version and two additional shorter and longer derivatives.

All of the above factors reinforce the selection of a 4,000 km design range with 200 PAX for the basic version and potentially a 2,500 km range for the shorter derivative and a 6,000 km range for the longer derivative with an appropriate number of PAX. This arrangement does not cross the slenderness limitation and highly respects the market request.

Appendix A shows more trends that are derived from range-PAX studies.

---

[9] Highest slenderness recorded by DC-8-71 is 14.2, single aisle with 259 PAX.

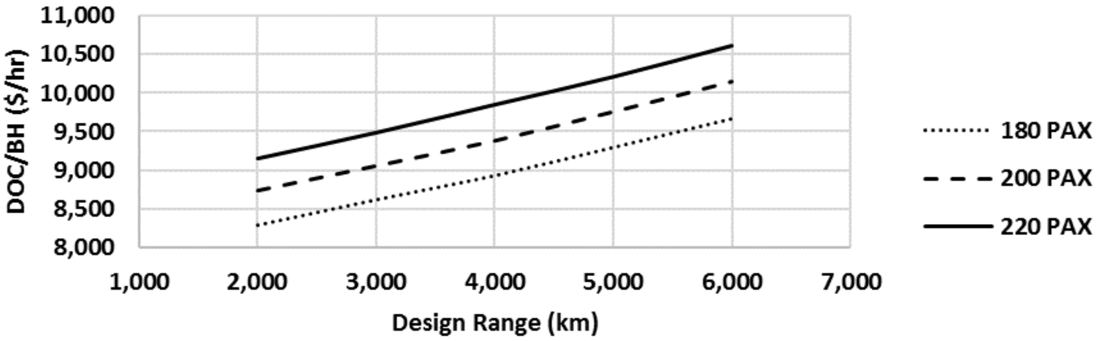

(a) NB DOC per BH for 2 $/kg fuel price.

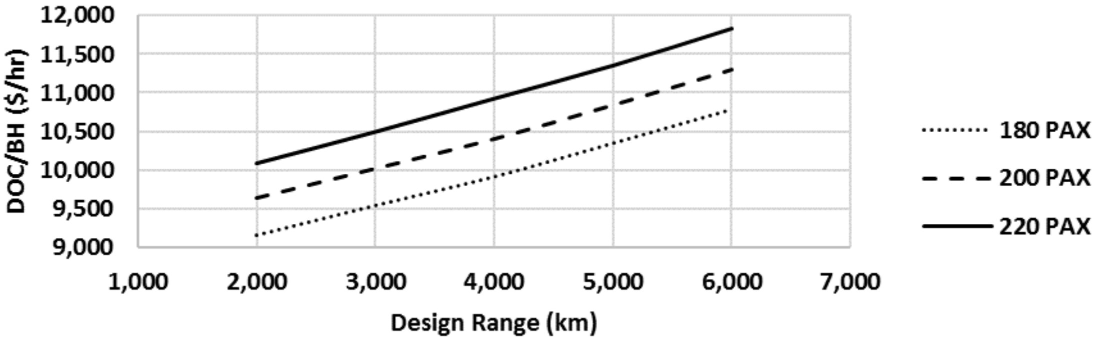

(b) NB DOC per BH for 3 $/kg fuel price.

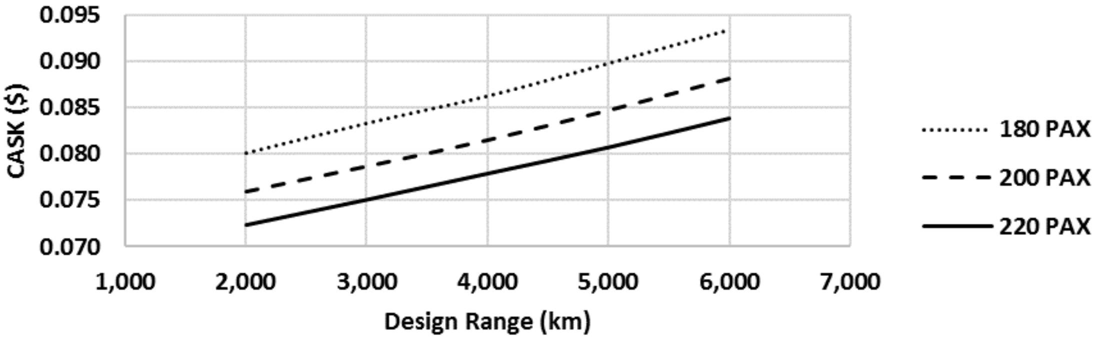

(c) NB CASK for 2 $/kg fuel price.

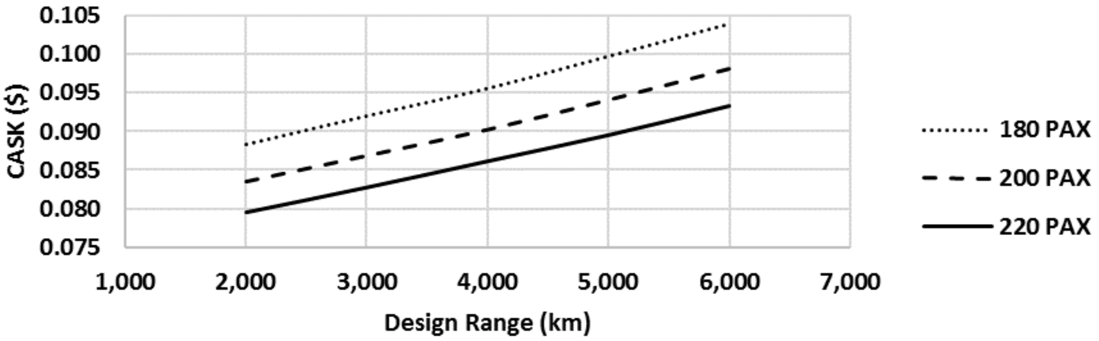

(d) NB CASK for 3 $/kg fuel price.

Figure 4.2: Trade off design range vs PAX for NB on DOC.

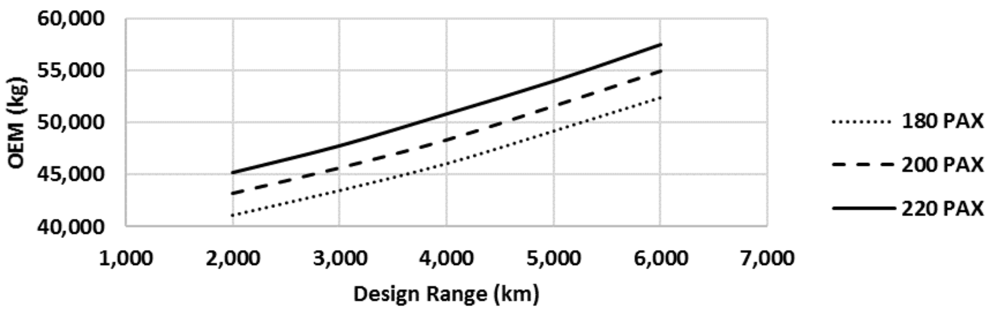

Figure 4.3: The effect of range and PAX on OEM for NB.

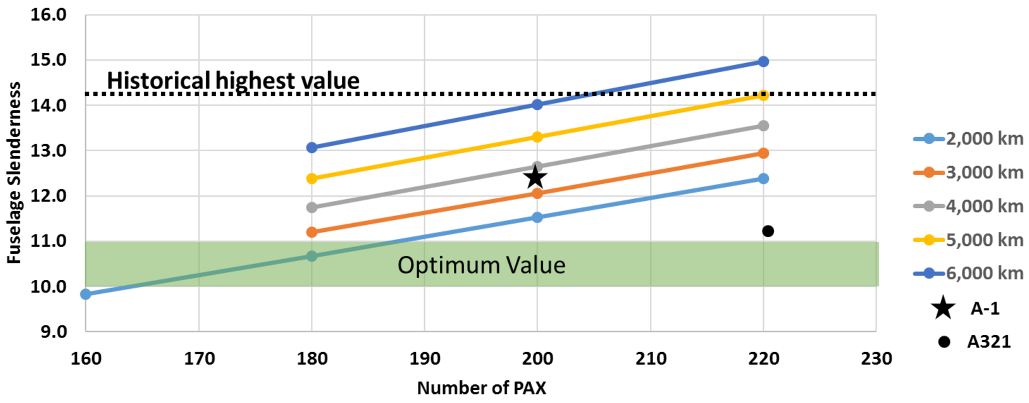

Figure 4.4: Fuselage slenderness for NB trade off cases.

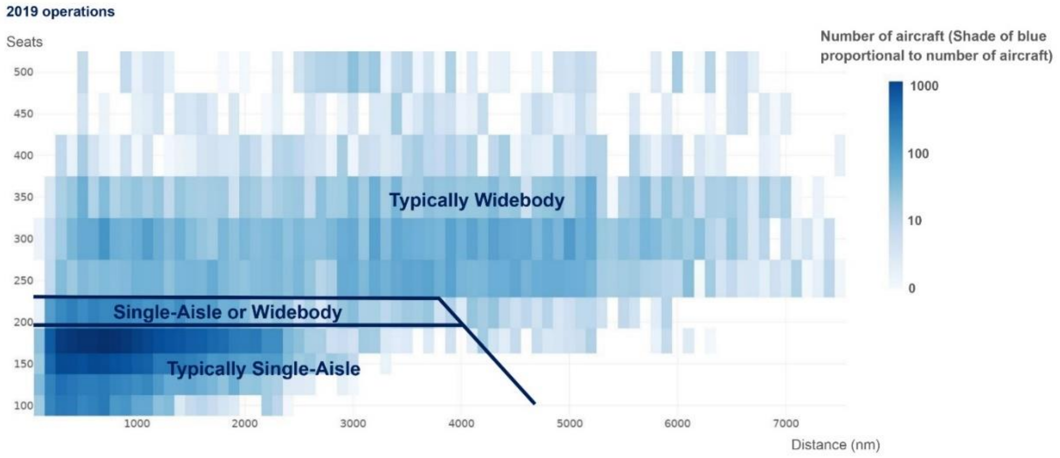

Figure 4.5: Current fleet concentrated zone up to 2,500 km and 200 PAX [25].

4.4. Wing Parameters Trade Off

The preliminary sizing trade studies allowed fine-tuning of wing parameters to obtain minimum DOC. This trade-off is not as effective as changing technology level or variations in design range or number of passengers on DOC. The maximum deviation of DOC and masses due to variation of wing parameters within a permissible range by this model is ±3% for DOC and ±5% for fuel mass and MTOM. Nevertheless, in the life cycle of an aircraft, these values would be remarkable.

To find the optimum values for the wing, a trade-off was carried out by dividing variable parameters into primary and secondary variables. The primary variables are wing sweep, AR, and t/c at a given value of Mach number, and the secondary variable is the variation of Mach (Refer to Section 4.5) at the optimum wing parameters.

In comparison between the sensitivity of DOC and fuel mass to the variables, the most significant parameter for both is AR. In the next level, t/c has remarkable effects on results, and eventually, the effects of sweep angle at a given t/c and AR are slightly fewer.

Figure 4.6 and Figure 4.7 show the variation of block fuel mass and MTOM due to wing parameters, and from Figure 4.8, it can be seen how DOC varies with the parameters for a 1,300 km stage length.

As would be expected, MTOM increases with lower t/c and higher AR. However, a higher AR causes lower induced drag and consequently lower fuel burn. In terms of DOC, the net effect of AR is an optimum point nearby AR=10.

From Figure 4.6 (at sweep angle of 25°), it is observed that changing the hydrogen price may lead to shifting the optimum point in terms of DOC. However, the variation is small, but it infers that making a decision based on minimum fuel mass is more reasonable.

With regards to the lowest points of average block fuel per hour, sweep angle of 25°, AR of 10, and t/c of 12%, a DOC close to the optimum is achievable, and the fuel used is also close to the minimum for the given stage length.

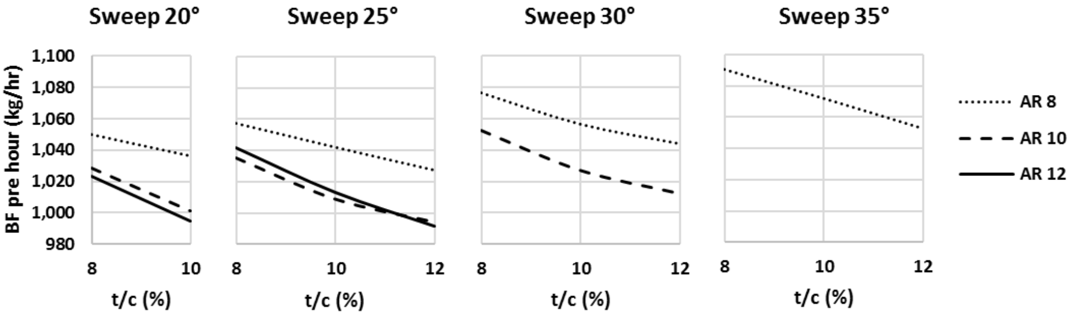

Figure 4.6: Block fuel per hour for NB wing parameters trade off.

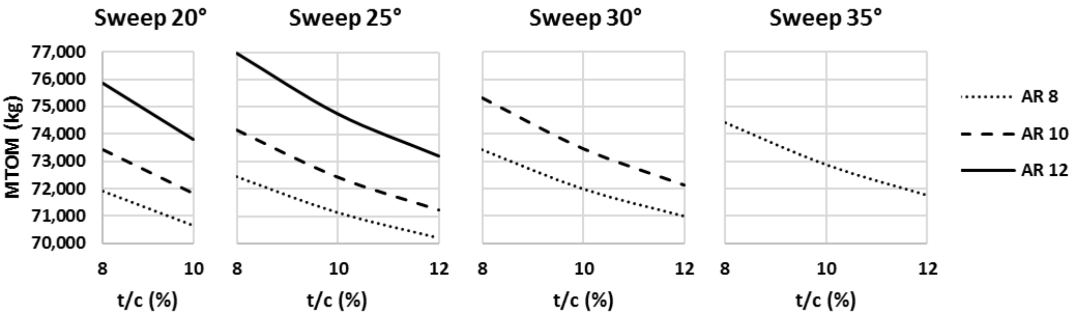

Figure 4.7: MTOM for NB wing parameters trade off.

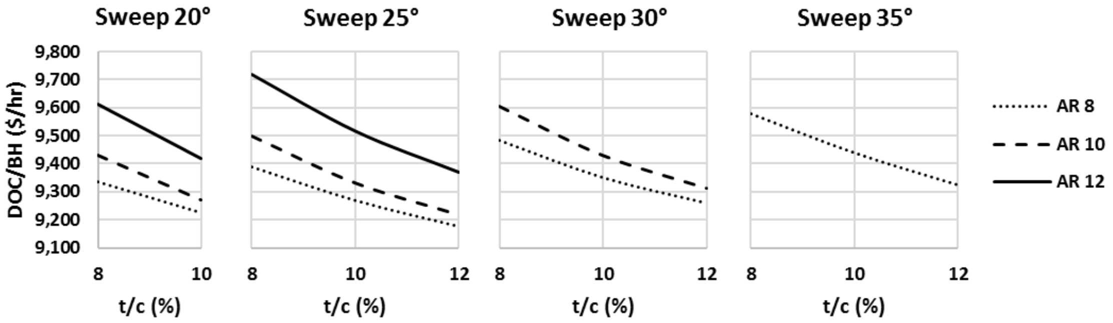

(a) DOC per BH for fuel price 2 $/kg.

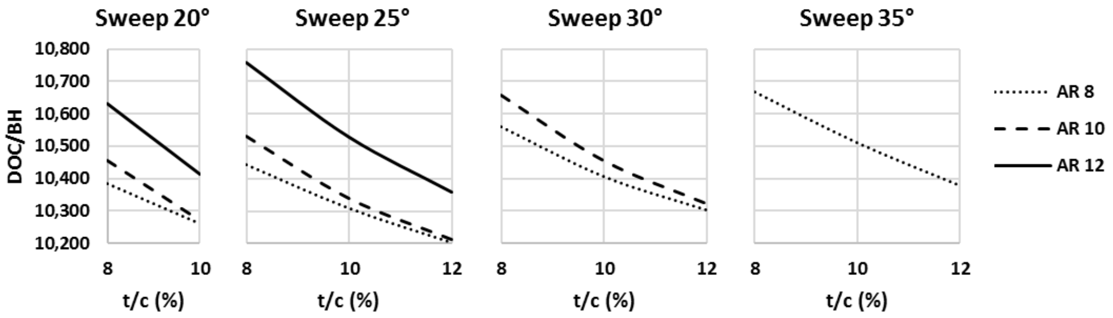

(b) DOC per BH for fuel price 3 $/kg.

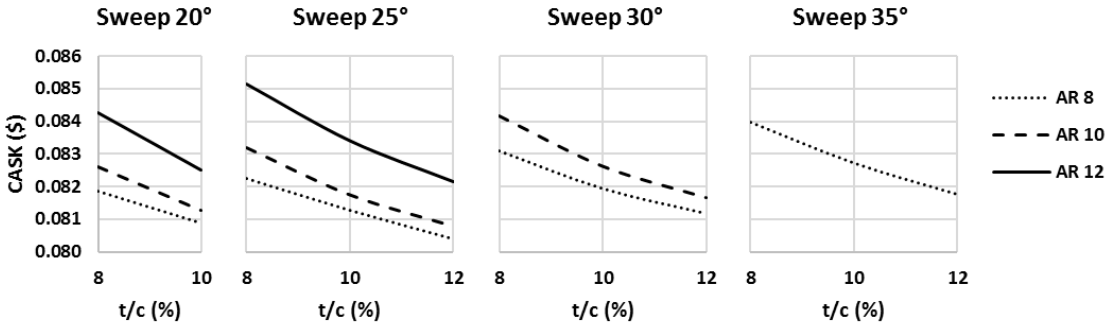

(c) CASK for fuel price 2 $/kg.

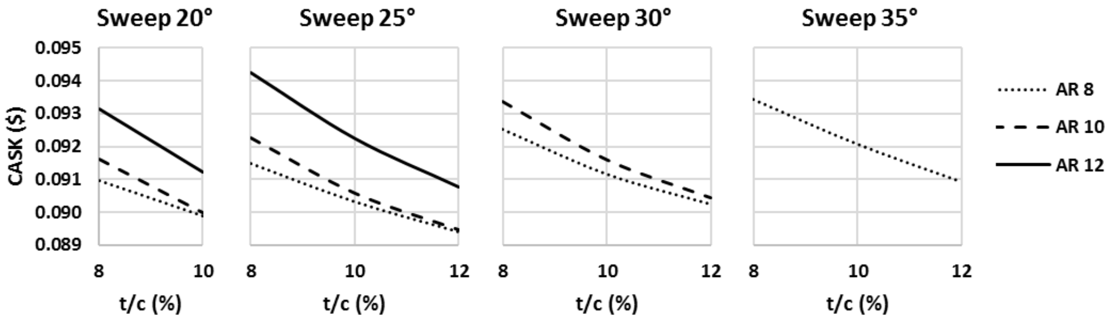

(d) CASK for fuel price 3 $/kg.

Figure 4.8: DOC of wing parameters trade off for NB.

4.5. Cruise Speed Trade Off

For the optimum point of wing parameters selected in Section 4.4, sizing was performed at different cruise Mach numbers. Figure 4.9 demonstrates how cruise speed affects DOC parameters. Increasing Mach number leads to decreasing block hour and also increases drag, consequently requiring more fuel. However, the reduction in cost parameters, which are dependent on block hour, takes precedence over fuel cost. Raising cruise speed greater than the optimum value dominates the fuel cost over other DOC components.

Hence, it can be stated that the optimum cruise Mach number is strongly dependent on fuel price. Figure 4.9 shows the variation in DOC with cruise Mach number at a 1,300 km stage length. A lower price shifts the Mach number to higher values.

In these cases, by increasing LH2 price from 1 $/kg to 3 $/kg, the optimum cruise speed would be decreased from M=0.84 to M=0.8. In other words, if expected fuel costs rise relatively more than other costs, the minimum DOC will be obtained at a slower cruise speed.

It can be concluded that CASK is extra sensitive to cruise Mach number rather than wing parameters. In practice, fluctuations in fuel prices during the lifespan of an aircraft are normal. There is likely to be little advantage in designing the wing exclusively and optimizing it based on a given fuel price for minimum fuel consumption.

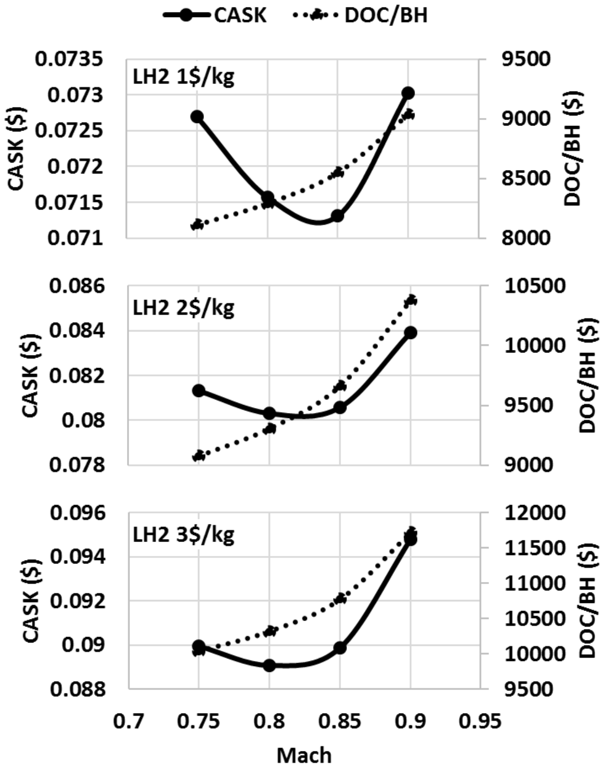

Figure 4.9: Effect of cruise Mach number on DOC for NB.

4.6. NB Design Solution

Preliminary sizing of the final solution for NB LH2 was conducted based on the more promising parameters observed in the systematic trade studies optimization. Table 4.3 reports the baseline (A-1), a middle case and the final solution (NB LH2), illustrating how the baseline was modified to achieve improved performance and FoM.

Regarding to the A-1 and NB LH2, some criteria, such as design range and cruise Mach number have been increased by 5% and 8% respectively, at the same expense of CASK. As a result, the increase in DOC/BH is due to increment of empty mass and purchasing price. To clarify of the effect of cruise speed on DOC, a case with design range of 4,000 km (same as NB LH2) was determined (A-1 4,000 km). As it has found, at the same design range, by increasing the cruise Mach number from 0.78 to 0.82 the CASK reduced by 1.2%.

Table 4.3: Design parameters of NB base line and final solution.

Parameters	**A-1**	**A-1 (4,000km)**	**NB LH2**	**ΔA-1**	**ΔA-1 (4,000km)**
Max Take off Mass (kg)	71,218	72,499	72,675	2.0%	0.2%
Operating Empty Mass (kg)	47,257	48,072	48,199	2.0%	0.3%
Empty Mass (kg)	43,658	44,473	44,600	2.2%	0.3%
Payload Weight (kg)	18,414	18,414	18,414	0.0%	0.0%
Fuel (kg)	5,344	5,809	5,859	9.6%	0.9%
Engine Mass (kg)	5,017	5,099	5,053	0.7%	-0.9%
Average Block Fuel per Hour (kg)	1,002	1,022	1,065	6.3%	4.2%
Wing Area (m^2)	112.5	114.5	114.8	2.0%	0.3%
Each Engine Thrust (kN)	126.3	128.6	127.1 (28,575 lb)	0.7%	-1.1%
Number of PAX	198	198	198	0.0%	0.0%
Design Range (km)	3,700	4,000	4,000	8.1%	0.0%
Cruise Mach Number	0.78	0.78	0.82	5.1%	5.1%
T/W	.362	0.362	0.357	-1.4%	-1.4%
W/S (N/m^2)	6,210	6,210	6,210	0.0%	0.0%
Wing Sweep c/4 (deg)	25	25	25	0.0%	0.0%
Wing Aspect Ratio	9.5	9.5	10	5.3%	5.3%
Average Wing t/c (%)	11	11	12	9.1%	9.1%
Wing Span (m)	32.7	33.0	33.9	3.7%	2.7%
Fuselage Length (m)	48.5	49.1	49.2	1.4%	0.2%
Fuselage Diameter (m)	3.99	3.99	3.99	0.0%	0.0%
LH2 Tank Length (m)	8.62	9.26	9.33	8.2%	0.8%
LH2 Tank Weight (kg)	2,559	2,746	2,766	8.1%	0.7%
BPR	12	12	12	0.0%	0.0%
DOC CASK ($) 1,300 km, LH2 2$/kg	0.081	0.082	0.081	0.0%	-1.2%
DOC / BH ($/hr) 1,300 km, LH2 2$/kg	9,229	9,329	9,527	3.2%	2.1%
Purchasing Price (M$)	119.8	121.4	121.7	1.6%	0.2%

Around a 1% reduction may not be considered a significant reduction through the optimization process. However, we should note that the baseline design parameters are selected to be close to A320 parameters, which is already a highly efficient aircraft.

Another point worth mentioning is the optimal cruise Mach number. In the optimal case, block fuel increases but we have a lower CASK with respect to A-1 4,000 km. This result stems from the fact that some components of DOC, such as ownership and insurance costs, are dependent on the flight cycle, while others, like crew costs, are dependent on flight hours. The block time would be reduced due to the higher cruise speed, but the reduction is not significant. However, due to the higher speed, there would be a higher flight cycle per year, which reduces the share of ownership costs and other expenses dependent on the flight cycle.

As explained in subsection 3.6, aircraft manufacturers determine the optimal cruise speed based on the maximum cruise efficiency parameter (ML/D), which represents the lower specific fuel consumption. Based on the findings and explanations in subsection 4.5, the economic cruise speed is strongly dependent on fuel price. Assuming a forecasted hydrogen price, it is estimated that a cruise Mach number of 0.82 is the optimum value.

For empty mass breakdown and more detail parameters of NB LH2, obtained by HYPERION, please refer to Appendix B. In addition, Figure 4.10 depicted a relative sizes comparison of NB LH2 with A321 aircraft that fuselage length and wing span is in the order of current NB aircraft.

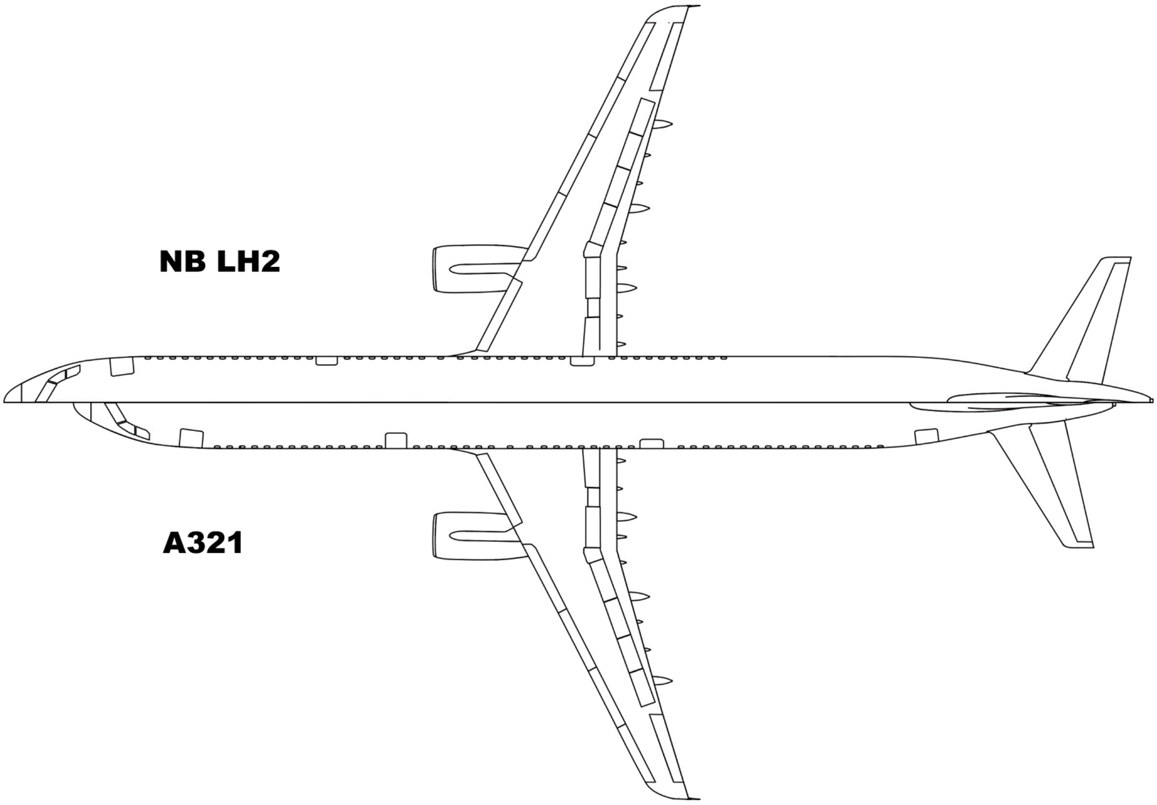

Figure 4.10: Size comparison of NB LH2 and A321.

The solution presented was sized based on a more likely fuel price of 2 $/kg in 2035. As mentioned in the previous section, changes in fuel price lead to variations in the optimum cruise Mach number, which in turn drives shifts in the optimum solution.

Figure 4.11 and Figure 4.12 shows the results of aircraft sizing for a range of cruise Mach numbers relative to an expected range of fuel prices. Based on these results, the deviation of optimum case MTOM and EM are 0.5% for each 1 $/kg variation in fuel price.

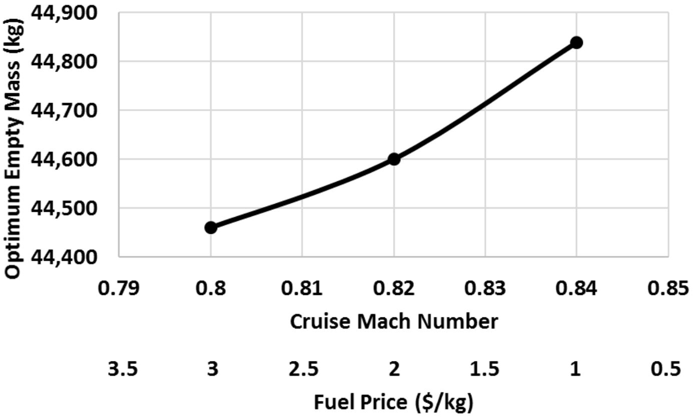

Figure 4.11: Effect of fuel price on empty mass of optimum solution for NB.

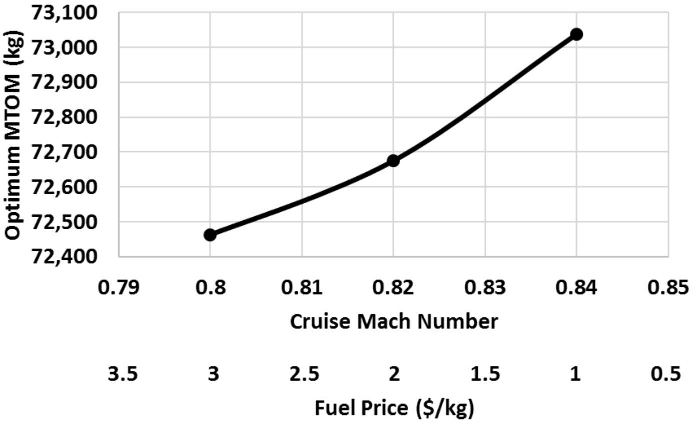

Figure 4.12: Effect of fuel price on MTOM of optimum solution for NB.

As mentioned in the previous sections, LH2 aircraft have a relatively lower wing area and higher drag coefficient compared to current passenger aircraft due to their lower MTOM and longer fuselage. This property affects the (L/D)max. As shown in Figure 4.13, the NB LH2 suffers from a 30% lower (L/D)max compared to kerosene burning airliners. To address this degradation, the implementation of an ultra-high aspect ratio wing is recommended.

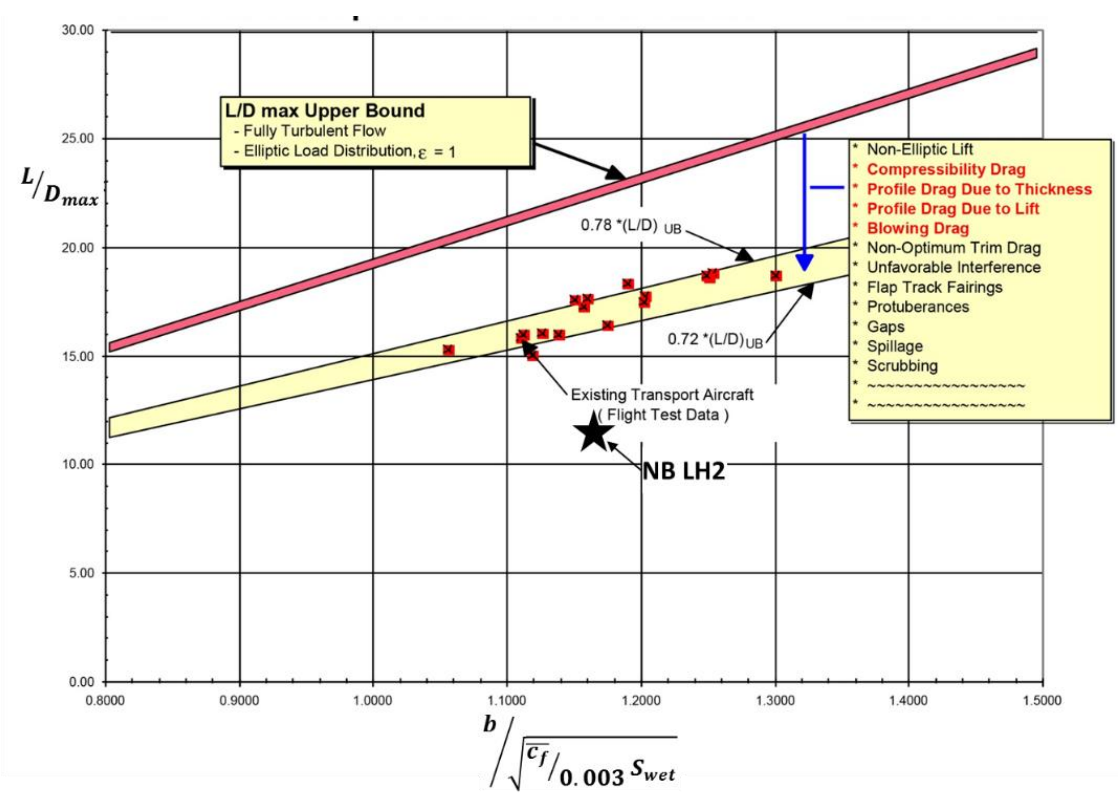

Figure 4.13: Potential L/D max for subsonic transport aircraft and NB LH2 [71].

5 Widebody Design Study

This chapter presents the results of the trade-off analysis for the WB aircraft. The range and capacity considered in the study cover the market demand beyond the capabilities of the NB aircraft. The chapter also includes the trade-off design and analysis results for the number of abreast variations, wing parameters, and the effect of cruise Mach number on DOC. The assessment procedure is the same as explained in Chapter 4.

5.1. Baseline WB Aircraft

The baseline for the WB trade study (B-1) is an aircraft with a capacity of 300 passengers, a seat pitch of 32 inches, and a design range of 14,800 km. It meets the performance requirements outlined in Table 1.3. The design characteristics and results of the B-1 case are listed in Table 5.1.

Table 5.1: WB baseline case design parameters.

Parameter	**B-1**
Max Take off Mass (kg)	191,909
Operating Empty Mass (kg)	127,613
Empty Mass (kg)	122,256
Payload Weight (kg)	27,900
Fuel (kg)	36,203
Engine Mass (kg)	13,674
Average Block Fuel per Hour (kg)	2,103
Wing Area (m^2)	260
Each Engine Thrust	371.4 kN (83,485 lb)
DOC CASK ($) @ 5,550 km stage, LH2 2 $/kg	0.069
DOC / BH ($/hr) @ 5,550 km stage, LH2 2 $/kg	16,872

5.2. Number of Abreast Trade Off

The number of abreast for the WB aircraft varies from 7 abreast in smaller WBs like the B767 to 10 abreast in larger WBs such as the A380 and B747, which are no longer in production. However, 8 and 9 abreast configurations are the most common.

From Table 5.2, it can be observed that the 8 abreast configuration has a lower DOC and MTOM compared to the 9 abreast configuration. Despite achieving a shorter fuselage length by changing from 8 to 9 abreast, the increase in fuselage diameter leads to an increase in fuselage mass, which offsets the mass savings from the fuselage length reduction.

In the 9 abreast configuration, MTOM increased by 0.6% and cost increased by 0.4%. The reduction in fuel mass by 0.4% indicates a decrease in drag due to the shorter fuselage length.

Table 5.2: Number of abreast effect on WB design parameters.

Parameters	**B-1**	**9 Abreast case**	**Δ%**
Max Take off Mass (kg)	191,909	192,988	0.6%
Empty Mass (kg)	122,256	123,475	1%
Fuel (kg)	36,203	36,063	-0.4%
Average Block Fuel per Hour (kg)	2,103	2,095	-0.4%
Wing Area (m^2)	260	262	-0.6%
Each Engine Thrust	371.4 kN (83,485 lb)	373.5 kN (83,954 lb)	0.6%
T/W	0.395	0.935	0%
W/S (N/m^2)	7,238	7,238	0.0%
CASK ($) @ 5,550 km stage, LH2 2 $/kg	0.069	0.069	0.4%
DOC/BH @ 5,550 km stage, LH2 2 $/kg	16,872	16,942	0.4%
Purchasing Price (M$)	323.5	326.2	0.4%

5.3. Range and PAX Trade off

A design range of 6,000 km to 12,000 km and a passenger capacity of 250 to 400 have been defined for the trade-off analysis. Similar to the NB aircraft, the CASK gain is greater at lower ranges and higher passenger capacities.

Figure 5.1 illustrates the relationship between passenger capacity and design range on the DOC parameter and in Figure 5.2 the effects of those parameters on OEM reported. The selection of the best basic version of the WB family is based on the slenderness parameter. The entire family must meet market requirements of a design range beyond 15,000 km and a passenger capacity of 400 (not necessarily concurrently).

To avoid surpassing the historical highest value, the design range limitation has been set at 15,000 km with 350 passengers (Figure 5.3). By limiting the design range of the WB basic version to 12,000 km with 350 passengers, it allows for longer versions with higher ranges and versions with more passengers to meet shorter-range demands.

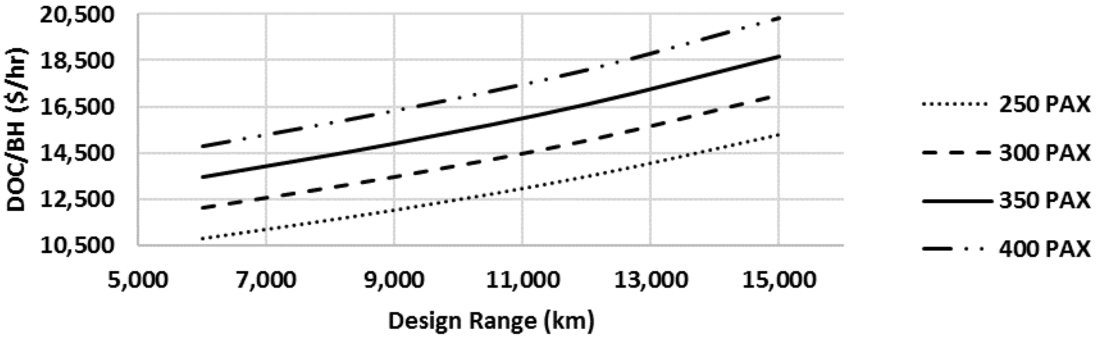

(a) WB DOC per BH for 2 $/kg fuel price.

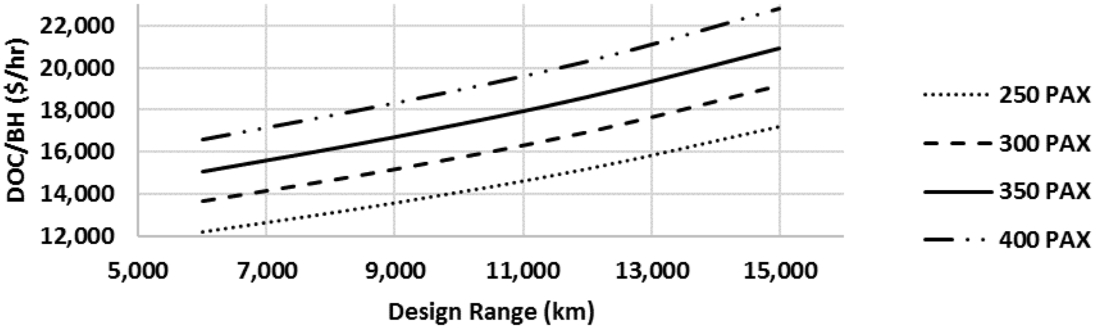

(b) WB DOC per BH for 3 $/kg fuel price.

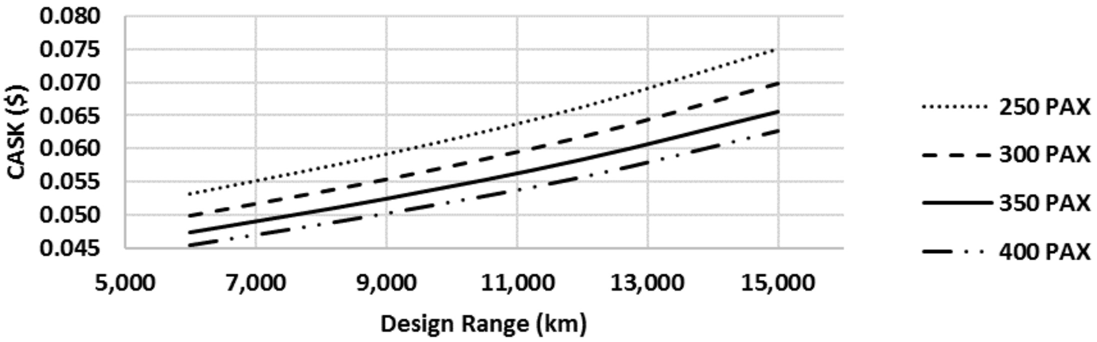

(c) WB CASK for 2 $/kg fuel price.

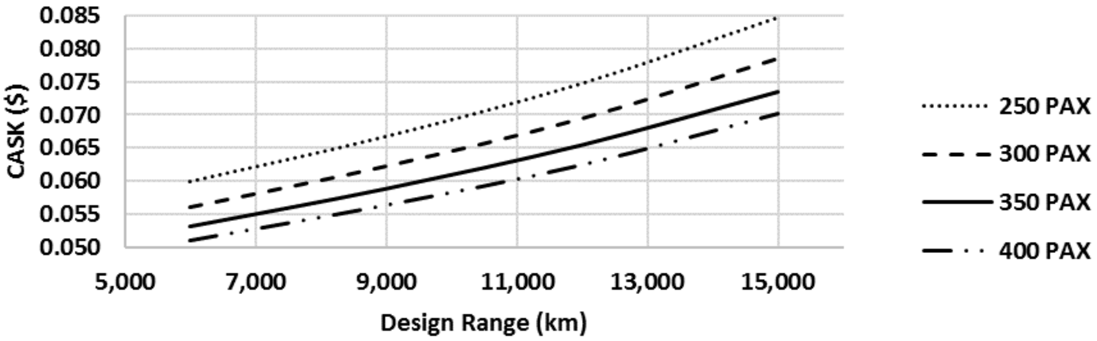

(d) WB CASK for 3 $/kg fuel price.

Figure 5.1: Trade off design range vs PAX for NB on DOC.

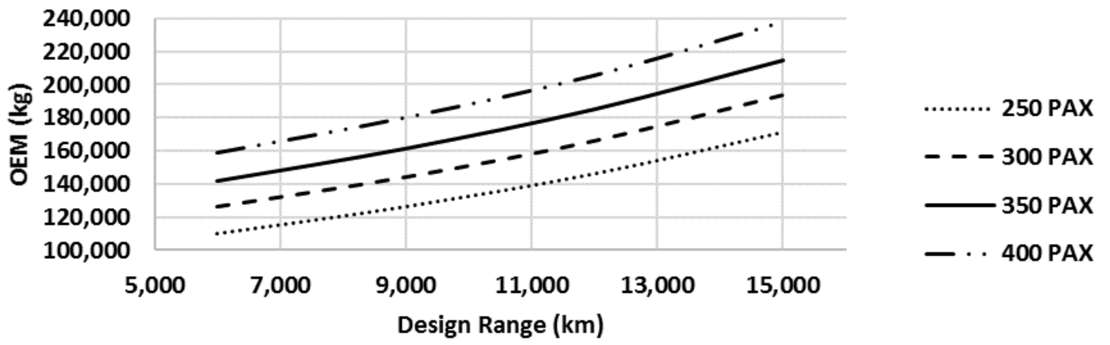

Figure 5.2: The effect of range and PAX on OEM for WB.

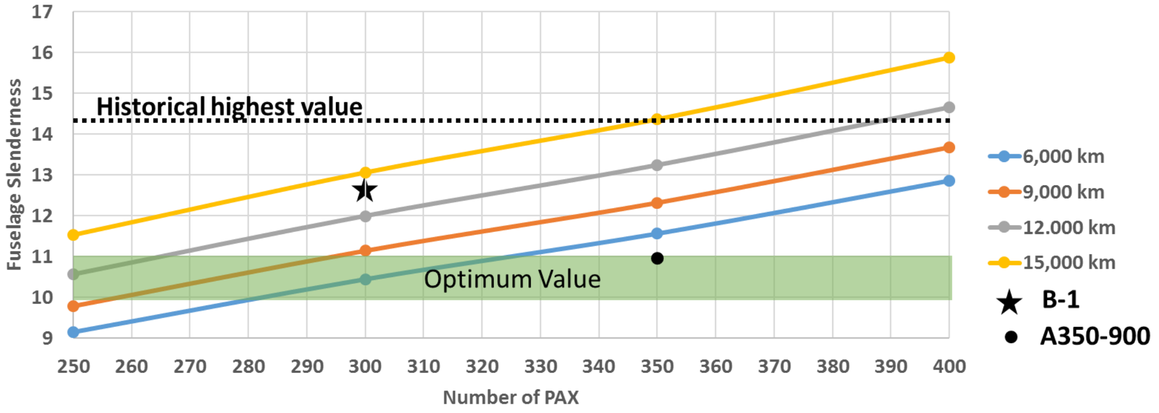

Figure 5.3: Fuselage slenderness for WB trade off cases.

5.4. Wing Parameters Trade Off

The trade off wing parameters present in Figure 5.6. As expected, all observations for wing sizing are the same as for the NB aircraft, except that due to the higher cruise Mach number, the sweep angle of 25° and 30° at AR=10 are closer to the optimum point of CASK.

Another observation is that, even though changing the t/c from 10% to 12% at a sweep angle of 30° changes MTOM (Figure 5.4) but does not have any variation in block fuel (Figure 5.4). To select the optimum point, a t/c of 12% would likely encounter aeroelastic issues or at least pose a risk of extensive development activities. It is within a safe margin to select an AR of 10, a sweep angle of 30°, and a t/c of 10% for the WB wing.

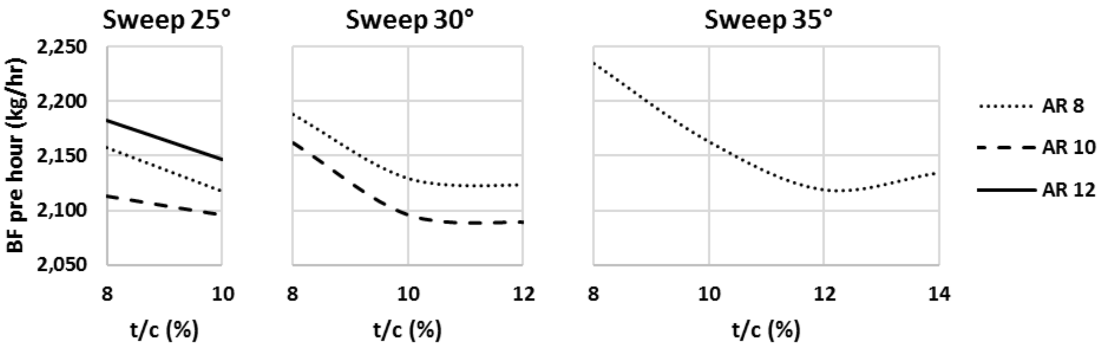

Figure 5.4: Block fuel per hour for WB wing parameters trade off.

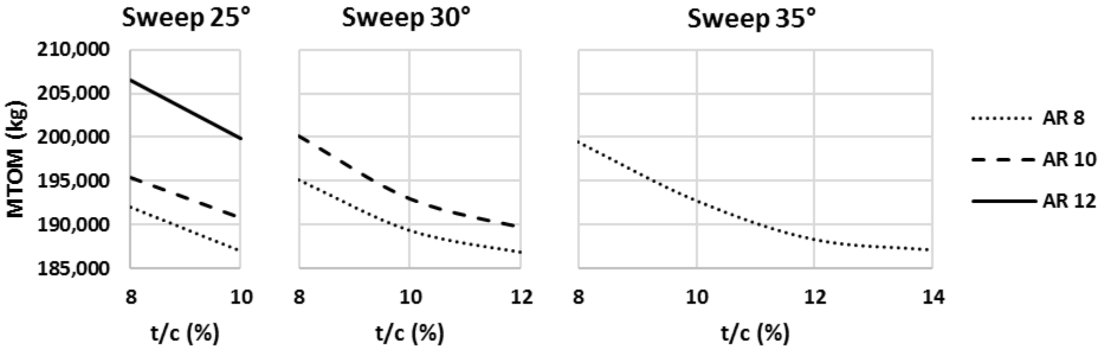

Figure 5.5: MTOM for WB wing parameters trade off.

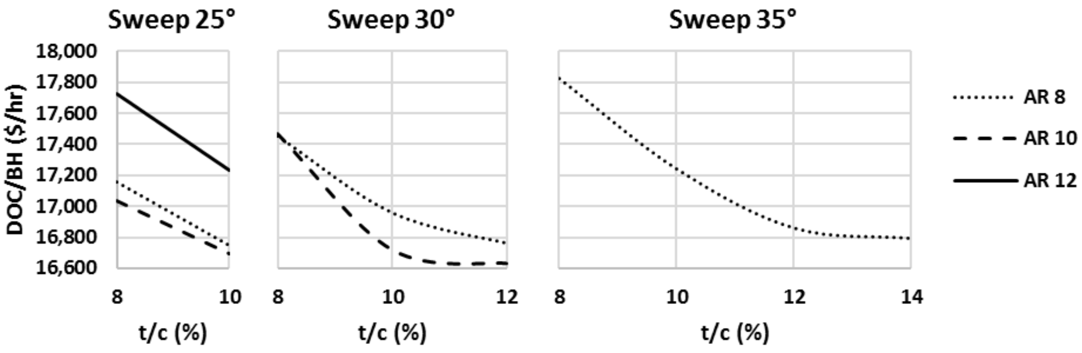

(a) DOC per BH for fuel price 2 $/kg.

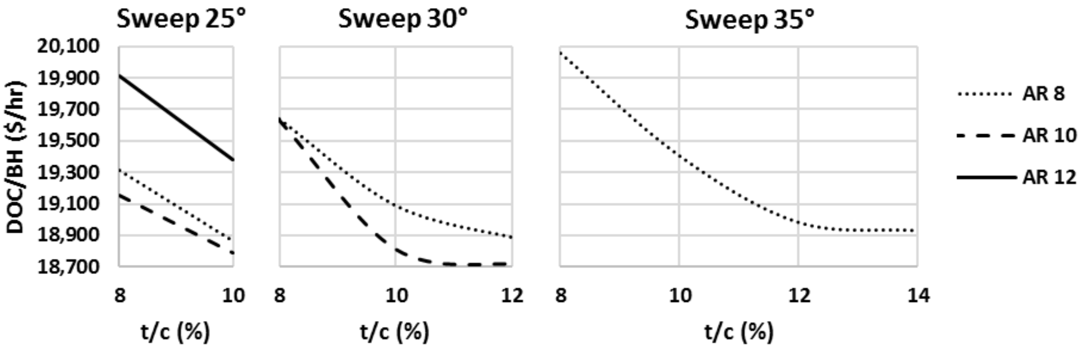

(b) DOC per BH for fuel price 3 $/kg.

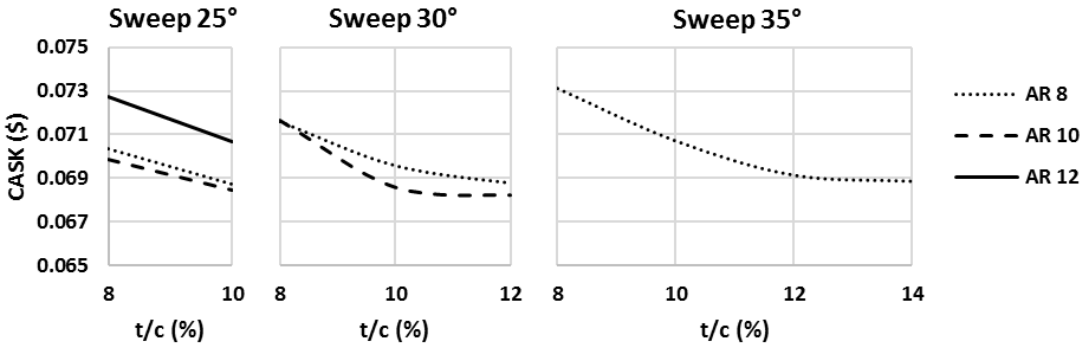

(c) CASK for fuel price 2 $/kg.

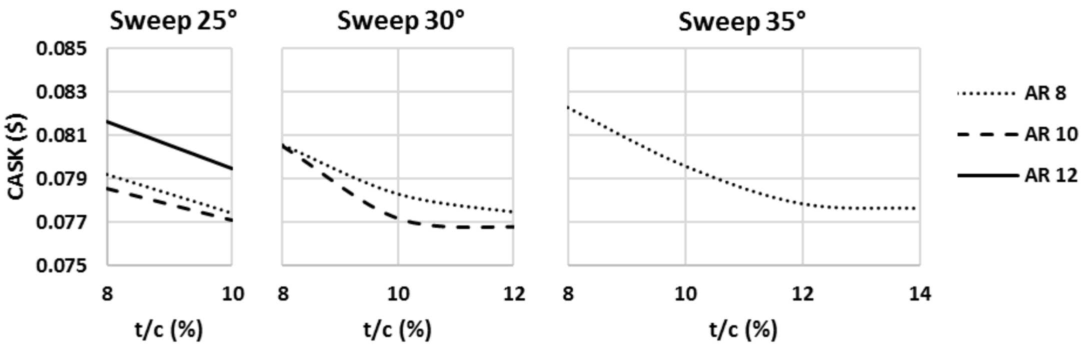

(d) CASK for fuel price 3 $/kg.

Figure 5.6: DOC of wing parameters trade off for WB.

5.5. Cruise Speed Trade Off

At the optimum point of wing parameters, a trade-off study on cruise Mach number was conducted. Figure 5.7 demonstrates how cruise speed affects DOC parameters for a stage length of 5,550 km.

In these cases, increasing the LH2 price from 1 $/kg to 3 $/kg would decrease the optimum cruise speed from M=0.87 to M=0.85. It is also observed that the sensitivity of CASK vs cruise Mach number is not as strong as in the NB case. A higher sweep angle results in a lower deviation of drag in the transonic regime.

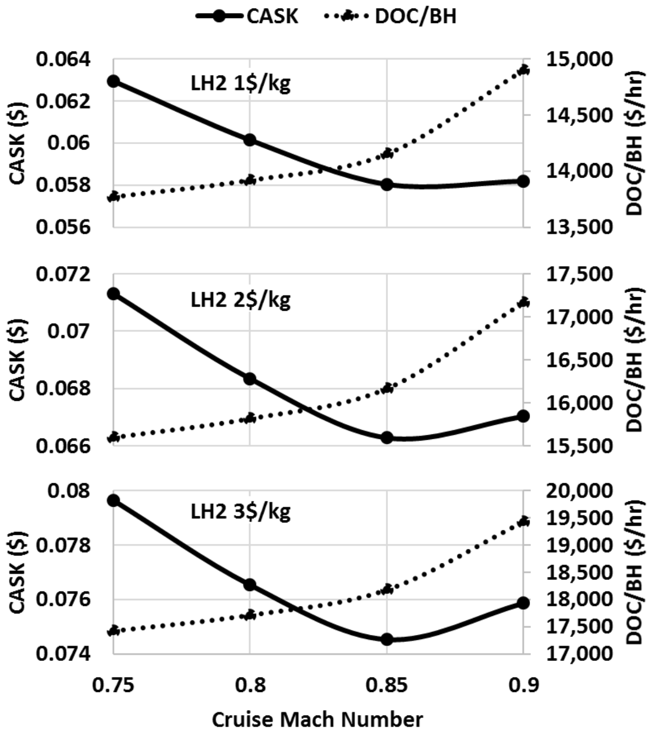

Figure 5.7: Effect of cruise Mach number on DOC for WB.

5.6. WB Design Solution

Preliminary sizing of the final solution for the WB LH2 aircraft was performed based on the parameters observed in the trade-off analysis. Table 5.3 presents the baseline (B-1) and final solution (WB LH2), showing that the optimum solution has a 17% higher payload weight, a 19% lower design range, and a 16% reduced CASK compared to the baseline.

For empty mass breakdown and more detail parameters of the WB LH2 aircraft, obtained by HYPERION, please refer to Appendix B. To compare the relative sizes of the current leading WB aircraft (B787-8) and WB LH2, Figure 5.8 is presented. Unlike the NB LH2, the elongation in fuselage is significant compared to the current WB aircraft. It conveys the massage that in the case of WB LH2 we need to taller LDG and have more issues related to airport handling, furthermore numerous considerations about the long fuselage.

Table 5.3: Design parameters of WB base line and final solution.

Parameters	**B-1**	**WB LH2**	**Δ%**
Max Take off Mass (kg)	191,909	185,238	-3.5%
Operating Empty Mass (kg)	127,613	124,150	-2.7%
Empty Mass (kg)	122,256	117,931	-3.5%
Payload Weight (kg)	27,900	32,550	16.7%
Fuel (kg)	36,203	28,350	-21.7%
Engine Mass (kg)	13,674	12,795	-6.4%
Average Block Fuel per Hour (kg)	2,103	1,647	-21.7%
Wing Area (m^2)	260	251	-3.5%
Each Engine Thrust	371.4 kN (83,485 lb)	345.8 kN (77,727 lb)	-6.9%
Number of PAX	300 (32″ seat pitch)	350 (32″ seat pitch)	16.7%
Number of Abreast	8	8	0.0%
Design Range (km)	14,800	12,000	-18.9%
Cruise Mach number	0.85	0.85	0.0%
T/W	0.395	0.381	-3.5%
W/S (N/m^2)	7,238	7,238	0.0%
Wing Sweep c/4 (deg)	30	30	0.0%
Wing Aspect Ratio	9.5	10	5.3%
Average Wing t/c (%)	10	10	0.0%
Wing Span (m)	49.7	50.1	0.8%
Fuselage Length (m)	76.7	78.2	2.0%
Fuselage Diameter (m)	5.91	5.91	0.0%
LH2 Tank Length (m)	23.7	19.0	-19.8%
LH2 Tank Weight (kg)	15,647	12,527	-19.9%
BPR	12	12	0.0%
CASK ($) @ 5,550 km stage, LH2 2 $/kg	0.069	0.058	-15.9%
DOC/BH ($/hr) @ 5,550 km stage, LH2 2 $/kg	16,872	16,432	-2.6%
Purchasing Price (M$)	323.5	309.3	-4.4%

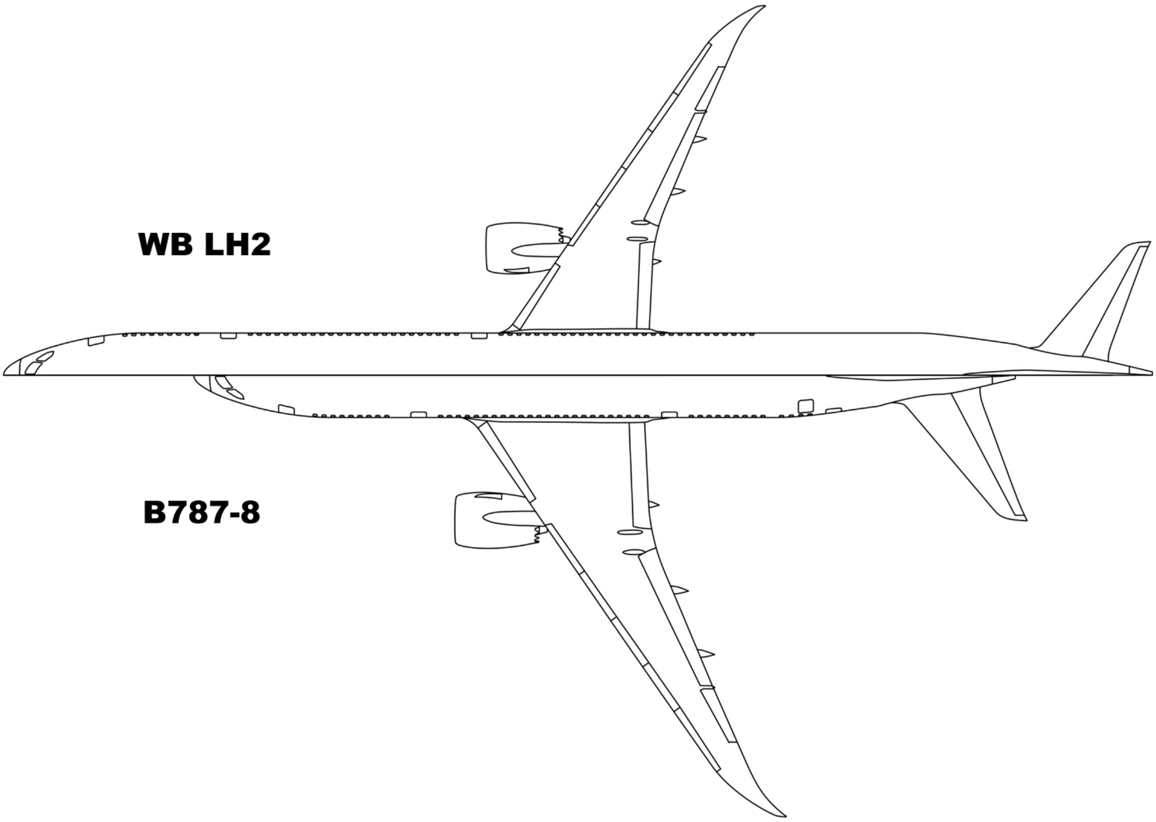

Figure 5.8: Size comparison of WB LH2 and B787-8.

The solution presented was sized based on a more likely fuel price of 2 \$/kg in 2035. Figure 5.9 and Figure 5.10 shows the results of aircraft sizing for a range of cruise Mach numbers that are relative to an expected range of fuel prices. It has been shown that the deviation of optimum case MTOM and EM is 0.2% for each 1 \$/kg variation in fuel price.

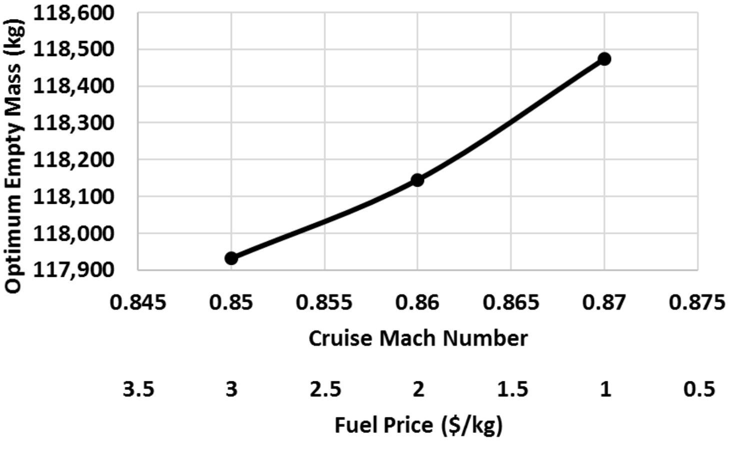

Figure 5.9: Effect of fuel price on empty mass of optimum solution for WB.

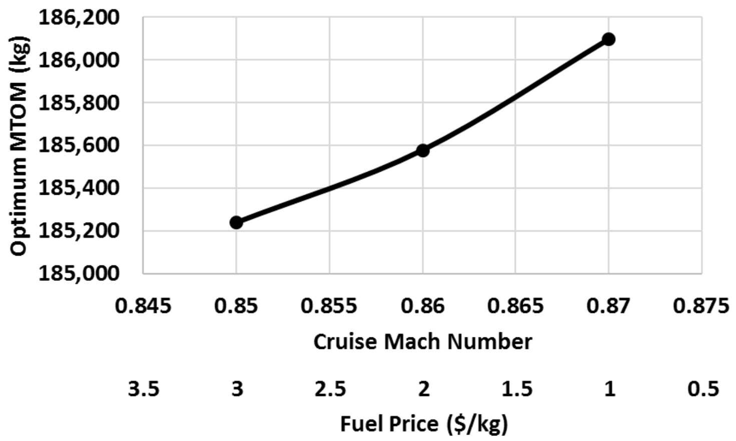

Figure 5.10: Effect of fuel price on MTOM of optimum solution for WB.

Same as NB solution, the WB LH2 also has degradation in term of (L/D)max. Its reported in Figure 5.11.

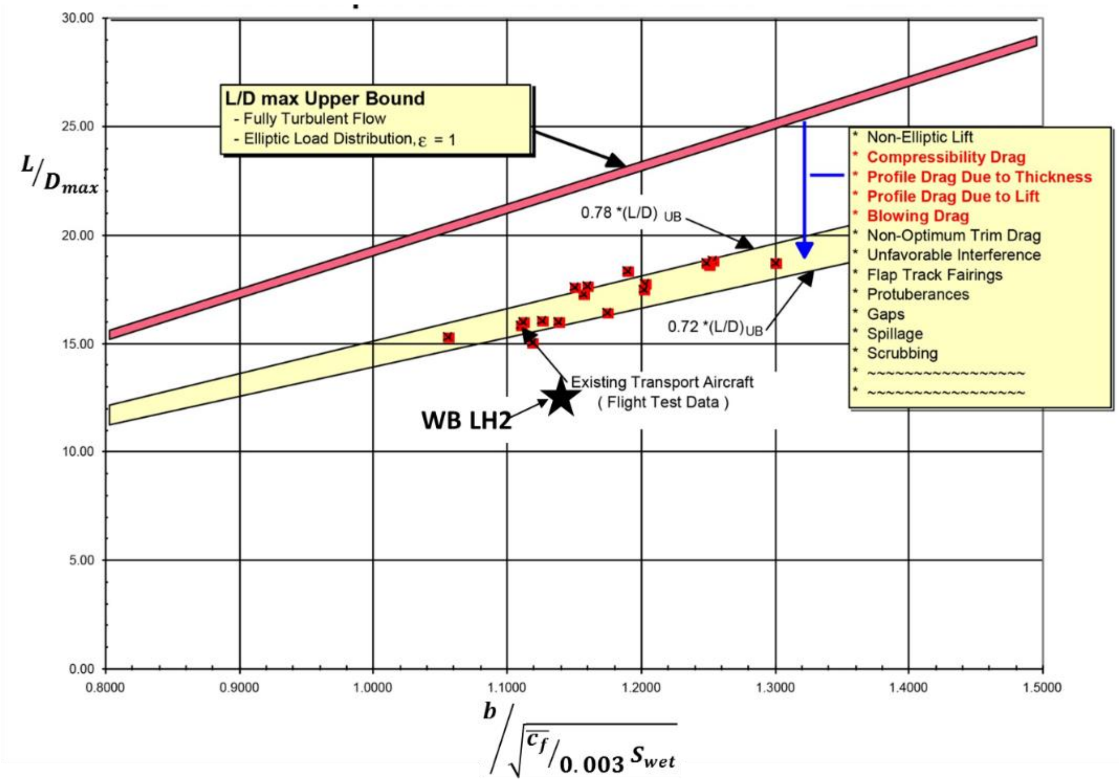

Figure 5.11: Potential L/D max for subsonic transport aircraft and WB LH2 [71].

6 Summary and Conclusion

The focus of this research is to incorporate liquid hydrogen (LH2) as an aviation fuel in narrow and widebody airliners. Directly burning LH2 in a gas turbine overcomes the limitations of other types of green energy, such as fuel cells and batteries, which have restrictions in terms of speed and range in aviation transport.

By applying the methodology and design tools reviewed in the project, the study explores the possibility of finding an optimum design solution in terms of economy. Through a family planning approach for both narrow-body and wide-body aircraft, it is potentially possible to cover almost the entire aviation transport market demand. Only in ultra-long flights, LH2 aircraft have limitations, but their contribution to these flights are insignificant in terms of flight frequency.

The research aims to adapt the current tube and wing jetliner configuration to avoid radical changes and new technology investments and offer a faster entry into service. To accommodate cryogenic tanks, the fuselage needs to be elongated by approximately 20% for narrow-body aircraft and 35% for wide-body aircraft. Additionally, LH2 aircraft have a naturally lower lift-to-drag ratio compared to kerosene-fueled aircraft, which poses another challenge. The lift-to-drag ratio of LH2-burning aircraft is typically around 11 to 12, while for kerosene-burning aircraft, it is in the range of 17 to 20.

The methodology used in this research involves the use of a design tool called HYPERION, which allows for the examination of different scenarios to find optimal solutions. The cost model used in the research accurately estimates Research, Development, Test, and Evaluation, Acquisition, and Direct Operating Cost. The sizing design tools and methodology, combined with the cost model, are accurate enough for conceptual design optimization and capable of calculating the optimum point the aircraft.

The goal is to find optimal solutions for narrow-body and wide-body aircraft that meet market demands while reducing environmental impact. The basic variant of NB with a range of 4,000 km and 200 passengers is the best option for NB, while the basic variant of WB with a range of 12,000 km and 350 passengers would be a good estimation. However, LH2-burning aircraft have limitations in terms of range and passenger capacity. The LH2 mid-range narrow-body class and ultra-long-range wide-body passenger aircraft have specific limitations in these aspects.

The project also found that production cost is the main driver of DOC. Technological advancements that improve fuel consumption do not significantly reduce DOC. The major variables in the trade-off sizing for DOC are technology level, number of passengers, and design range. For example, applying more than 50% composite materials and using an engine with a BPR of 12 can decrease DOC by 14% and fuel consumption by 36% in comparison of A320-200 technology level. However, the wing's optimization within the range of aspect ratio 8 to 12 has not a significant influence on the overall DOC. The effect would be around 3% to 5% on DOC dependent to the payload-range parameters.

Furthermore, the project found that LH2-burning aircraft have higher operational empty mass by 15% for NB and 5% for WB, as well as lower maximum takeoff mass by 1% for NB and 19% for WB compared to kerosene versions. These numbers strongly vary depending on the aircraft payload weight and design range. In addition, in the case of different basic variant with changing in payload-range parameter, the order of numbers would by varied.

In addition, the analysis takes into account the impact of fuel prices on operational assumptions. It is found that while fuel prices do have an impact on the operational scenario, they have a negligible effect on the optimal solution.

Further research is needed to fully assess the capability and economic viability of using LH2 in commercial aircraft compared to current kerosene-burning aircraft. Collaboration with industry stakeholders, regulatory bodies, and research institutions is essential to address regulatory and certification challenges associated with LH2 use in commercial aircraft. By addressing these challenges and conducting comprehensive research, the aviation industry can make significant progress towards adopting LH2 as a sustainable fuel option and achieving its goals of decarbonizing aviation.

In this regard and in line with the initial goals of the project, the following activities are proposed to address the limitations identified in this study:

1. The method for DOC estimation in this project, although able to follow the trend of cost versus changes in other driver parameters and has enough accuracy to be used in cost optimization, lacks sufficient information on the actual values of DOC. In order to provide a justification that accurately determines the cost change from switching to a hydrogen burning aircraft (which most likely it forces higher operational cost) from a kerosene burning one, a more precise DOC method is required. Initially, the lack of real data on DOC components of airliners is acknowledged. Additionally, it is necessary to obtain an accurate flyaway cost for LH2 aircraft. Based on these considerations, it is recommended to conduct a project that focuses on extracting real DOC data and calibrating the current method accordingly. Furthermore, the cost estimation method should be calibrated to accurately determine the realistic flyaway cost of a hydrogen burning aircraft.

2. Design study on utilization an ultra-high aspect ratio wing, in the order of 20, to achieve increase in aerodynamic efficiency as close as possible to L/D_{max} upper bound (Figure 4.13 and Figure 5.11) and the effect on DOC reduction. This study will focus on analyzing the design parameters and configurations that can optimize the wing's parameters for maximize potential L/D and minimizing of DOC.

3. Design study on the possibility and effects of incorporating split main tanks and added auxiliary fuel tanks in and ahead of the center wing for longer range variants of the aircraft. This study will refine the current design study and investigate the impact on overall range capabilities and effect on DOC.

4. Research study on solutions to address maintenance, repair and overhaul issues related to cryogenic fuel tanks and their impact on DOC. This study will explore potential issues and solutions of reliability, maintainability, and operability of cryogenic fuel tanks, which can contribute to changing operational costs.

These topics reflect the valuable insights into improving aerodynamic efficiency, extending range capabilities, optimizing wing design, and addressing issues related to cryogenic fuel tanks that have remarkable impacts on DOC.

Bibliography

[1] E.v.d Sman, B. Peerlings, R. Lieshout, T. Boonekamp, "Destination 2050 - A route to net zero European aviation", NLR, NLR-CR-2020-510, 2021.

[2] "Net zero resolution", International Air Transport Association, 2022. Available: www.iata.org/flynetzero

[3] "The future of aviation: no longer one size fits all", Aviation Week & Space Technology, February 7-20, 2022.

[4] M. Bruno, "Tectonic shift, sustainability's effects on air transport may be capped", Aviation Week & Space Technology, May 30-June 12, 2022.

[5] B. Graver, K. Zhang, D. Rutherford, "CO2 emissions from commercial aviation 2018", International Civil Aviation Organization, A40-WP/560, 2019.

[6] K. Michaels, "Farewell to fast growth why it's a big deal", Aviation Week & Space Technology, October 10-23, 2022.

[7] “The high energy cost of decarbonizing aircraft propulsion", Aviation Week & Space Technology, May 23 - June 4, 2023.

[8] H. Webber, S. Job, "Primary energy source comparison and selection", Aerospace Technology Institute, FZ_0_6.1, 2021.

[9] G.D. Brewer, “Hydrogen aircraft technology", CRC Press, 1991.

[10] L.M. Nicolai, G.E. Carichner, "Fundamentals of aircraft and airship design, Volume I - Aircraft design", AIAA, 2010.

[11] E. Torenbeek, "Advanced aircraft design: conceptual design, analysis, and optimization of subsonic civil airplanes", John Wiley and Sons, 2013.

[12] J. Roskam, "Airplane design, part I: preliminary sizing of airplanes", Roskam Aviation and Engineering Corporation, 1985.

[13] L. Caccetta, "Preliminary sizing of hydrogen burning jet aircraft", M.S. thesis, Politecnico di Milano, 2022.

[14] L. Trainelli, C.E.D. Riboldi, F. Salucci, A. Rolando, "A general preliminary sizing procedure for pure-electric and hybrid-electric airplanes", Aerospace Europe Conference, 2020.

[15] L. Trainelli, C.E.D Riboldi, A. Rolando, F. Salucci, F. Oliviero, J. Pirnar,T. Koopman, A. Žnidar, " The design framework for an NZE 19-seater", 2020, Available: https://pipistrel.sharepoint.com/sites/UNIFIER19.

[16] G. Norris, "Engine makers face hydrogen combustion challenges", Aviation Week & Space Technology, October 12-25, 2020,

[17] "Tupolev Tu-155", Wikipedia.com, https://en.wikipedia.org/wiki/Tupolev_Tu-155 (accessed Aug. 1, 2023).

[18] "Tupolev develops ecologically clean Tu-156", Flight International, May 9-15, 1990.

[19] A. Postlethwaite, "East-West hydrogen fuel pact", Flight International, May 30 - June 5, 1990.

[20] "Liquid hydrogen fuelled aircraft - System analysis", Airbus Deutschland GmbH, 2003.

[21] "Enableh2", www.enableh2.eu, https://www.enableh2.eu/project-structure (accessed Aug. 1, 2023).

[22] G Norris, G. Warwick, "Green trio", Aviation Week & Space Technology, April 4-17, 2022.

[23] A.P.K. Helen, H. Leadbetter, C. Pickard, "Hydrogen infrastructure and operations", FZO-CST-POS-0035, 2022.

[24] J. Flottau, T. Dubois, "Airbus' big bet", Aviation Week & Space Technology, September 28 - October 11, 2020.

[25] "Global Market Forecast 2022", Airbus, 2022, Available: https://aircraft.airbus.com/en/market/global-services-forecast-gsf-2022-2041.

[26] "The next commercial aircraft battleground", Aviation Week & Space Technology, July 3-16, 2023.

[27] "Commercial Market Outlook 2022–2041", Boeing, 2022, Available: https://www.boeing.com/commercial/market/commercial-market-outlook/index.page.

[28] "Cirium Fleet Forecast, 2022-2041 Executive Summary", Cirium, 2023, Available: https://www.cirium.com/solutions/cirium-fleet-forecast/.

[29] "Orders and deliveries Commercial Aircraft", www.airbus.com, https://www.airbus.com/en/products-services/commercial-aircraft/market/orders-and-deliveries (accessed Aug. 1, 2023).

[30] "Orders & Deliveries", www.boeing.com, https://www.boeing.com/commercial/ (accessed Aug. 1, 2023).

[31] R. Aboulafia, "NMA delay, Why a Boeing launch is far from certain", Aviation Week & Space Technology, February 25 - March 10, 2019.

[32] R. Aboulafia, “Widebody woes", Aviation Week & Space Technology, May 2-15, 2022.

[33] R. Aboulafia, "World aircraft overview", Teal Group Corporation, 2021.

[34] "List of busiest passenger air routes", Wikipedia.com, https://en.wikipedia.org/wiki/List_of_busiest_passenger_air_routes (accessed Aug. 1, 2023).

[35] "Busiest routes", OAG, 2019, Available: https://www.oag.com/webinars/busiest-routes-2019.

[36] M.K. Jones, "Airbus begins tests to extend service life of A320 family", Flight International, 2008.

[37] D. Debney, "Zero-carbon emission aircraft concepts", Aerospace Technology Institute, FZO-AIN-REP-0007, 2022.

[38] J. Cole, W. McClintock, L. Powis, "Market forecasts & exploitation strategy", Aerospace Technology Institute, FZO-CST-REP-0043, 2022.

[39] M.K. Jones, "The long and short of it", Flight International, June 13-19, 2017.

[40] "Jane's all the world's aircraft in service 2020-2021", Jane’s Group, 2020.

[41] D.P. Raymer, "Aircraft design: a conceptual approach", AIAA, 2006.

[42] R. Aboulafia, “Glimmers of light why 2022 will be a better year", Aviation Week & Space Technology, January 10-23, 2022.

[43] R. Doganis, "Flying off Course The economics of international airlines", Routledge, 2002.

[44] "After many false starts, hydrogen power might now bear fruit", The Economist, July 7, 2020.

[45] W.M. Swan, N. Adler, " Aircraft trip cost parameters: A function of stage length and seat capacity", Elsevier, Transportation Research Part E 42 (2006) 105–115, 2005.

[46] E. Torenbeek, “Synthesis of Subsonic Airplane Design", Delft University Press, 1982.

[47] M. Fioriti, V. Vercella, N. Viola, "Cost-Estimating Model for Aircraft Maintenance", AIAA, Journal Of Aircraft, 2017.

[48] S. Ackert, "Aircraft maintenance handbook for financiers", Aircraft Monitor, ICAS 2021, 2018.

[49] C. Cabaleiro, M. Fioriti, L. Boggero, S. Corpino, P.D. Ciampa, B. Nagel, "Assessment of new technologies in a multi-disciplinary design analysis and optimization environment including rams and cost disciplines", ICAS, 2021.

[50] R. Falsetti, "Business jet conceptual design: a cost-driven approach", M.S. thesis, Politecnico di Milano, 2023.

[51] M. Daly, "Jane's aero-engine 2011", Jane' s Group, 2011.

[52] S. Ackert, "Commercial aspects of aircraft customization", Aircraft Monitor, 2013.

[53] G. Warwick, "Can new concepts reshape the narrowbody market", Aviation Week & Space Technology, June 17-30, 2019.

[54] A.S.J. van Heerden, M.D. Guenov, A.M. Cristóbal, "Evolvability and design reuse in civil jet transport aircraft", Elsevier, Progress in Aerospace Sciences 108 (2019) 121–155, 2019.

[55] B. Probert, "Aspects of wing design for transonic and supersonic combat aircraft", RTO NATO, RTO EN-4-19, 1998.

[56] S. Gudmundsson, "General aviation aircraft design: applied methods and procedures", Elsevier, 2014.

[57] D. Scholz, " Wing Design", Hamburg University of Applied Sciences Lecture Note,

[58] E. Obert, "Aerodynamic design of transport aircraft", Delft University Press, 2009.

[59] A.P. Hays, W.E. Beck, W.H. Morita, B.J. Penrose, R.E. Skarshaug, B. S. Wainfan, " Integrated Technology Wing Design Study", NASA, NASA CR-3586, 1982.

[60] R. Stüssel, "The airbus family progress and set-backs in development of European commercial aircraft", AIAA, AIAA-2003-2884, 2003.

[61] J.C. Fuchte, "Enhancement of Aircraft Cabin Design Guidelines with Special Consideration of Aircraft Turnaround and Short Range Operations", Ph.D. dissertation Hamburg University of Technical, 2014.

[62] "MPC75 aerodynamic data base", Deutsche Airbus GmbH, EF 14- /90, 1990.

[63] I. Kroo, "Drag due to lift: concepts for prediction and reduction", Annu. Rev. Fluid Mech. 2001. 33:587–617, 2001.

[64] R.S, Shevell, "Fundamentals of flight", Pearson, 1988.

[65] M. Nita, D. Scholz, " Estimation the Oswald factor from basic aircraft geometrical parameters", Deutscher Luft- und Raumfahrtkongress 2012, DocumentID: 281424, 2012.

[66] R.D. Schaufele, "The elements of aircraft preliminary design", Aries Publications, 2007.

[67] O. Samoylovitchq, D. Strelets, “Determination of the Oswald efficiency factor at the aeroplane design preliminary stage", Elsevier, Aircraft Design 3 (2000) 167-174, 2000.

[68] S. Howe, A.J. Kolios , F.P. Brennan, " Environmental life cycle assessment of commercial passenger jet airliners", Elsevier, Transportation Research Part D 19 (2013) 34–41, 2013.

[69] O. Criou, " A350 XWB family & technologies", Airbus, 2007.

[70] F. Lutsch, "Preliminary Aircraft Design", Design course at University of Stuttgart, 2007.

[71] B.M. Kulfan, "Revolutionary and evolutionary aspects of breakthrough supersonic technologies", The National Research Council, 2001.

[72] P. Belobaba, " Airline operating costs", Istanbul Technical University, 2014.

[73] McKinsey, "Hydrogen-powered aviation A fact-based study of hydrogen technology, economics, and climate impact by 2050", 2020.

[74] T. Hays, Private communication, Sep, 2023.

[75] Bjorn Fehrm, Bjorn's Corner: The challenges of hydrogen. Part20. Hydrogen airliner weight shift, January 15, 2021,

https://leehamnews.com/2021/01/15/bjorns-corner-the-challenges-of-hydrogen-part-20-hydrogen-airliner-weight-shift/, (accessed Sep. 1, 2023)

[76] T. Hays, Lecture note "Aerodynamic Analysis", 2003, Available: https://www.adac.aero

[77] F.T. Lynch, "Commercial Transports—Aerodynamic Design for Cruise Performance Efficiency", AIAA, 1982

A Appendix A

To supplement trend data related to DOC, number of PAX and design range are presented in this section.

A.1. NB trade off trend

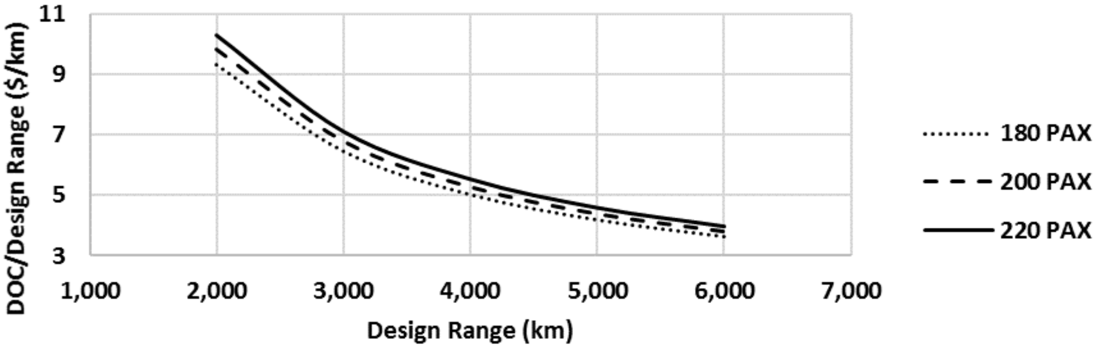

Figure A.1: NB trend of DOC per design range vs PAX and range for LH2 2 $/kg.

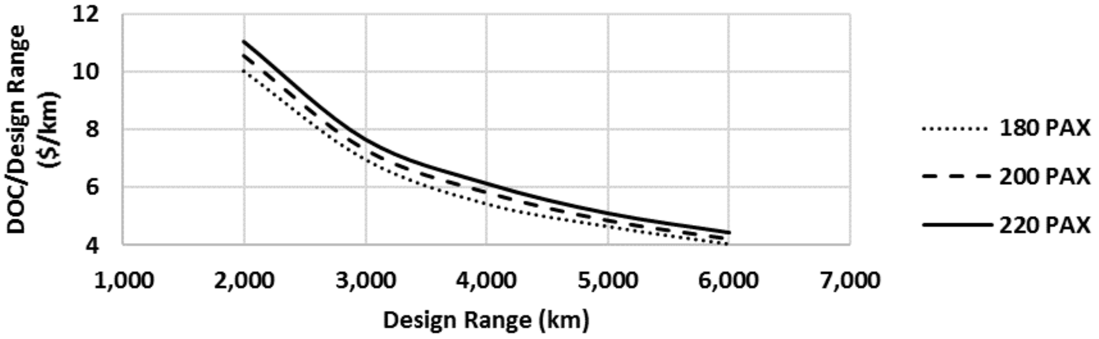

Figure A.2: NB trend of DOC per design range vs PAX and range for LH2 3 $/kg.

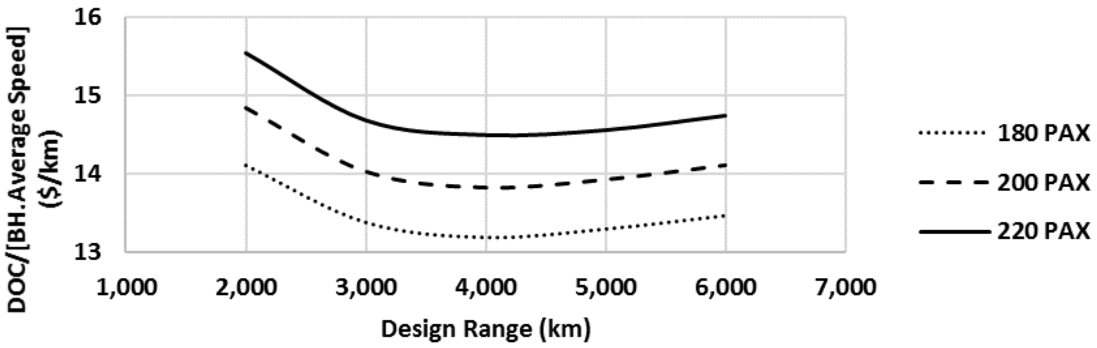

Figure A.3: NB trend of DOC per BH and average speed vs PAX and range for LH2 2 $/kg.

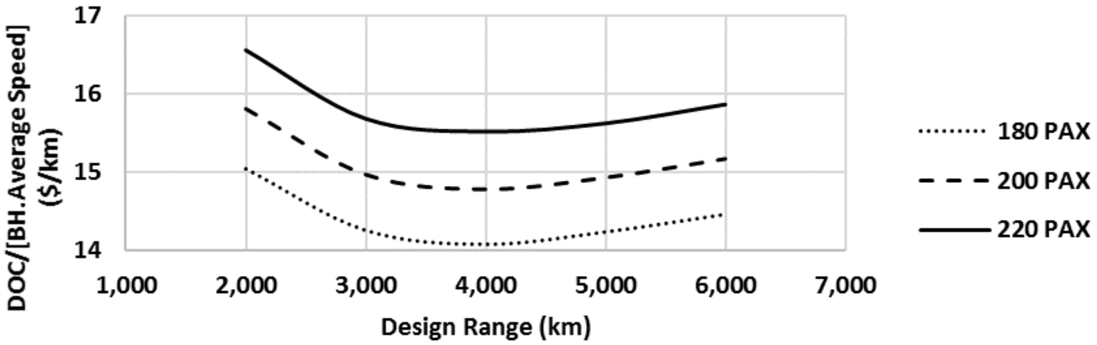

Figure A.4: NB trend of DOC per BH and average speed vs PAX and range for LH2 3 $/kg.

A.2. WB Trade off trend

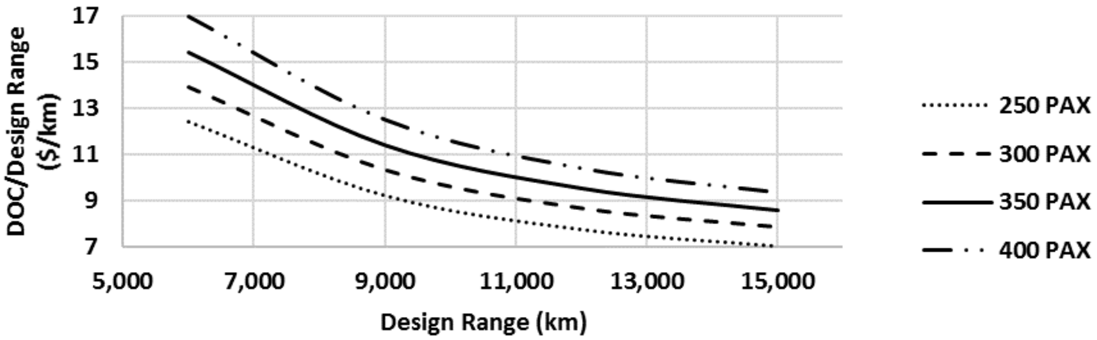

Figure A.5: WB trend of DOC per design range vs PAX and range for LH2 2 $/kg.

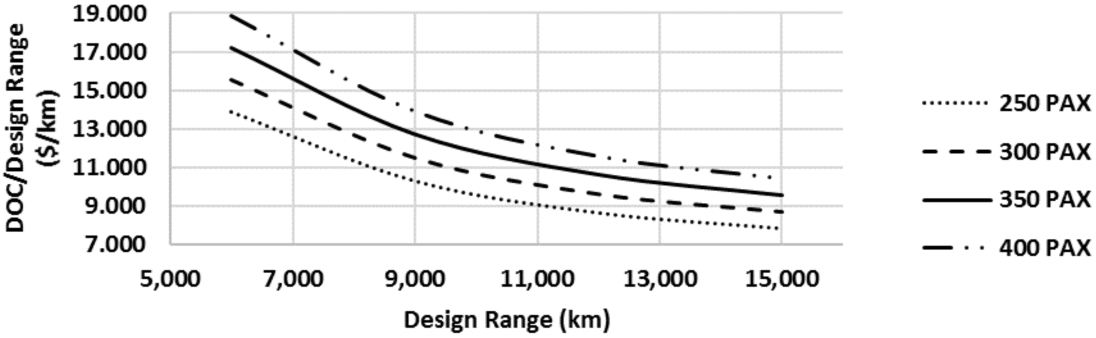

Figure A.6: WB trend of DOC per design range vs PAX and range for LH2 3 $/kg.

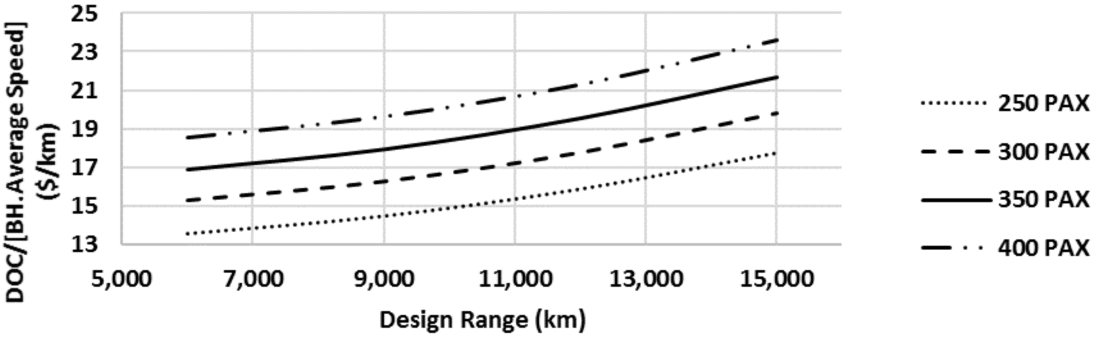

Figure A.7: WB trend of DOC per BH and average speed vs PAX and range for LH2 2 $/kg.

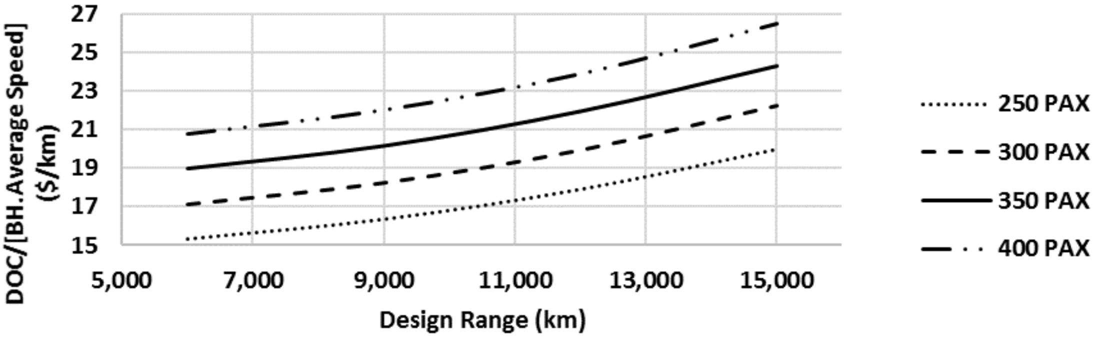

Figure A.8: WB trend of DOC per BH and average speed vs PAX and range for LH2 3 $/kg.

B Appendix B

In this section results of final solution of NB and WB which obtained by HYPERION are presented.

B.1. NB HYPERION Output of Final Solution

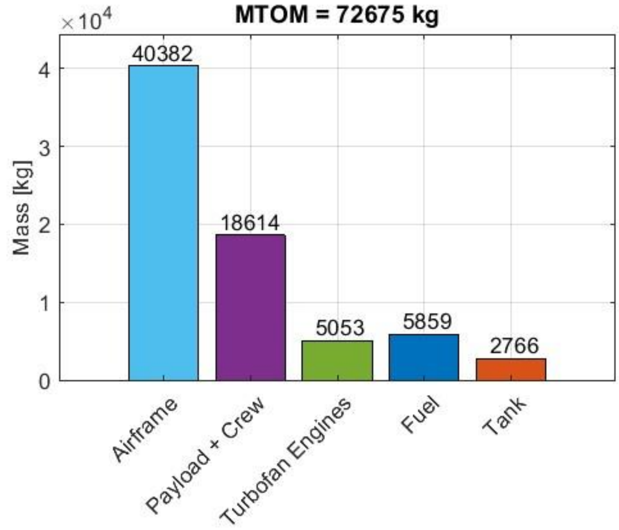

Figure B.1: MTOM and its components of NB LH2.

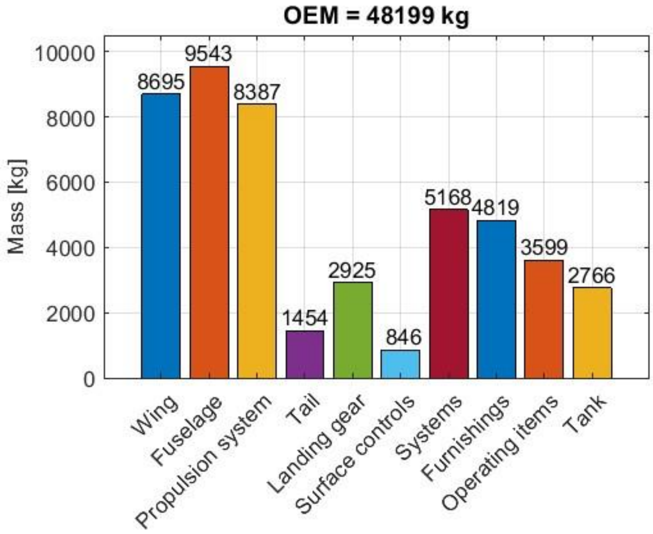

Figure B.2: OEM and its components of NB LH2.

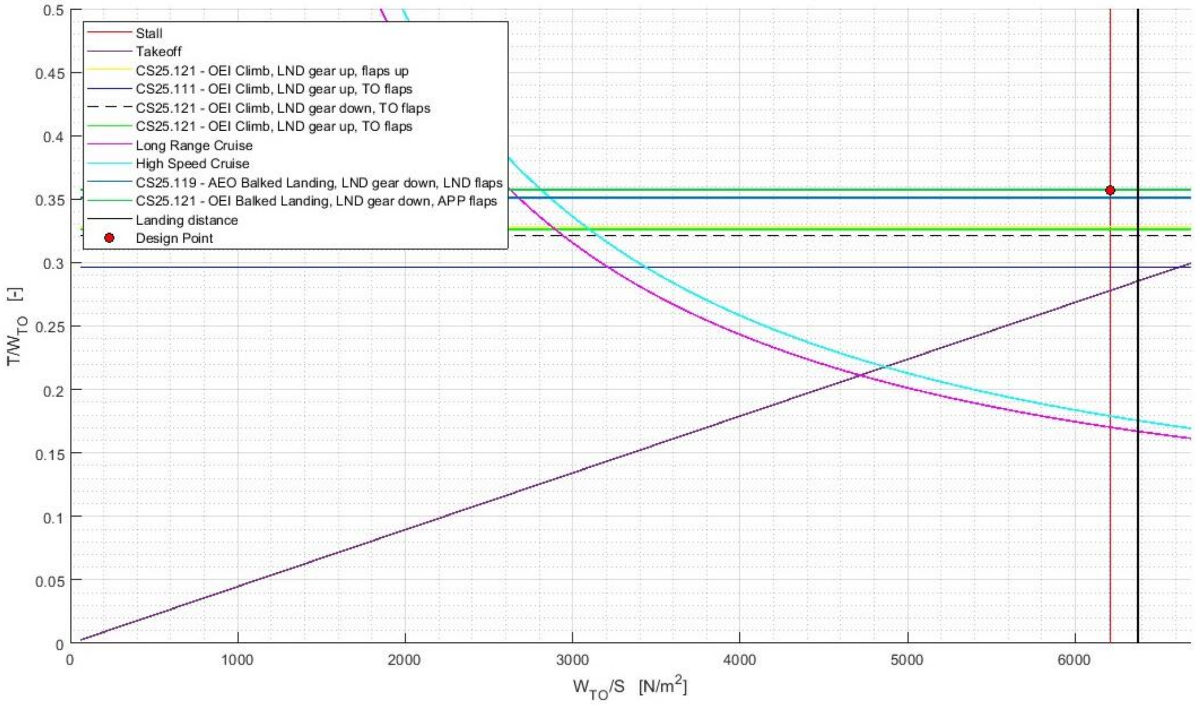

Figure B.3: Sizing matrix plot of NB LH2.

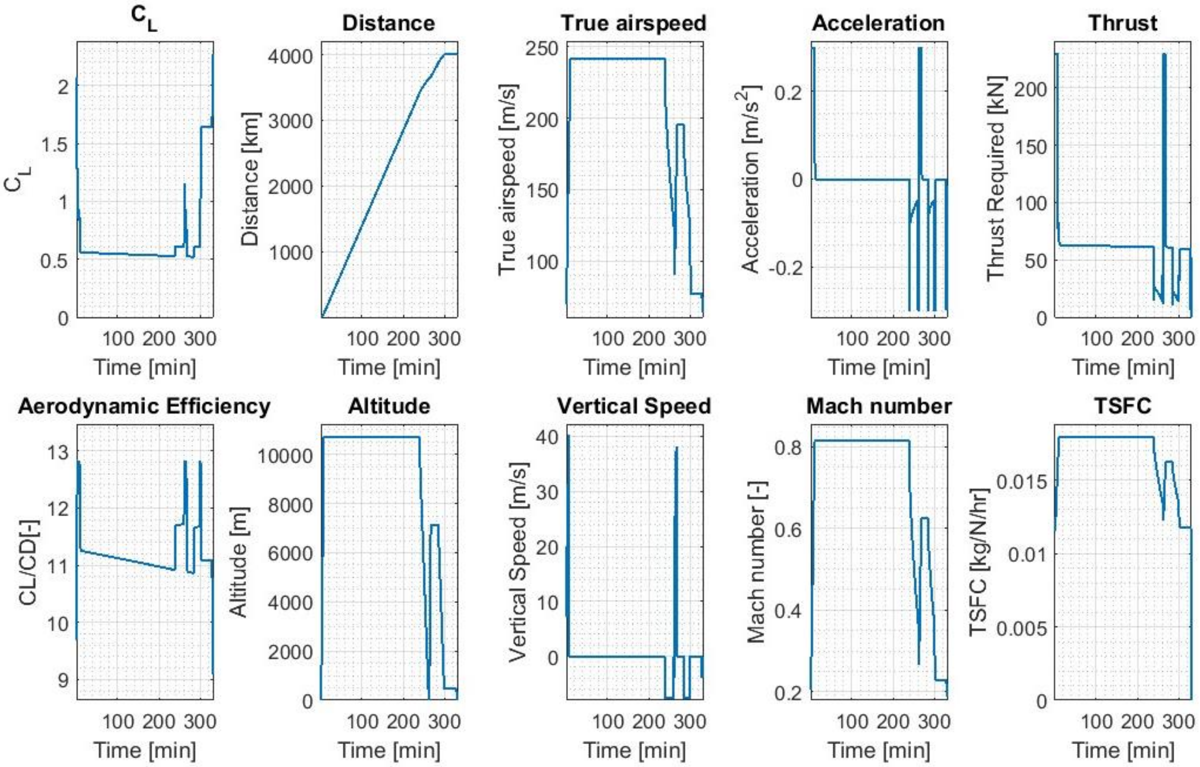

Figure B.4: Mission parameters histogram of NB LH2.

B.2. WB HYPERION Output of Final Solution

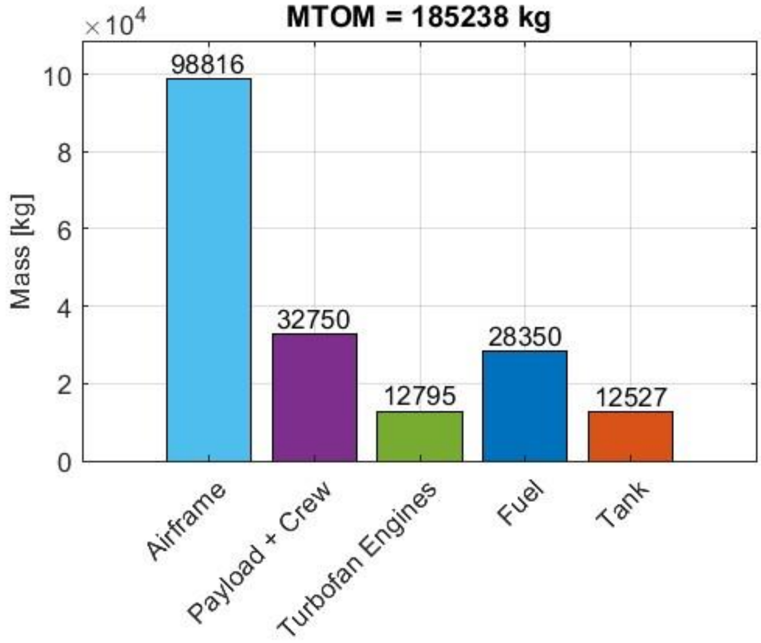

Figure B.5: MTOM and its components of WB LH2.

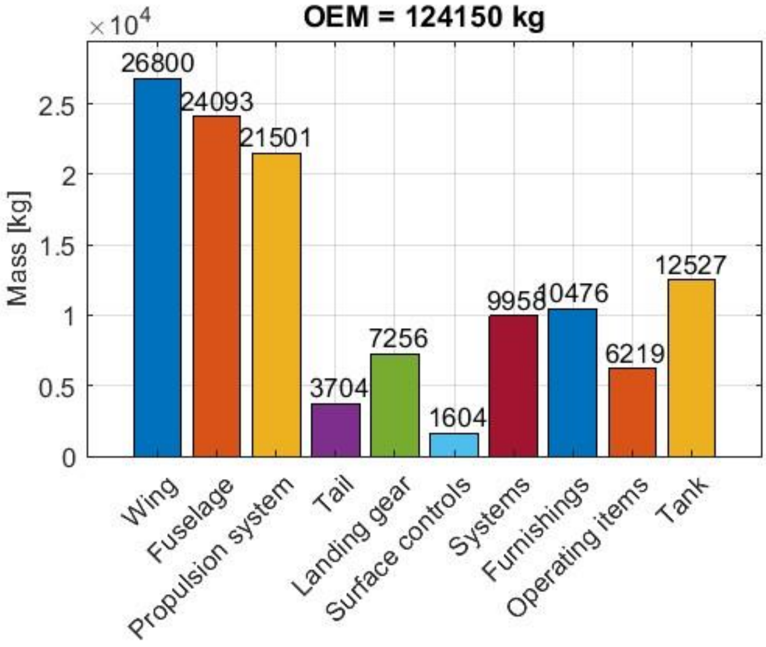

Figure B.6: OEM and its components of WB LH2.

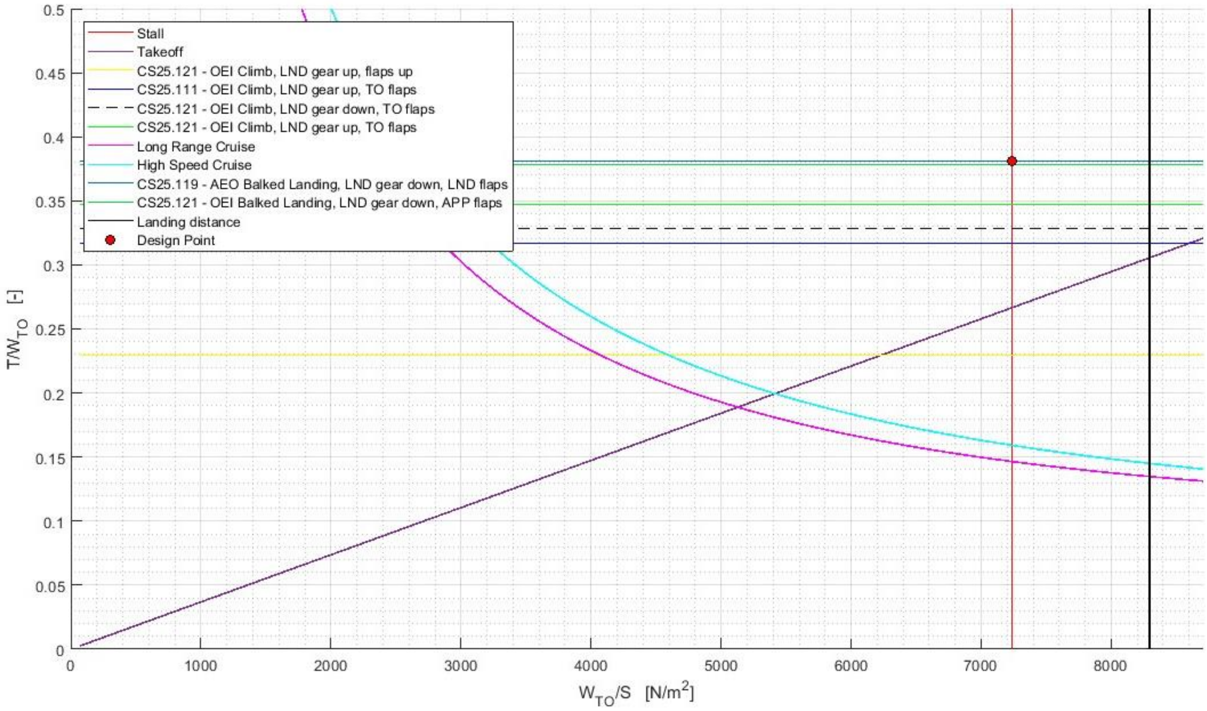

Figure B.7: Sizing matrix plot of WB LH2.

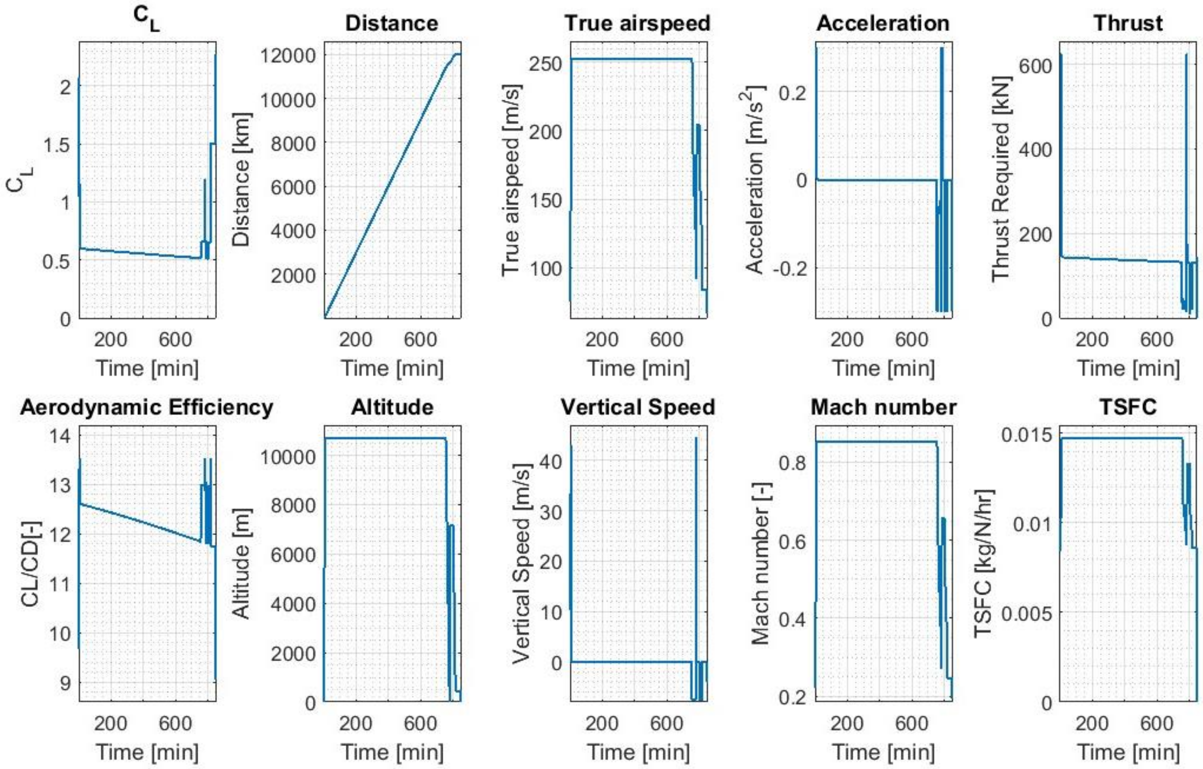

Figure B.8: Mission parameters histogram of WB LH2.

List of Figures

Figure 0.1: Aviation carbon emissions to be subsided by 2050 [2]. 13

Figure 0.2: Share of global flights and CO2 emissions vs flight distance [3]. 14

Figure 0.3: CO2 emissions in 2018 by operations and aircraft class [5]. 14

Figure 0.4: Contribution to achieving Net Zero Carbon in 2050 [2]. 15

Figure 0.5: Efficiency of energy delivery to the aircraft propulsion [7]. 16

Figure 0.6: The range of cases in terms of PAX and design range evaluated for NB and WB. 17

Figure 0.7: Relative tank size for different zero-carbon emission fuels, with kerosene provided for comparison [8]. 18

Figure 0.8: Schedule of the civil airplane development process [11]. 19

Figure 0.9: The three phases of aircraft design [10]. 20

Figure 0.10: Evolution of mission specification and its relation to preliminary sizing [12]. 20

Figure 0.11: Project Bee, Hydrogen powered B-57B [16]. 23

Figure 0.12: General arrangement LH2-fueled subsonic passenger, 400 PAX, 5500 nm, M 0.85. [9]. 24

Figure 0.13: General arrangement LH2-fueled supersonic passenger, 234 PAX, 4200 nm, M 2.7 [9]. 24

Figure 0.14: Tu-155 inboard profile [18]. 25

Figure 0.15: Hydrogen fueled Airbus A300 [19]. 25

Figure 0.16: CRYOPLANE concept for short and medium range aircraft [20]. 26

Figure 0.17: ATI concepts for FlyZero [23]. 26

Figure 0.18: Airbus concepts for low carbo aviation. 27

Figure 1.1: World annual air traffic [25]. 30

Figure 1.2: Trend of GDP vs air trip [26]. 30

Figure 1.3: World 2019 fleet share [27]. 31

Figure 1.4: Current fleet share by type [28]. 31

Figure 1.5: Demand for new aircraft by 2041 [6]. 32

Figure 1.6: Forecast of NB aircraft Orders [33]. 33

Figure 1.7: Forecast of WB aircraft Orders [33]. 34

Figure 1.8: Average flight stage divided in short, medium and long haul. 35

Figure 1.9: Relation between stage length and cruise speed with flight cycle. 35

Figure 1.10: Relationship between aircraft size and sector distance in NB [38]. 36

Figure 1.11: Relationship between aircraft size and sector distance in WB [38]. 36

Figure 2.1: DOC items. 42

Figure 2.2: Flight profile for NB cases analysis. 43

Figure 2.3: CASK vs flight distance based on airlines data in 2012 [72]. 43

Figure 2.4: The impact of sector distance on fuel burn of A321-200 on routes from London [43]. 44

Figure 2.5: Cost of LH2 per kg, fiscal base year 2019 [44]. 44

Figure 2.6: Items of RDT&E and ACQ cost. 49

Figure 2.7: Rolls-Royce Trent family thrust vs price (based on 2020) [51]. 51

Figure 2.8: CASK vs sector distance for Airbus A321 on routes from London (2020) [43]. 53

Figure 2.9: A321 DOC at stage length 1,300 km. 53

Figure 3.1: Boeing 737 nacelle evolution [54]. 55

Figure 3.2: Effects of turbofan BPR on TSFC in cruise conditions [11]. 56

Figure 3.3: Empirical pitch-up boundary for sweep back wing [56]. 57

Figure 3.4: M_{DD} definition. 58

Figure 3.5: Improvement of drag rise Mach number by advancement of aerodynamic at constant wing seep, t/c and lift coefficient [59]. 59

Figure 3.6: Fuselage cross section in NB and WB. 60

Figure 3.7: Mach number time aerodynamic efficiency of DC-10 [64] [76]. 64

Figure 3.8: Typical trade off cruise Mach number optimization for DOC [76]. 65

Figure 3.9: Method trade off sensitivity study for a kerosene burning aircraft in class of A320. 66

Figure 4.1: Share of materials in new and old passenger aircraft, A350 and A320 [68] [69]. 68

Figure 4.2: Trade off design range vs PAX for NB on DOC. 70

Figure 4.3: The effect of range and PAX on OEM for NB. 71

Figure 4.4: Fuselage slenderness for NB trade off cases. 71
Figure 4.5: Current fleet concentrated zone up to 2,500 km and 200 PAX [25]........... 71
Figure 4.6: Block fuel per hour for NB wing parameters trade off. 72
Figure 4.7: MTOM for NB wing parameters trade off. 72
Figure 4.8: DOC of wing parameters trade off for NB. 73
Figure 4.9: Effect of cruise Mach number on DOC for NB. 74
Figure 4.10: Size comparison of NB LH2 and A321. 76
Figure 4.11: Effect of fuel price on empty mass of optimum solution for NB. 77
Figure 4.12: Effect of fuel price on MTOM of optimum solution for NB. 77
Figure 4.13: Potential L/D $_{max}$ for subsonic transport aircraft and NB LH2 [71]. 78
Figure 5.1: Trade off design range vs PAX for NB on DOC. 81
Figure 5.2: The effect of range and PAX on OEM for WB. 82
Figure 5.3: Fuselage slenderness for WB trade off cases. 82
Figure 5.4: Block fuel per hour for WB wing parameters trade off. 83
Figure 5.5: MTOM for WB wing parameters trade off. 83
Figure 5.6: DOC of wing parameters trade off for WB. 84
Figure 5.7: Effect of cruise Mach number on DOC for WB. 85
Figure 5.8: Size comparison of WB LH2 and B787-8. 87
Figure 5.9: Effect of fuel price on empty mass of optimum solution for WB. 87
Figure 5.10: Effect of fuel price on MTOM of optimum solution for WB. 88
Figure 5.11: Potential L/D $_{max}$ for subsonic transport aircraft and WB LH2 [71]. 88
Figure A.1: NB trend of DOC per design range vs PAX and range for LH2 2 $/kg. ... 99
Figure A.2: NB trend of DOC per design range vs PAX and range for LH2 3 $/kg. ... 99
Figure A.3: NB trend of DOC per BH and average speed vs PAX and range for LH2 2 $/kg. 100
Figure A.4: NB trend of DOC per BH and average speed vs PAX and range for LH2 3 $/kg. 100
Figure A.5: WB trend of DOC per design range vs PAX and range for LH2 2 $/kg. 100
Figure A.6: WB trend of DOC per design range vs PAX and range for LH2 3 $/kg. 101
Figure A.7: WB trend of DOC per BH and average speed vs PAX and range for LH2 2 $/kg. 101

Figure A.8: WB trend of DOC per BH and average speed vs PAX and range for LH2 3 $/kg. 101
Figure B.1: MTOM and its components of NB LH2. 103
Figure B.2: OEM and its components of NB LH2. 103
Figure B.3: Sizing matrix plot of NB LH2. 104
Figure B.4: Mission parameters histogram of NB LH2. 104
Figure B.5: MTOM and its components of WB LH2. 105
Figure B.6: OEM and its components of WB LH2. 105
Figure B.7: Sizing matrix plot of WB LH2........ 106
Figure B.8: Mission parameters histogram of WB LH2. 106

List if Tables

Table 1.1: Selected performance parameters of NB aircraft [40]. 38

Table 1.2: Selected performance parameters of WB aircraft [40]. 39

Table 1.3: Performance parameters aimed for LH2 NB and LH2 WB aircraft. 39

Table 2.1: Crew wage. 45

Table 2.2: MMH/FH for selected aircraft [10]. 46

Table 2.3: Maintenance cost for selected aircraft, based on 2013 [47]. 46

Table 2.4: Overhaul cost of selected engine [48]. 46

Table 2.5: En-route charges for Airbus A321, 2001 (per 700 km overflight) [43]. 48

Table 2.6: Labor rate at 2020 [15]. 50

Table 2.7: Material factor [15]. 51

Table 3.1: Typical cabin parameters dimension. 60

Table 3.2: C_{Lmax} at landing and takeoff configuration of selected aircraft [58]. 61

Table 3.3: C_{Lmax} at landing and takeoff configuration for NB and WB. 61

Table 3.4: $\Delta C_{D\,LDG}$ and $\Delta C_{D\,Flap}$ for selected aircraft. 62

Table 3.5: $\Delta C_{D\,LDG}$ and $\Delta C_{D\,Flap}$ for NB and WB. 62

Table 3.6: Real and estimated Oswald factor of A320 in cruise condition. 63

Table 4.1: NB baseline case design parameters. 67

Table 4.2: The Effect of implement higher technology in NB cost and design parameters. 68

Table 4.3: Design parameters of NB base line and final solution. 75

Table 5.1: WB baseline case design parameters. 79

Table 5.2: Number of abreast effect on WB design parameters. 80

Table 5.3: Design parameters of WB base line and final solution. 86

List of abbreviations

ACQ	Acquisition
APU	Auxiliary Power Unit
AR	Aspect Ratio
ATC	Air Traffic Control
ATI	Aerospace Technology Institute
BF	Block Fuel
BH	Block Hour
BPR	Bypass Ratio
BWB	Blended Wing Body
CAGR	Compound Annual Growth Rate
CAO	Civil Aviation Organizations
CASK	Cost of Available Seat Kilometer
c.g.	Center of Gravity
CO2	Carbon Dioxide
DAPCA	Development and Procurement Costs of Aircraft
DOC	Direct Operating Cost
DP	Depreciation Period
EIS	Entry Into Service
EM	Empty Mass
FC	Flight Cycle
FH	Flight Hours
FoM	Figures of Merit
GDP	Gross Domestic Product
GFM	Global Market Forecast
Gt	Giga ton
GTF	Geared Turbofan
HYPERION	HYbrid PERformance SimulatION
IATA	International Air Transport Association
IOC	Indirect Operating Cost
IR	Interest Rate
ISA	International Standard Atmosphere

LCC	Life Cycle Cost
LDG	Landing Gear
LE	Leading Edge
LH2	Liquid Hydrogen
LLP	Life-Limited Parts
M	Mach
M$	Million US dollar
MH	Man Hour
MJ	Mega Joule
MLM	Max Landing Mass
MMH	Maintenance Man-Hours
MMT	Million Metric Tons
MTOM	Max Takeoff Mass
N/A	Not Available
NB	Narrowbody
NMA	New Midsize Airplanes
OEM	Operating Empty Mass
OPR	Overall Pressure Ratio
PAX	Passenger
RDT&E	Research Development, Test, and Evaluation
ROC	Rate of Climb
RPK	Revenue Passenger Kilometers
SAF	Sustainable Aviation Fuel
SAR	Specific Air Range
S/L	Sea Level
TBD	To be Defined
TET	Turbine Entry Temperature
TLR	Technology Readiness Levels
TSFC	thrust-specific fuel consumption
WB	Widebody

List of symbols

Variable	Description	SI unit
a	Speed of sound	m/s
$A-0$	NB case with A320-200 technology level	-
$A-1$	NB baseline case	-
b	Wing span	m
$B-1$	WB baseline case	-
$C_{aircraft}$	Flyaway cost of aircraft	$
C_{avio}	Avionic cost	$
C_D	Drag coefficient	-
C_{dev}	Development support cost	$
C_{Di}	Induced drag coefficient	-
$C_{D\,wave}$	Wave drag coefficient	-
C_{D0}	Zero lift drag coefficient	-
C_{eng}	Engineering cost	$
C_{FT}	Flight test cost	$
$C_{interior}$	Interior cost	$
C_L	Lift coefficient	-
$C_{L\,max}$	Max lift coefficient	-
$C_{L\,max\,1g}$	Max lift coefficient in steady rectilinear flight	-
C_{mat}	Manufacturing material costs	$
$C_{RDTE\,+\,ACQ}$	RDTE and ACQ cost	$
$\overline{c_f}$	Equivalent flat-plate friction drag coefficient	-

Variable	Description	SI unit
$c/4$	25% of chord	-
D_f	Distance departure arrival airport	km
D_{Fus}	Fuselage diameter	m
DOC_{arp}	Airport fee per flight	$
DOC_{crw}	Cost of crew per flight	$
DOC_{fuel}	Cost of fuel per flight	$
DOC_{ins}	Cost of insurance per flight	$
DOC_{Nav}	Navigation fee per flight	$
DOC_{own}	Ownership cost per flight	$
e	Oswald efficiency factor	-
f_{ins}	Insurance factor	%
f_{invest}	Investment factor	%
f_{mat}	Material factor	-
$f_{mat\ i}$	Each material factor	-
f_{RV}	Residual value factor	%
f_{spares}	Spares factor	-
H_{eng}	Engineering hours	hr
H_{mfg}	Manufacturing hours	hr
H_{qc}	Quality control hours	hr
H_{tool}	Tooling hours	hr
$L_{Cabin\ actu}$	Actual length of cabin	m
$L_{Cabin\ theo}$	Theoretical cabin length	m
$L_{Flight\ deck}$	Flight deck length	m
L_{Fus}	Fuselage length	m
$L_{seat\ pitch}$	Seat pitch	m

Variable	Description	SI unit
L/D	Lift to drag ratio	
M_{CR}	Cruise Mach number	-
M_{cr}	Critical Mach number	-
M_{DD}	Drag divergence Mach number	-
M_e	Empty mass	kg
$n_{Abreast}$	Number of abreast	-
N_{CP}	Number of co pilot	-
N_{eng}	Number of engine	-
N_{FA}	Number of flight attendant	-
N_P	Number of pilot	-
n_{PAX}	Number of passenger	-
P_{ac}	Aircraft purchase price	$
P_{fuel}	Fuel price	$
Q	Production Quantity	-
R_e	Rate engineering	$/hr
R_m	Rate manufacturing	$/hr
R_q	Rate of quality control	$/hr
R_t	Rate of tooling	$/hr
$S_{cp/h}$	Copilot wage	$/hr
$S_{fa/h}$	Flight attendant wage	$/hr
$S_{p/h}$	Pilot wage	$/hr
S_{wet}	Wetted area	m^2
t/c	Thickness to chord ratio	-
$\overline{(t/c)}$	Average thickness to chord ratio	-
T/W	Thrust to weight	-

Variable	Description	SI unit
$\boldsymbol{V}$	Cruise speed	Km/hr
$\boldsymbol{W}$	Weight	N
$\boldsymbol{W/S}$	Wing loading	kg/m^2
$\boldsymbol{W_{Aisle}}$	Width of aisle	m
$\boldsymbol{W_{Armrest}}$	Width of armrest	m
$\boldsymbol{W_{Cabin}}$	Width of cabin	m
$\boldsymbol{W_{Clearance}}$	Width of clearance gap between window seat and cabin wall	m
$\boldsymbol{W_{Seat}}$	Width of seat	m
$\boldsymbol{W_f}$	Fuel weight	N
$\Delta \boldsymbol{C_D}$	Drag coefficient increment	-
$\boldsymbol{\lambda}$	Taper ratio	-
$\boldsymbol{\Lambda_{c/4\ limit}}$	Sweep limitation at 25% of chord	deg
$\%_{\boldsymbol{mat\ i}}$	Percent of each material in weight	%

Acknowledgments

I would like to express my sincere gratitude to my thesis supervisor, Prof. Lorenzo Trainelli, for his continuous critical review during the preparation of the thesis and for the valuable skills I was able to obtain through his courses at Politecnico di Milano.

I would also like to thank Mr. Gabriele Sirtori for his invaluable professional assistance and consultation on working with HYPERION and other subjects related to the thesis.

Special thanks go to Mr. Tony Hays for his valuable comments and hints during the review phase of my thesis. I have learned a lot from his lecture notes and our conversations, which helped me, identify the strengths and weaknesses of my project. I would also like to express my gratitude to Prof. Mohammad Ali Vaziry for providing valuable feedback after reading the draft version of the thesis, as well as to Prof. Carlo E.D. Riboldi for his contribution in supervising the thesis.

I am grateful to my friends at Polimi, especially Martina Ghioni, for guiding me through the entire paperwork process in Italy and providing great help in getting acquainted with student life there. I would also like to extend my appreciation to Rafael Rego Lima, Benedetta Invernizzi, and Sofia Fasolato for sharing their valuable knowledge and supporting me throughout my studies.

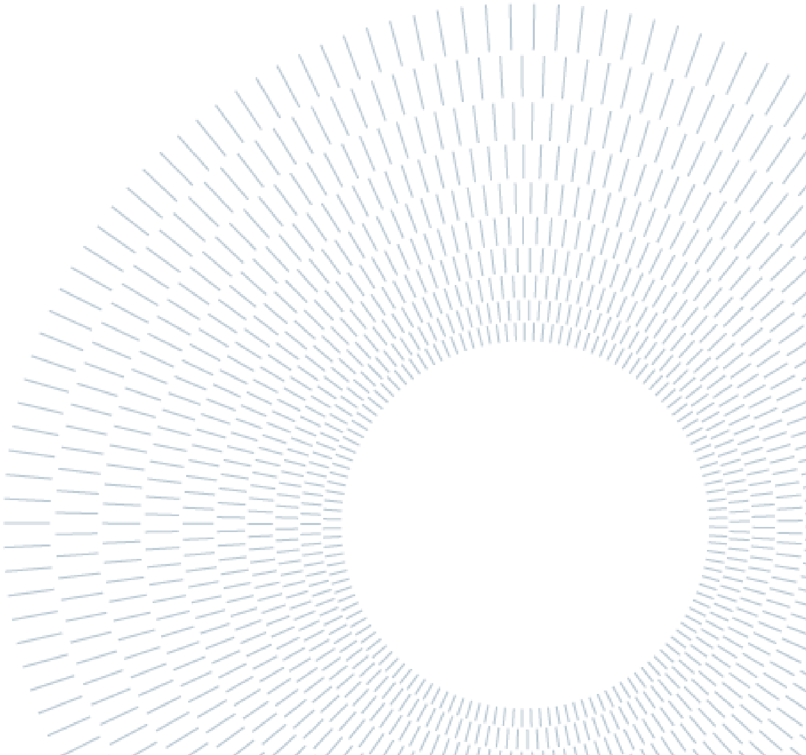Lastly, I am eternally grateful to my wife Niayesh and my parents for their unwavering support and tolerance throughout my entire graduate studies. My journey in MSc would not have been possible without them.